Republic of Iraq
Ministry of Higher Education and Scientific Research
University of Babylon
College of Materials Engineering
Department of Polymer Engineering and Petrochemical Industries

Study the effect of carbon fibers on the crystallization degree of the PEEK polymer

A Thesis
Submitted to the Council of the College of Materials Engineering / University of Babylon in Partial Fulfillment of the Requirements for the Master Degree in Materials Engineering / Polymer

Kawthar kareem degheim
(B. Sc. in engineering Polymer and petrochemical industries, 2017)
Supervisors
Prof. Dr. Najm Abdul Ameer Saad (Ph.D.)
Assist .Prof. Dr. Asra Ali Hussein

2021 A.D **1442 A.H**

بِسْمِ اللَّهِ الرَّحْمَٰنِ الرَّحِيمِ

قُلْ هُوَ اللَّهُ أَحَدٌ ۝١ اللَّهُ الصَّمَدُ ۝٢

لَمْ يَلِدْ وَلَمْ يُولَدْ ۝٣ وَلَمْ يَكُن لَّهُ كُفُوًا أَحَدٌ ۝٤

بِسْمِ اللَّهِ الرَّحْمَٰنِ الرَّحِيمِ

قُلْ أَعُوذُ بِرَبِّ الْفَلَقِ ۝١ مِن شَرِّ مَا خَلَقَ ۝٢

وَمِن شَرِّ غَاسِقٍ إِذَا وَقَبَ ۝٣ وَمِن شَرِّ النَّفَّاثَاتِ فِي الْعُقَدِ ۝٤

وَمِن شَرِّ حَاسِدٍ إِذَا حَسَدَ ۝٥

بِسْمِ اللَّهِ الرَّحْمَٰنِ الرَّحِيمِ

قُلْ أَعُوذُ بِرَبِّ النَّاسِ ۝١ مَلِكِ النَّاسِ ۝٢ إِلَٰهِ النَّاسِ ۝٣

مِن شَرِّ الْوَسْوَاسِ الْخَنَّاسِ ۝٤ الَّذِي يُوَسْوِسُ فِي صُدُورِ النَّاسِ ۝٥

مِنَ الْجِنَّةِ وَالنَّاسِ ۝٦

Supervisors Certification

We certify that this thesis entitled (study the effect of crystallization factor on the mechanical properties of semi crystalline polymers for transport applications) was prepared by (Kawthar kareem degheim) under our supervision at Babylon University / College of Materials Engineering / Department of polymer and petrochemical industries, in Partial Fulfillment of the Requirements for the Award Master Degree of Science in Materials Engineering / Polymers Engineering.

Signature :

Name : Prof. Dr. Najm Abdul Ameer Saad
(Supervisor)

Date : / / 2021

Signature :
Name: Assist Prof . Dr. Asra Ali Hussein
(Supervisor)

Date : / / 2021

Dedicationn

TO

The one who worth's praise and Thanks….
The one who Revives the skies by his Throne and Decorates the Universe by his mention…..Allah

TO

Our great Prophet Mohammad and his Relative (Peace and Blessings of Allah be Upon Him and Them)……

TO

The one who embraced me like my mother…..
The one who is the light in my life….

TO

The one who is my angel on earth….
The secret of my existence, strength and joy…..My father

TO

The whispers of flowers and fragrance of morning….
The shoulder of tenderness and miracle of all time…. My brothers and sister

TO

Who supported me and was with me ……To my loved ones

TO

the one who helped me and was with me……..

Acknowledgment

Firstly, all the thank and praise be to Allah, who has given me the ability and desire to finish this task.

****

I would like to share my deepest appreciation and deepest gratitude to Assist. Prof. Dr. Najm Abdul Amir - and Assist Prof. Dr. Asra Ali Hussein - for their continued encouragement, knowledgeable advise, guidance and support throughout this study.

****

I do not know how can I reach my big respect and thank to my family for their care, patience and encouragement throughout the study period, I am really indebted to them.

****

I do not know how I can express my gratitude to those who helped me and was with me in difficult matters.

With Respect *Kawthar*

2021

Examination Committee Certification

We certify that we had read this thesis entitled **(Study the effect of carbon fiber on the degree of crystallinity of PEEK)** and as an Examination committee examined the student **(Kawthar kareem degheim)** in its contents and that in our opinion it meets the standard of a thesis and is adequate for the award of the Degree of Master in Material's Engineering / Polymer.

Signature:
Prof.Dr. Zoalfokkar Kareem Mezaal
Polymer and Petrochemical Industries
Department Material Engineering
Date: / / 2021
(Chairman)

Signature:
Asst. Prof. Dr. Qahtan Adnan Hamad
University of Technology-Iraq
composite materials
Department Material Engineering
Date: / / 2021
(Member)

Signature:
Asst. Prof. Dr. Ammar Emad Al-kawaz
University of Babylon
Polymer and Petrochemical Industries
Department Material Engineering
Date: / / 2021
(Member)

Signature:
Prof . Dr. Najm Abdul Ameer Saad
University of Babylon
Polymer and Petrochemical Industries
Department Material Engineering
Date: / / 2021
(Supervisor)

Signature:
Asst .Prof. Dr. Asra Ali Hussein
University of Babylon
Polymer and Petrochemical Industries
Department Material Engineering
Date: / / 2021
(Supervisor)

Signature:
Approval of Polymer and Petrochemical Industries Department
Head of Department
Prof.Dr. Zoalfokkar Kareem Mezaal
Date: / / 2021

Signature:
Approval of Material's Engineering Collage
Dean collage
Asst.Prof.Dr. Emad Disher
Date: / / 2021

Chapter One

Introduction

Chapter One

Introduction

1.1Generall Introduction

Polymers form a shape broad category of materials, without which life appears to be quite complicated, they are used every day and everywhere around us: Rubber, resins, and adhesives are all examples [1]. In industrial applications, crystalline polymers represent a category of remarkable engineering plastic materials, these materials vary from small molecular materials include organics and metals, completely crystalline polymers cannot be acquired utilize standard processing conditions[2]. Polymer crystallization depends on nucleation and growth possibilities, and the polymer's structural regularity has a profound effect on both[3].Within the same polymer matrix, semi-crystalline polymers include both amorphous and crystalline zone, due to intermolecular and/or intramolecular forces, molecular movement does not happen to the identical grade in the crystalline section several polymers crystallize beneath the melting point very quickly and others crystallize much slowly, To achieve their equilibrium crystallization stages, various crystalline polymers crystallizee at various average and grades, need long periods and probably after crystallization period .

The Figure (1.1) shows the crystalline region is surrounded by a circle, other regions with indiscriminate chains are amorphous [4].

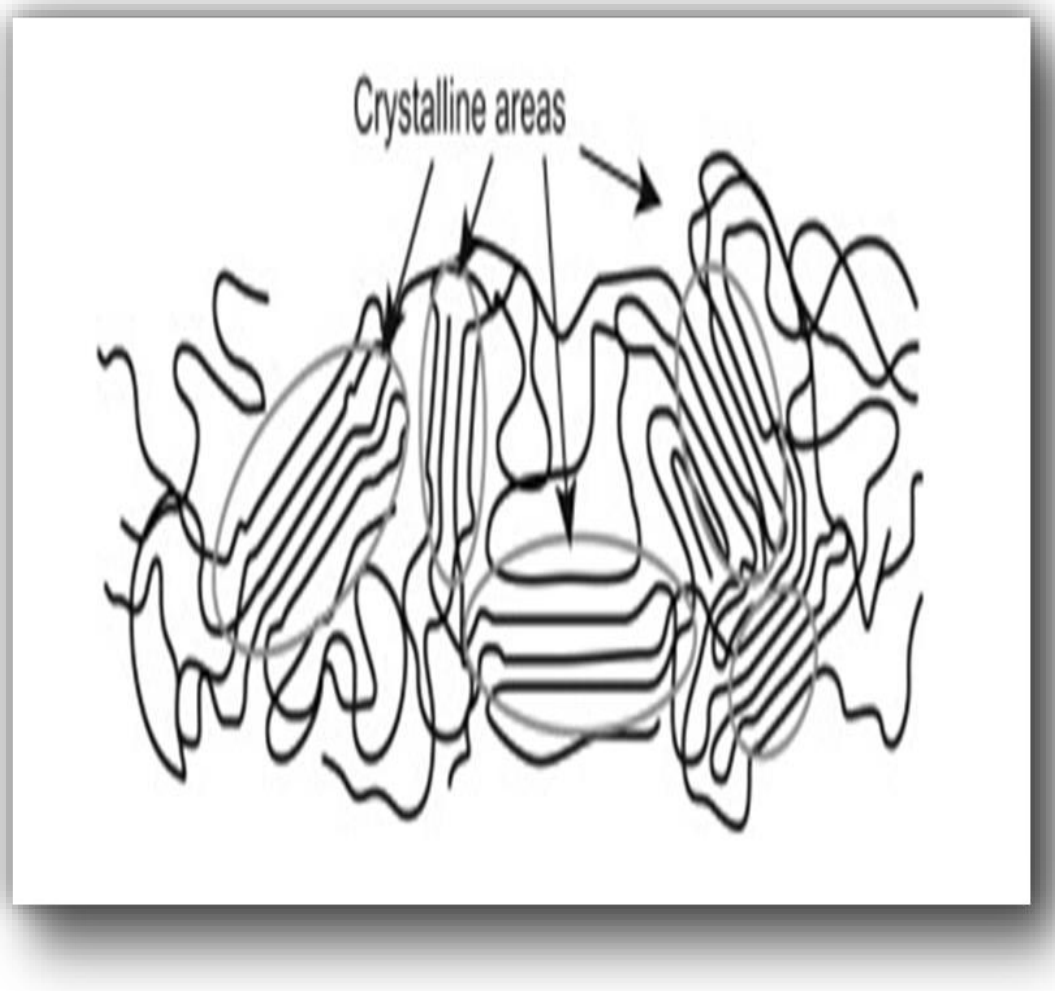

Figure (1.1): Offer a semi crystalline polymer structure

understanding the crystallization behavior of polymers is becoming increasingly important, significant material characteristic that defines many of their physical properties is crystallinity in polymers that are semi crystalline. In polymer science, crystallization of polymers has been a very important subject ,the state of crystallization appear an salient aspect in the polymeric materials' ultimate structure and physical characteristics [5]. Crystallization is in control of the structural formation of polymeric materials and hence of the properties of the final polymer product, Primary nucleation and crystal growth are typically two distinct processes of polymer crystallization[6].Crystalline or strictly semi-crystalline polymers includes together crystalline and amorphous zones , and the

relative amounts of crystalline polymers are defined by the degree of crystallinity that can be measured using different methods, including precise density measurement, thermal analysis, and X-ray diffraction wide-angle[7]. The degree of crystallinity has an important effectiveness on material features like hardnesss, density, melting point, transparency, and diffusion, No polymers exist which are 100% crystalline as there estimated quantity from content of amorphous in the plastics morphology [8]. Polyethylene in Linear state (PE), Polyethylene terephthalate (PET), Polytetrafluoroethylenee (PTFE), or Isotacticc polypropylene(PP) are epitome of semi-crystalline polymers[9].

1.2 The aim of this work

- Study of the effect of carbon fiber reinforcement on (PEEK) polyetheretherketone polymer crystallization.
- Study of the effect of the degree of crystallization on the mechanical properties of a (PEEK) polyetheretherketone polymer.

Because the property of crystallization has a very big impact on the use of this materials(PEEK composite) in transport applications such as cars and aircraft.

Chapter Two

Theoretical part & Literature Review

Chapter Two

Theoretical part & Literature Review

2.1 Introduction

A composite is a structural substance made up of two or more components blended together , that they are not soluble in one another, and are combined at a macroscopic stage. The reinforcing process is called one constituent and the other in the matrix is the one that is embedded. Fibers, fragments, or flakes can be in the form of the reinforcing phase material. In general, the matrix phase materials are continuous [10]. In systems for industrial such as automotive, naval and aerospace, composite materials are commonly used, where cyclic fatigue loading is also subject to them. Microstructure production for high-performance advanced composites has concentrated primarily on reaching high intensity and high modulus. However, such materials must, in addition to their high strength, also absorb power and withstand cyclic fatigue loads [11]. The aim of incorporating fibers into composites is to bear the load that is applied to it, the matrix on the other hand holds and protects the fibers, spreading the load between them [12]. Crystallization takes place under very harsh conditions in most industrial conversion processes, usually at high cooling rates and, in many cases, with shear or extension flow and under strain. Therefore, when developing a polymer for certain applications, crystallization kinetics are of vital importance in order to extract the desired properties from the morphology formed during solidification[13]. Crystallization in polymer has always attracted a lot of scientific and academic attention, since polymers are considered to have a wide range of structures at different length scales, such as unit cell, lamella, and spherules. It's an intriguing phase transition property that defines the final properties of many technologically important and

scientifically fascinating structures [14, 15]. Higher crystallinity results in a substance that is stronger and more thermally stable, but also more porous, while some elasticity and impact resistance are given by the amorphous regions[16,17]. Thermoplastics come in a variety of shapes and sizes and in common use in today, Polyetheretherketone (PEEK) and Polyphenylene sulfide (PPS) are currently the most commonly reported thermoplastic resins in the field of high performance thermoplastics [18].

2.2 Morphology

2.2.1 Amorphous polymers

Amorphous polymers are the polymers that contain amorphous regions where molecules are arranged randomly. Are polymers that are composed of amorphous regions where molecules are randomly arranged. Polymers can be either completely amorphous or mixed with both amorphous and crystalline regions. Amorphous polymers possess widely different mechanical and physical properties owing to their structure and temperature Below glass transition temperature (Tg), amorphous polymers exhibit glassy, hard and brittle properties. As the temperature is increased, while it passes the Tg, amorphous polymers form cross-links and show elastic properties. Tg is defined as the temperature at which the polymer becomes soft due to the long-range coordinated molecular motion. Natural rubber latex, styrene-butadiene rubber (SBR) are good examples of amorphous polymers below the glass transition temperature.

2.2.2 Crystalline polymers

Crystalline polymers are the polymers with crystalline regions where molecules are arranged in a partial pattern. Not a single polymer is crystalline because all the crystalline polymers contain considerable amounts of amorphous material, Thus, crystalline polymers are generally called semi crystalline polymers. Crystalline polymers show X-ray

diffraction patterns due to the existence of specific partial patterns of molecules in the polymer chains and exhibit a crystalline melting temperature. X-ray diffraction, density measurements and heat of fusion are detected in order to determine the fraction of crystalline substances present in a particular polymer[19].

2.2.3 Difference Between Amorphous and Crystalline Polymers

- Amorphous polymers do not have uniformly packed molecules , but crystalline polymers have uniformly packed molecules.
- Amorphous polymers do not have a sharp melting point, but crystalline polymers have a sharp melting point.
- Amorphous polymers are transparent , but crystalline polymers are opaque/ translucent.
- Amorphous polymers have a low shrinkage, but crystalline polymers have a high shrinkage.
- Amorphous polymers have a poor chemical resistance, but crystalline polymers have a good chemical resistance.
- Amorphous polymers are soft, but crystalline polymers are hard [20,21].

2.3 Crystallization mechanisms

2.3.1 Solidification from the melt

Melt crystallization is an important separation, purification, and concentration technique used in the chemical, pharmaceutical, and food industries. Crystallization from melt is a very powerful separation process for the purification of organic compounds up to very high purities of 99.99 percent. Therefore, the objectives of melt crystallization (i.e., purity, separation, or concentration) are quite often different from crystallization from solution (i.e., purity and defined crystal size distribution)[22].

2.3.2 Crystal growth from the melt

The addendum of polymer chain segments that are folded achieves crystal growth and occurs just at temperatures below the temperature for melting Tm and above the temperature of the glass transition Tg , Higher temperatures break molecular structure and the movement of chains of molecules is frozen below the temperature of the glass transition. This method affects the mechanical features of polymers and reduces their volume due to a more compact packaging of the polymer chains aligned[23].

2.3.3 Crystallization by stretching

The polymer is being pushed through a nozzle that produces tensile stress which in this process partially aligns its molecules, Such alignment can be called crystallization and influences the material's properties و In the longitudinal direction, the strength of the fiber is considerably increased[24]. By stretching , it is possible to partially align some polymers that do not crystalline from the melt [25].

2.3.4 Crystallization from solution

Crystallization from solution is a separation technique where a solid phase is separated from a matrix liquor. In contrast to other separation processes, however, the dispersed phase consisting of numerous solid particles also forms the final product, that has to meet the required product specifications[26].

2.3.5 Confined crystallization

Nucleation and growth can be significantly affected when polymer chains are enclosed in a dimensioned space of a few tens of nanometers equivalent to or smaller than the thickness of the gyration radius or the lamellar crystal. As an example, The lamellar crystals' isotropic spherulitic organization is hindered when a polymer in a confined ultra-

thin layer crystallizes, and confinement can create specific orientations of lamellar crystals[27].

2.4 Thermal and mechanical properties

Amorphous polymers are typically hard and brittle below their glass transition temperature because of their molecules' low mobility. Molecular motion is caused by increasing the temperature, resulting in traditional rubber-elastic properties. A constant force at temperatures above Tg applied to a polymer results in a viscoelastic deformation, the polymer starts to creep. For amorphous polymers, $heat_t$ resistance is typically offered only below the temperature of the glass transition [28]. A distinctive feature of semi-crystalline polymers is the solid anisotropy of their mechanical properties along and perpendicular to the direction of molecular alignment[29]. In a polymer that is semi-crystalline, amorphous chains are ductile above the glass transition temperature and are capable of plastically deforming, the amorphous regions are bound by crystalline areas of the polymer. The semi-crystalline polymer first deforms elastically when tensile stress is applied, While the crystalline areas remain unaffected by the stress applied[30].

2.5 Optical property

Owing to light scattering on the various borders between the crystalline and amorphous areas, crystalline polymers are typically opaque,the density of such boundaries is smaller and therefore lower, the transparency is higher .Atactic polypropylene, for instance, is normally amorphous and translucent, whereas syndiotactic polypropylene is typically transparent, opaque with a crystallinity of ~50 percent [31].

Crystallinity also affects polymer dyeing : As the dye molecules penetrate into amorphous regions with greater ease, crystalline polymers are harder to stain than amorphous ones [32].

2.6 Composite materials

A composite is a material made up of two or more different materials that, when combined, these constituent materials have notably dissimilar chemical or physical properties and are merged to create a material with properties unlike the individual elements. Within the finished structure, the individual elements remain separate and distinct, distinguishing composites from mixtures and solid solutions[33][34].

Typical engineered composite materials include:

- Reinforced concrete .
- Composite wood such as plywood.
- Reinforced plastics, such as fibre-reinforced polymer or fiberglass.
- Ceramic matrix composites (composite ceramic and metal matrices).
- Metal matrix composites and other advanced composite materials.

Fiber-reinforced polymer and fiberglass are examples of reinforced plastics, composite materials are currently described as materials with continuous or non-continuous strong fibers encased in a weaker matrix material, The matrix serves to distribute the fibers and also to transmit the load to the fibers[35].Because of their intricate geometry and the behavior of their constituents, to ensure a successful design of a part or structure, composites need intense tests, this testing is carried out during the design process [36]. Metals have a lower fatigue threshold stress than composite materials, when this limit is reached, When it comes to fatigue, composites exhibit more scatter than metals [37].

2.6.1 Structure of Composite Material

1.Matrix Phase

2. Reinforcement Phase - fiber.

3.The Fiber-Matrix Interface.

The figure (2.1) show the composite material structure.

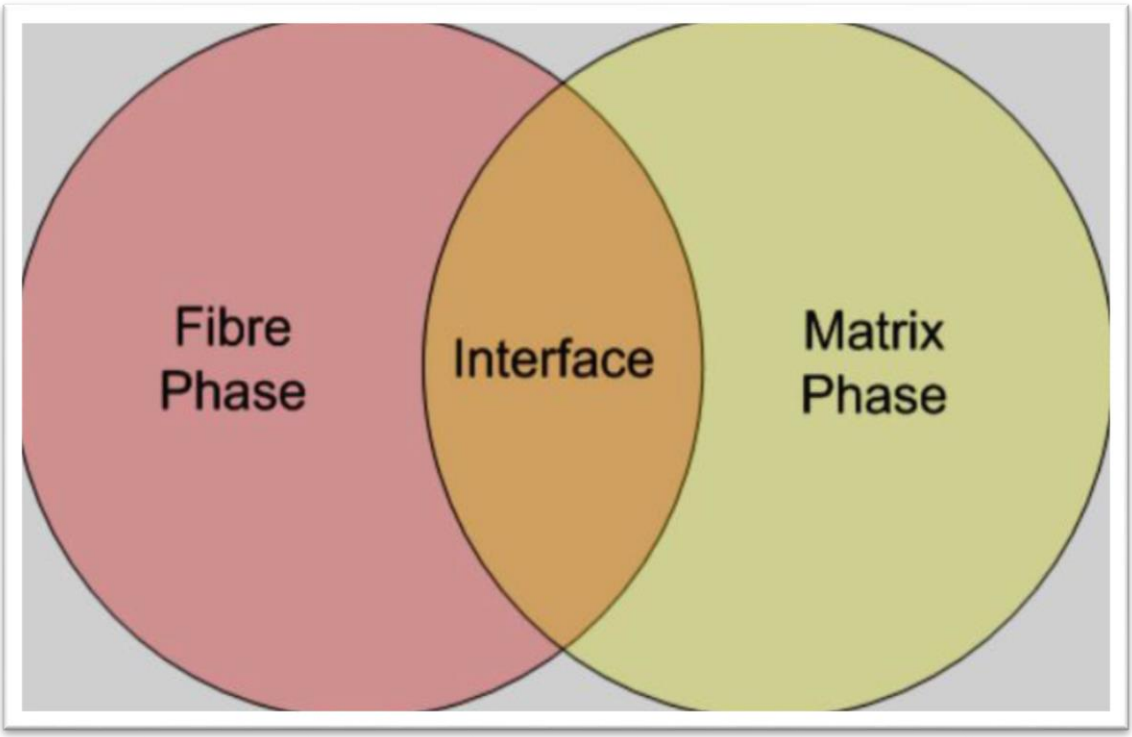

Fig (2.1): Composite Materials Structure [38].

2.6.1.1 Matrix Phase

Normally, the key stage with a continuous Permanent description is more ductile and less complex. The object of the matrix is, it comes back to its coherent and adhesive properties , to tie the reinforcements together, to move the load to and between the reinforcements and to protect the reinforcements from the environment and handling [39].

2.6.1.2 Reinforcement Phase – Fiber

Second phase is included in the matrix in a discontinuous manner, generally more powerful than the matrix. Consequently, it is sometimes called the reinforcement stage. The main purpose of the reinforcement is to provide the composite with superior strength and rigidity levels [40].

2.6.1.3 The Fiber-Matrix Interface

The interphase is formed by chemical reactions between the materials of the fiber and the matrix , or by the use of fiber protective coatings during

production. The fiber-matrix interphase structure and properties the mechanical and physical properties of composite materials play a major role. particularly, it is important to communicate the broad differences between the elastic properties through the interphase of the matrix and of the fibers, or in other words, to transmit the stresses acting on the matrix [41].

2.6.2 Classification of Composite Material

2.6.2.1 Polymer Matrix Composites (PMC)

Its fundamental mechanical properties are the primary factor in a matrix selection, The most desirable mechanical properties for high-performance composites of a matrix are: high tensile modulus that affects the composite's compressive strength and strong tensile strength, which controls the internal cracking of a laminate composite, High fracture toughness, controls delamination of layers growth and crack formation.

There may be other considerations for a polymer matrix composite. for instance good dimensional stability at high temperatures and resistance to moisture or solvents where the polymer does not melt. In hot-wet environments or when exposed to solvents, they swell, crack, or otherwise degrade. Thermoplastic polymers typically have greater strain-to-failure than thermoset polymers [42].

2.6.2.2 Metal Matrix Composite (MMC)

In application requires long- term possibility to extreme conditions, like high temperatures, the metal matrix has an advantage over the polymer matrix. For composite applications requiring high transverse strength and modulus beside compressive strength; Many metals' yield strength and modulus are more than those for polymers, and this is a significant factor. Another advantage of using metals is that a range of thermal and mechanical treatments will plastically deform and reinforce them. Metals, however, have a range of drawbacks, including high densities, high

melting points (hence high process temperatures),and a corrosion propensity at the interface of the fiber- matrix [42].

2.6.2.3 Ceramic Matrix Composite (CMC)

Ceramics are recognized for their stability in high temperatures, high resistance to thermal shock ,high modulus ,high hardness, high resistance to corrosion, and low density. They are brittle compounds, however, and have poor crack propagation tolerance, which is reflected in their low strength to fracture. Growing its fracture toughness is the key justification for reinforcing a ceramic matrix[42].

2.6.2.4 Carbon and Graphite Matrices (CGM)

In composite material choices, carbon and graphite have a special location. Just as many composites have proven that be much preferable at these temperature, carbon -carbon composites should not implementation at rising temperatures. Their capacity to retain their characteristics at room temperature beside temperature in the 2400^{o}C range and its dimensional stability, however; In most aeronautics, they make them an ignorant alternative , military, industrial and space applications[43].

2.7 Poly ether ether ketone (PEEK)

2.7.1 Introduction

PEEK is a semi-crystalline thermoplastic with a crystalline melting point around T = 613 K (340°C) and a glass transition around T =416 K (143°C). It is a tough aromatic thermoplastic polymer with properties that make it very desirable for use as high-quality engineering thermoplastic. It has an excellent high-temperature stability due to its relatively stiff backbone. It has a high continuous service temperature and the benefits of injection molding and other thermoplastic polymer processing techniques. The chemical structure of poly ether ether ketone is shown in Figure (2.2)[44].

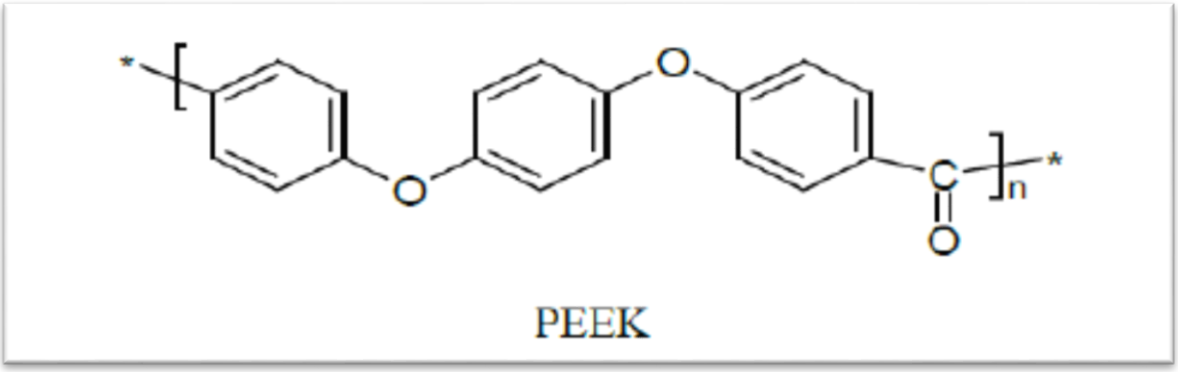

Figure(2.2):Poly(oxy-1,4-phenyleneoxy-1,4-phenylenecarbonyl-1,4 phenylene) (PEEK)[44].

The stability of the aromatic backbone, which makes up the majority of the uni monomer, is credited with the polymer's excellent thermal properties. Polymers with aromatic carbon and/or heterocyclic ties in the polymer main chain, like PEEK, have specific pyrolysis and char yield characteristics. The following are some of these characteristics:

Thermal stability and yield are also improved by the the number of aromatic groups in the main chain per repeat unit of the polymer chain. Pyrolysis usually starts with the weakest bonds in the bridging between aromatic ring groups[45].

The following are some of PEEK's (polye therether ketone) main characteristics:

- At temperatures as high as 315°C (600°F), useful mechanical properties are retained.
- PEEK is extremely fatigue resistant. When the temperature cycle is less than 150°C (300°F), it is also resistant to thermal fatigue.
- PEEK has a higher impact strength than most thermoplastics but a lower impact strength than other metals.
- Despite the fact that mechanical properties decrease after the glass transition.

- PEEK is much stronger than most other materials at high temperatures, At higher temperatures, thermoplastics are used.
- Biocompatibility, mechanical efficiency, and stress crack resistance are all advantages.
- Because of their susceptibility to creep, many thermoplastics are resistant to continuously applied loads. PEEK has a higher creep tolerance over a large temperature range.
- PEEK has a 50-100 times higher fracture toughness than epoxies.
- It has a poor water absorption rate of less than 0.5 percent at 23 degrees Celsius (73 degrees Fahrenheit), compared to 4-5 percent for traditional aerospace epoxies.
- PEEK provides good resistance to wear and chemicals.
- It has strong gamma radiation tolerance, making it suitable for use as a wire covering material for control cabling inside nuclear reactor containment areas[46].

2.7.2 Applications of Poly ether ether Ketone (PEEK)

2.7.2.1 PEEK replaces Metal Tubing

For weight savings, equivalent strength/mass, chemical resistance, and hardness, PEEK is an excellent substitute for stainless steel, other forms of metal tubing, and even glass. PEEK, above all, is equal in terms of quality. Stainless steel is stronger, but it is also heavier and more expensive. Since PEEK tubing is made of silicone, the risk of corrosion, outgassing, or leaching (which can lead to contamination) is low. For most acids and bases, PEEK is chemically resistant and inert. Thin-walled PEEK tubing can be designed to be more versatile than stainless steel or titanium tubing, and can easily be cut to length with a razor blade. PEEK is weldable, machinable, and can be used with existing stainless steel or

polymer fittings. PEEK can be bonded with epoxies, cyanoacrylates, polyurethanes, or silicones [47].

2.7.2.2 Chemical Processing

PEEK is used in the chemical manufacturing industry because it is inherently pure and has excellent chemical resistance. Unlike most metals, such as stainless steel or aluminum, PEEK can be used in long-term continuous service applications with minimal degradation of the chemicals being processed. PEEK has been shown to outperform fluoro-polymers with its excellent fatigue resistance and general mechanical properties [47].

2.7.2.3 Medical Applications

PEEK have high resistance to chemical and radiation degradation, compatible with different fibers and have high strength ,and elastic modulus for structural application. It is an appropriate biomaterial for orthopedic and spine implants due to its stability, biocompatibility, radiolucency, and mechanical properties. PEEK and PEEK composite biomaterials are biocompatible however, its bio inert does not easily allow protein adsorption on its surface. Therefore, when present as a bulk PEEK polymers are known to be inert (bioinert) in hard and soft tissues. An Important advantage of bio inert material it is that does not have revers reaction or release ions or ingredient. In order to make PEEK polymers bioactive, it must be mixed or coated with some inorganic [48].

2.7.2.4 HPLC Applicationss(High Performance Liquid Chromatograph)

PEEK For HPLC analytical science applications, it has become the gold standard due to its purity, high burst strain, and chemical inertness and resistance. It is also resistant to solvents that are both organic and inorganic. For its power, versatility, and ease of cutting, chromatographers value PEEK [49].

2.7.2.5 Aerospace application

Lighter weight, the ability to configure lay-ups for optimum strength and rigidity, improved fatigue life, corrosion resistance, and lower assembly costs due to fewer detailed parts and fasteners with good design practices are just a few of the advantages of high-performance composites[50].

2.7.3 Poly ether ether ketone Matrix

PEEK is now being used as a polymer matrix for thermoplastic composites, suspending carbon, glass or aramid fibers for a composite material that can substitute metals and thermosets for aerospace, medical and industrial applications. PEEK ability resilience continuous operating temperaturess of reach to 260°C and 120 °C in aerospace structural applications, One of the first reinforcing additives to increase the strength and rigidity of PEEK was carbon and glass fillers [51].

2.8 Reinforcing materials

2.8.1 Carbon Fiber

In nature, we can say that carbon is the more impressive element, by tailoring the carbon structure, a surprising number of various structures can be obtained at differing lengths scales , as Graphene, carbon fiber, nanotubes and fullerenes [52,53,54,55]. One of the interesting carbonaceous materials with excellent mechanical characteristics and optimum chemical stability is carbon fiber [56]. These fibers have mechanical and physical properties that are highly enhanced[57, 58, 59, 60]. Not restricted to high tensile strength (2.7GPa), significant compressive strength, high Young's modulus (200-900GPa), low densityy(1.75-2.20g/cm^3),low thermal expansion, outstanding thermal and electrical conductivity(~800$Wm^{-1}K^{-1}$) [61, 62, 63]. Excepting in the existence of hot air/flame , carbon fiber as well progress high chemical resistivity to all chemical species [64]. With very strong creep resistance ,low densities (ρ= 1.75-2.00 $g.cm^{-3}$) and high module(HM) up to

(E≤900GPa),carbon fibers has high tensile strength(HT)up to(7GPa), lack of oxidizing agent resistance such like hot air and fires, but are resistant to all other chemical species. The strong mechanical properties make carbon fiber desirable in the form of woven textiles, as well as continuous or chopped fabrics[65,66]. Carbon fibers are produced at a temperature between 1000^{o}C and 3500^{o}C by carbonizing a fiber precursor[67]. Carbon fibers typically have outstanding tensile characteristics, low density, high thermal and chemical stability, strong thermal and electrical conductivity, in the absence of oxidizing agents, outstanding fatigue resistance and excellent creep resistance. They are widely used in composites in the form of woven textiles, pre-pregs, continuous fibers/ rovings, and chopped fibers [68].Carbon fiber use is increasing in a variety of applications, including aerospace, sporting goods, and a variety of commercial/industrial applications , development is at its fastest in commercial/industrial applications[69].

2.8.2 Effects of Fillers on Structure and Properties

The following attractive are carbon fiber polymer-matrix composites.

- Low density (40 percent least than aluminumn).
- .High-intensity strength (strong as high-strength steels).
- High stiffness (More stiff than titanium, though much smaller in density).
- Strong resistance to fatigue (A nearly unlimited life under the loading of fatigue).
- Strong resistance to creeps.
- Low coefficient of friction and strong wear resistance (at 40 wt. percent).The composite nylon-matrix carbon fibre with a coefficient of friction almost as low as Teflon and unlubricated wear properties near those of lubricated steel).

- By using laminate, hardness and damage resistance can be built.
- Orientation to be stronger than metals and more harm-tolerant.
- Chemical resistance (polymer-controlled chemical resistance from the matrix).
- Resistance to Corrosion (Corrosion-impermeable).
- Dimensional stability (It can be designed to achieve zero thermal expansion coefficient.
- Damping capacity of vibration (Excellent damping of the structure when Compared to metal).
- Poor Resistivity to electricity.
- Efficacy Shielding of high electromagnetic interference (EMI).
- Elevated heat conductivity

Most notably, carbon fiber is utilized to reinforce composite materials, especially the category of materials recognized polymers reinforced with carbon fiber or graphite, For carbon fibers as the matrix, it is also possible to use non-polymer materials[70]. Carbon fiber reinforced plastics (CFRPs) have the highest strength-to-weight, greater anti-fatigue and anti-aging properties than conventional metal products. CFRPs increasingly are used in automotive, aviation, aerospace, wind energy and another industries with the characteristics of lightweight and high performance[71]. PEEK is one of the widely used to mix with carbon fibers, but in order to destroy the PEEK matrix's previous thermal history, processing must be carried out done at a sufficiently high temperature. Fiber-matrix adhesion in a combined system is dependent on the molding temperature, the melt temperature residence time, and the cooling rate[72].

2.9 Literatures Review

Alexander Tregub, et al.(1993)[73], studied investigated the effect of the degree of crystallinity on the mechanical properties specifically affect the flexural fatigue, of the as-received performance of carbon-fiber-reinforced PEEK, where they are examined at two crystallinity composites levels (35%) and of damped composites (10%). The results shows the higher the crystallinity degree, the higher the static flexural strength and modulus, as well as the longer the fatigue life.

G. Swallowe, et al.(1997)[74], studied crystallinity increases in semi-crystalline polymers during high rate testing. Where crystallinity in the polymers PEK,PEEK , and PET.is addressed when they are at a range of temperatures compressed at high strain rates. During low rate deformation in tension semi-crystalline polymers, strain caused by crystallization may occur, resulting in an increase in flow stress. When measured at high rates, all three polymers show substantial increases in crystallinity, with PEK and PEEK showing increases only at rates of 10'1s. The evidence presented here indicates that such increases are real, at least in semi-crystalline polymers, and are thought to be caused by the high strain intensity's combination of increased crystallinity and crystalline perfection.

Bhanu Nandan ,et al.(2003)[75], studied crystallization and melting behavior of poly(ether ether ketone)/Poly(aryl ether sulfone) blends. (PES) prepared by melt mixing the blend use investigated by using differential scanning calorimetry (DSC) and wide angle X-ray scattering (WAXS), show that the presence of PES in PEEK/PES blends has a significant impact on the crystallization behavior of PEEK, particularly when present in small quantities . In the presence of PES from the melt and in the rubbery state, the crystallization kinetics of PEEK is slowed. The melt crystallization exotherm of PEEK in the presence of PES

indicates a slower rate of nucleation and a broader crystallite size distribution. Because of the dilution effect of PES, the degree of crystallinity in PEEK-rich formulations is lower than in pure PEEK.

M.C. Kuoa , et al.(2004)[76], They studied PEEK, composites reinforced by nano-sized SiO_2 and Al_2O_3 particulate ,filled with nano-sized silica or alumina measuring (15-30nm) to (2.5-10wt%).Have been prepared by vacuum hot press molding is used at 400◦C, the composition have been examined by crystallinity degree testing and the thermal stability of the PEEK resin with nanoparticles is investigated using X-ray diffraction, differential scanning calorimetry, and other techniques thermos gravity analyzer. this show that nano composites containing 5–7.5 wt% SiO2 or Al_2O_3 nanoparticles boost stiffness, elastic modulus, and durability the most , as compared to unfilled PEEK, the composites improve tensile strength by 20–50% while losing tensile ductility. It is also discovered that the composites have a higher crystallinity fraction and degradation temperature.

Liliana B, et al.(2006)[77], studied crystallization behavior of poly(phenylene sulfide), Poly(phenylene sulfide) (PPS),by differential scanning calorimetry (DSC)which is a technique for determining the temperature (DSC) and PLM techniques. Can they find Thermal treatment has an effect on polymer morphology. The temperature must be calculated to avoid self-nucleation. The presence of remnant crystals in the melting phase will interfere with crystal nucleation during cooling, preventing precise control of the final composite microstructure and resulting in a material with poor mechanical properties.

M. Rahail Parvaiz ,et al.(2010)[78], studied Polyetheretherketone (PEEK) Composites Reinforced with Fly Ash and Mica , Polyetheretherketone (PEEK) composites were developed using fly ash and mica as fillers, PEEK composites of 5-30 wt% loading were

compounded using twin screw extruder. The effect of fly ash and mica on the percentage crystallinity of PEEK composites was studied by using modulated differential scanning calorimeter (MDSC), Uniaxial tensile testing was carried out using Universal Tensile Testing Machine Flexural properties were measured, Tensile strength of Polyetheretherketone composite initially increased with the content of fillers after reaching a maximum value at 20 wt % filler (fly ash and mica) and then decreased, there is increase in effective surface fracture energy, size of voids and agglomeration of filler particles, there is no significant change in the melting points (Tm) of both filled and unfilled samples of mica and fly ash PEEK composites.

T. Yu ,et al.(2011)[79], studied effects of crystalline morphologies on the mechanical properties of carbon fiber reinforcing polymerized cyclic butylene terephthalate composites, Carbon./polymerized cyclic butylene terephthalate (pCBT) Tensile, flexural, short beam shear, and impact tests were performed on the composites using a modified film stacking technique. As a result, the crack started and spread along with ‘weak' spherulite/trans crystalline boundary regions, resulting in low mechanical properties. The highest mechanical properties were found in the Carbon/ pCBT sample crystallized at 210°C with high crystallinity and highly disordered spherulitic crystallites without spherulite/trans crystalline boundary lines or boundary crystals.

Lanzhu Zhang , et al.(2012)[80], studied the mechanical properties of PEEK composites polyetheretherketone (PEEK) composite ,

which were reinforced with short fibers like short carbon fiber (SCF), short glass fiber (SGF.), or filled with Polytetrafluoroethylenee (PTEF), expanded graphite, and TiO_2 nanomaterial. The tensile properties of polyetheretherketone (PEEK) composites were investigated. The results show that the weight content of short fibers, PTFE, and extended graphite

was varied between 0 and 15%, and that the weight content of TiO2 were varied between 0 and 8%. The tensile efficiency (tensile strength and modulus) of PEEK composites improved rapidly as the weight content of short fibers increased. The tensile strength increased at first, but gradually decreased as the PTFE content was increased. Despite the shift in PTFE material, the tensile modulus remained constant..

R. Hemanth1, et al.(2014)[81], studied the effects of fibers and fillers on mechanical properties of thermoplastic composites result Thermoplastic copolyester elastomer (TCE,) and Polyoxymethylene(POM)filled Polytetrafluoroethylenee (PTFE) composite, reinforced with short glass fiber (SGF) and different shape microfillers Melt mixing with a twin screw extruder created short carbon fiber (SCF), silicon carbide (SiC), and alumina (Al_2O_3),which were then injection molded. Mechanical properties such as tensile, flexural and impact strengths were studied. The mechanical properties test results show that short glass fiber increases the strength of TCE and POM filled PTFE composites, while different form ceramic fillers minimize the tensile and bending properties of TCE filled PTFE composites. However, different shape microfillers have a synergistic effect on the tensile and bending properties of POM and PTFE at the same time.

Iskender Ozsoy,et al (2015)[82], studied the influence of micro and nano filler content on the mechanical properties of Epoxy Composites ، Micro- fillers, such as aluminum oxide(Al_2O_3),titanium dioxide (TiO_2) At a weight ratio of 10% to 30%, fly ash and other materials were added. Nano-fillers such as aluminium oxide (Al2O3), titanium dioxide (TiO2), and nano clay were applied in weight ratios ranging from 2.5 to 10%.show that The strength of clay epoxy composites decreased as the filler ratio was increased. The tensile modulus and flexural modulus of micro-filler Al_2O_3, TiO_2, fly ash and nano-fillers Al_2O_3, TiO2 clay epoxy

composites increased with increasing filler content. In general, With the filler content, the hardness of the micro-filler Al2O3, TiO2, fly ash and nano-fillers Al2O3, TiO2, clay epoxy composites increased. With the addition of the filler, epoxy composites become brittle. At higher nano-filler ratios, the issue of filler agglomeration is present.

S. Selvam , et al. (2016)[83], studied Development and Investigation of Mechanical Properties of PEEK Fine Particles Reinforced UHMWPE Composites , novel Ultra-high molecular weight polyethylene (UHMWPE) composites reinforced with 3wt. %, 6wt. %, 9wt. %, 12wt. % and 15wt. % PEEK particles are fabricated by using hot compression moulding technique and mechanical properties are investigated. The results have revealed that the addition of PEEK to the UHMWPE reduced tensile strength and elongation at break, whereas the Young's modulus of the composites was increased, The morphologies of the fractured surface are analyzed under field emission scanning electron microscope. The results have indicated poor interfacial bonding between PEEK and UHMWPE

Jianhua Li, et al.(2019)[84], studied crystalline characteristics, mechanical properties, thermal degradation kinetics and hydration behavior of biodegradable fibers melt -spun from polyoxymethylene /Poly(l-lactic acid) Blends ,were prepared by melt extrusion. Melt-spinning was used to produce the bicomponent fibers, and the thermal degradation kinetics were thoroughly investigated. As a result, the bicomponent fibers achieved a tensile strength of 791 MPa , which is very strong. And it has partial hydration potential in acid and alkali media, so it could meet the requirements for being used as a form of biodegradable fiber. The addition of PLLA to the bio component fibers decreased their thermo-oxidative aging property and thermal stability slightly.

Dong-Hyun Kim et al.(2020)[85], studied an investigation of mechanical and microscopic properties for the semi -crystalline polypropylene Polymer Via experiments and molecular dynamics. With related to the degree of crystallinity , mechanical properties and moisture absorption characteristics were investigated using both experiments and molecular dynamics. Crystal structure and crystallinity were tested using XRD, DSC, and a tensile test, and the calculated values of crystallinity for the regular and annealed samples were (46.5% and 50.1% respectively),crystalline and amorphous layers were used to build semi-crystalline MD models with varying degrees of crystallinity. The crystallinity values measured for the MD models were (47.8% and 53.8 percent)respectively, suggesting that an improvement in crystallinity increased stiffness and strength for the PP , It was discovered that higher crystallinity resulted in less moisture absorption.

M. Doumeng , et al .(2021)[86],studied A comparative study of the crystallinity of polyetheretherketone by using density, DSC, XRD, and Raman spectroscopy techniques , the microstructure of Polyetheretherketone is first analyzed with usual techniques such as density, Differential Scanning Calorimetry, X-ray Diffraction, and secondly, compared with Raman Spectroscopy, The density measurement gives the highest most trusted absolute uncertainty for the degree of crystallinity, around 4%, compared to the other techniques. , overestimates up to 18% the degree of crystallinity due to a competitive phenomenon between crystallization and melting of PEEK over the same temperature range, and a fast crystallization. When Analyzing the X-ray Diffraction data, the degree of crystallinity is underestimated up to 11% as a consequence of the broad amorphous halo. Lastly, our investigation proves that Raman microspectroscopy is appropriate to determine the

local crystallinity on the sample surface and compares 18 indicators in the same study.

Chapter Three

Experimental Work

Chapter Three

Experimental Work

3.1 Introduction

The experimental part includes a study of mechanical , structural and thermal characteristics of high performance material of PEEK and its composite reinforced by (20% and 30% carbon fiber), where the structural tests include FTIR, X-ray and SEM, The mechanical tests include tensile, impact strength and hardness, thermal properties including Tg , Tm and Tc by using DSC instrument.

3.2 Materials Used in the Study

Three types of material sheets have been used in this work with dimensions of (6×700×700mm) supplied by Tangyin Sanyou Engineering Plastic Co. Itd /China .

1.Pure PEEK

2. PEEK + 20% CF

3. PEEK + 30% CF

3.3 Procedure of the Work

The pure poly ether ether ketone (PEEK), (PEEK+20%CF) and (PEEK+ 30% CF) are subjected to these tests in the following flow chart (3.1).

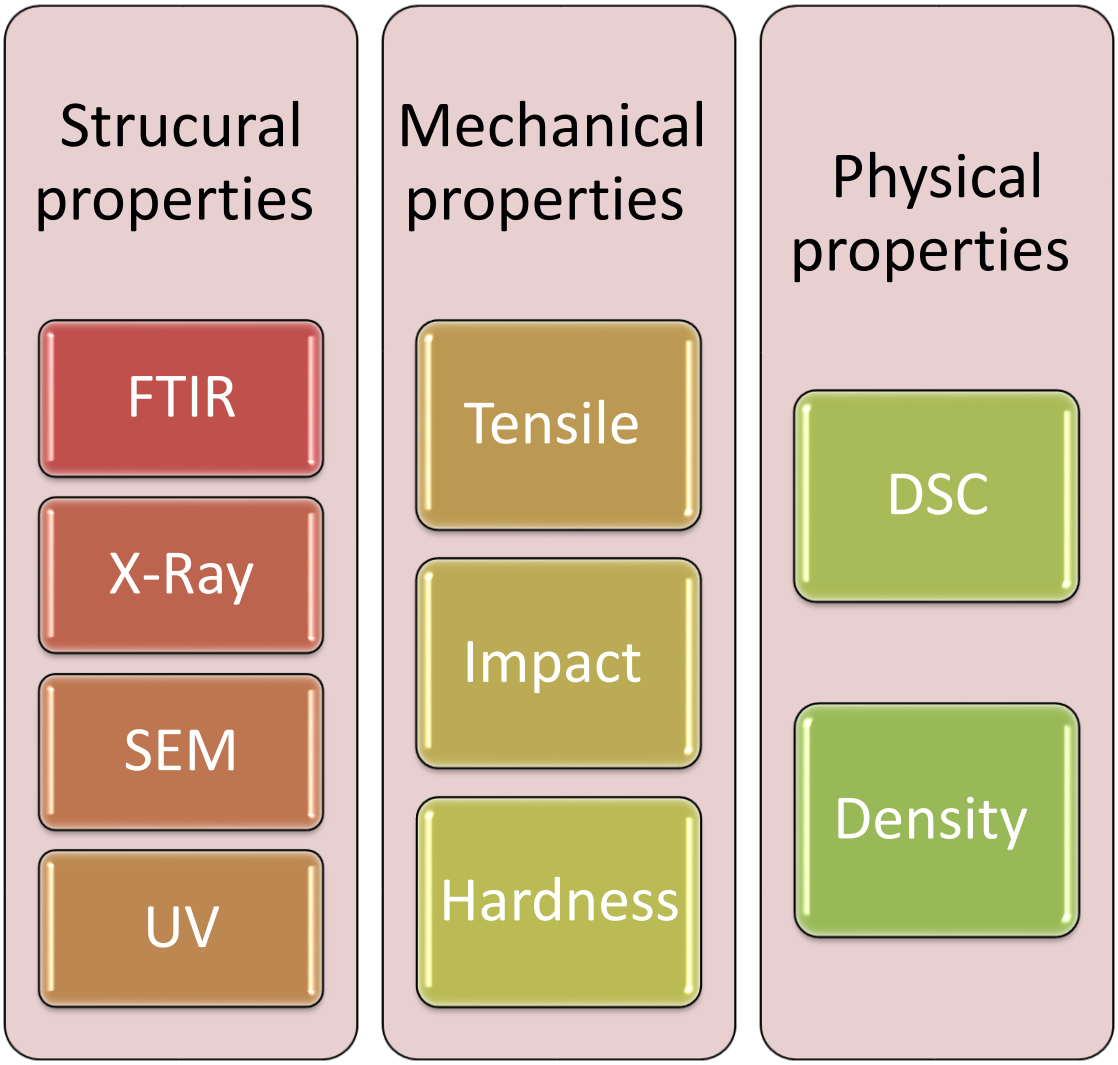

Figure(3.1) Shows Simple Schematic Procedure of the Experimental Work.

3.4 Structural Properties

3.4.1 Fourier Transform Infrared Spectrometry(FTIR)

In IR Spectroscopy the sample is prepared as a powder mixed with transparent material KBr with ratio 1:3.Then the mixture is well crushed. to receive homogeneous material, and compressed in a disc to reach its form to experiment. At the end of the test, the IR spectroscopy prepare a chart between transmittance and number of waves, showing chemical

structure of material then the graph is comparison to the standard scheme to differentiate the real material . This experiment takes place by using, (FTt-IR -OPUS -7.0 industrialization by shimadzn Company, the Figure (3.2)show the FTIR test instrument.

Figure (3.2) FTIR test Instrument.

3. 4. 2 X - Ray Diffraction Test (XRD):

Diffraction X-ray technique was utilized to specify the state of polymer, either crystalline, semi crystalline or amorphous , Also to see if 20% and 30% of carbon fibers cause an appearance in new peaks to note if chemical or physical reaction occurs between fibers and matrix. This test is executed by employing XRD 6000 instrument which made by (SHIMADZU)-japan as appear in Figure (3.3). Small pieces of the sheets

from virgin (PEEK), (PEEK+20%CF) and (PEEK+30%CF) are used as samples. At the end of the test, the XRD instrument provides a chart between intensity and 2θ showing the state of polymer and if carbon fibers cause in appearance new peaks.

Figure (3.3) XRD Instrument.

The degree of crystallinity or the region of crystalline diffraction peaks is determined from equation (3.1)[87].

$$\chi c = \frac{Ac}{Ac+Aa} \qquad (3.1)$$

χc : The degree of crystallinity .

Ac: The area of crystalline peaks of diffraction .

Aa: The area of amorphous peaks of diffraction.

3.4.3 Density Test

Density tests have been carried out about room temperature by using Matsu Haku High accuracy DENSITY TESTER G12OS , g/cm ^{3}.as shown in the Figure (3.4). According to the ASTM D-792,this test is used to measure the density according to Archimedes low. The Crystallinity Degree χc can be calculated by using the equation (3.2)

Knowledgeable the amorphous phase theoretical density ρa and the Crystalline phase theoretical density ρc, 1.263g/cm^3 and 1.400g/cm ^{3} respectively [88].

$$\chi c = \frac{\rho - \rho a}{\rho c - \rho a} \qquad (3.2)$$

Where Four percent is absolute uncertainty by considering $\Delta\rho a$, $\Delta\rho$, the theoretical values showed a value equal to zero.

χc : The degreee of crystallinity.

ρ : The density of Calculated in the laboratory.

ρa : The amorphous phase density.

ρc : The Crystalline phase density.

Figure(3.4) Density measurement device

3.4.4 Scanning electron microscopy(SEM)

Scanning Electron Microscope(SEM) and element analysis with Oxford Inca Energy 250X EDS system are used to provide microscopes with first class detectors also used to show the initial crack on the sample's surface based on the technology of synthetic crystals. The instrument (Tescan –company, model vega ii) is used in this test .Tescan detectors provide very fast and efficient solutions that enhance high imaging quality. Initially, the specimens were prepared by chopping up the fracturared sample into a rectangular block (5 ×5.6 ×15mm) and then a thin layer of sputter coating of gold a utilization sputter -coating unit (EM Technologies LTD company , UK). Samples are measured in Razi metallurgical research center of the Islamic republic in Iran.

Analytical scanning electron microscope (SEM), model (JEOL6400F) is used to examine the morphology of microspheres according to (ASTM 986-04).

3.4.5 Ultraviolet-visible spectrophotometer test

UV - Visible spectrophotometer is used, type UV- 1800, (Shimadzu-Japan) .The sample was placed in the device's quartz cell (1 cm). The aim of this test is to identify the permeability. Figure (3.5) show the UV test devise.

Figure (3.5) UV- Visible device

3.5 Mechanical properties

3.5.1 Tensile Test

This test was performed by using (Universal test machine model WAW-1000)china origin industry instrument .The tensile device applies load

range (40-400KN) with speed range (0.1-50 mm/min). This test was performed by using (Universal test machine model WAW-1000) instrument . A characteristic of polymers in the tensile diagrams relies on the dimensions and shape of the specimen. Figures (3.6),(3.7) show the specimens and instrument of tensile test which can be used for the testing depending on ASTM_638.

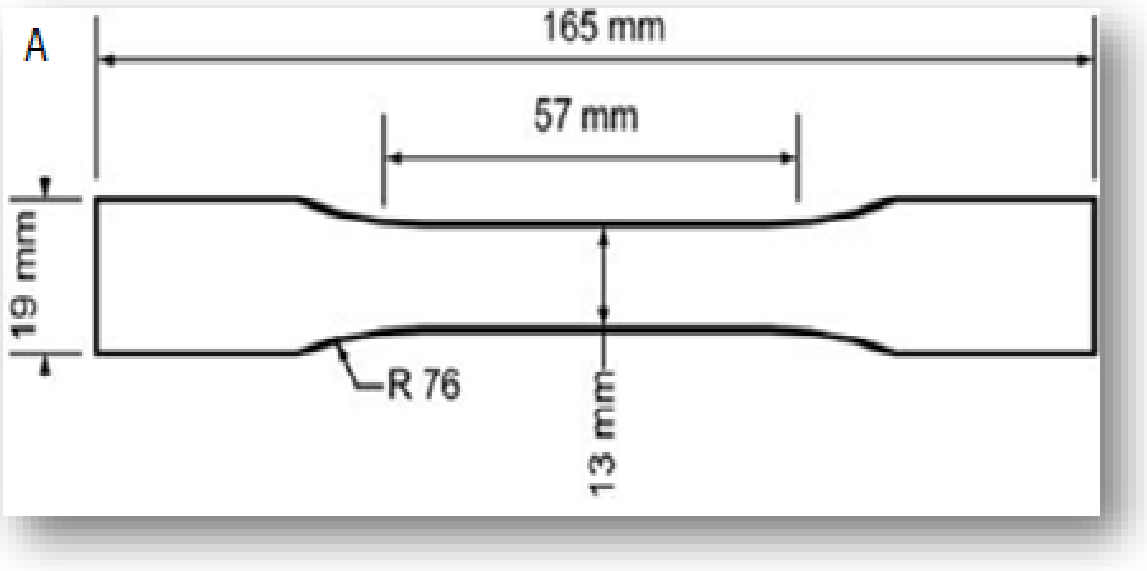

Figure (3.6) Tensile Schematic Specimen (ASTM D638)

Figure (3.7) Experimental Tensile Specimen

The test was conducted at room temperature. After the sample was fixed, load can be applied on it by making the upper grip moving handle up with a speed of (5mm/min), though stationary the lower grip was before failure happened. Then the relationship between Stress-Strain on a graph paper is obtained from the machine. The avarge of three samples is expressed by the result, Figure(3.8)show the tensile test instrument.

Figure (3.8) Tensile Instrument.

3.5.2 Impact Test

Decidedly, the impact testing has received attention ,Impact tests consist of be made up of striking an acceptable specimen with a blow that is regulated and measurement of the energy consumed by bending or

splitting the sample. The energy value shows the toughness of the substance being tested, The concept of "toughness" is one that most people can readily appreciate and a broadly accepted definition is the work done in breaking a test piece or object. It is one of the most common tests for determining the impact resistance of plastics. Notch and un- notch specimens are prepared according to ASTM D 256-87, the test was conducted about room temperature. Each energy value in this test represents the average of three samples.

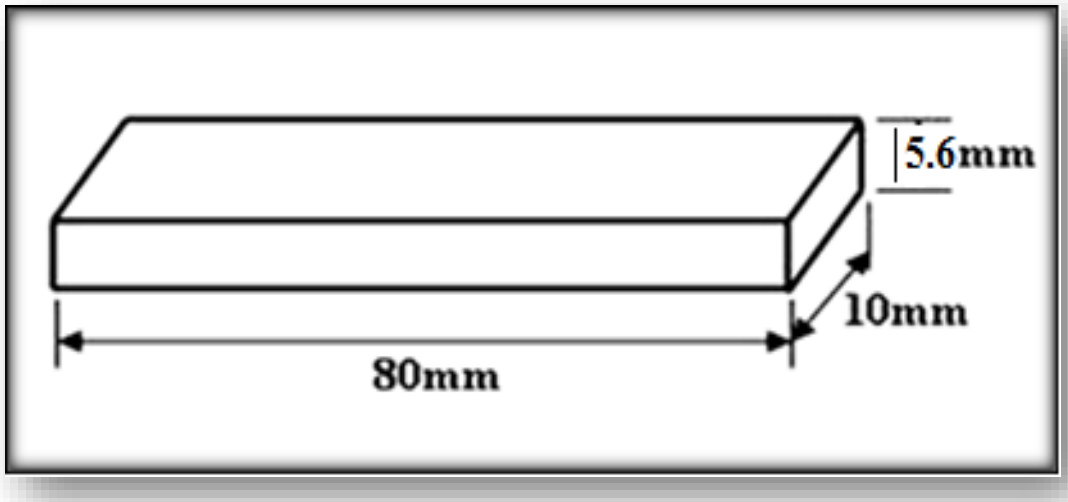

Figure (3.9): Impact Schematic Specimen without Notch (ISO 179)

In this test in a cantilever position, the specimen is placed. A pendulum's arm kicks the specimen. The energy consumed in the breaking process by the specimen is defined as a breaking energy. It is possible to calculate the breaking energy by joule unit. German pendulum impact tester, gant (HAMBURG)company , Model WP400 chirpy type as shown in Figure (3.10).

Figure (3.10) Impact Machine Used in the Test .

The impact energy and the toughness of fracture It was based on the measurement of the fracture energy required, following equation the impact strength were calculated .

Impact strength = (Fracture energy)/(cross section area)

3.5.3 Hardness Test

The hardness is generally understood as a modulus dependent calculation, From the material's resistance towards Blank space but was as well added to scratch resistance and resilience. Although hardness is included almost invariably, it is also commonly applicable to metals with rubber properties, Far less frequently, it has been used for plastics.

Shore Durometer (shore D)

Possibly the most common scale is in two of his primary variants, Shore A and Shore D respectively , as shown in the Figure(3.11), the Shore durometer hardness .Shore scales typically measure the hardness of

polymers (rubbers, plastics). For measuring soft elastomers (rubbers) and other soft polymers, the Shore A scale is used. Shore D scale calculation of the toughness of hard elastomers and most other forms of polymer materials (thermoplastics , thermosets). The common both shore variants are unified in ISO 868. Samples prepared according to this test are in compliance with ASTMD 2240 by employment Chinese Hardness Device , Model TH 200 for hardness measurements of (PEEK), (PEEK+20% CF), and (PEEK+30% CF). In this test, each value of hardness represents the average of the sample.

Fig (3.11) Hardness test device

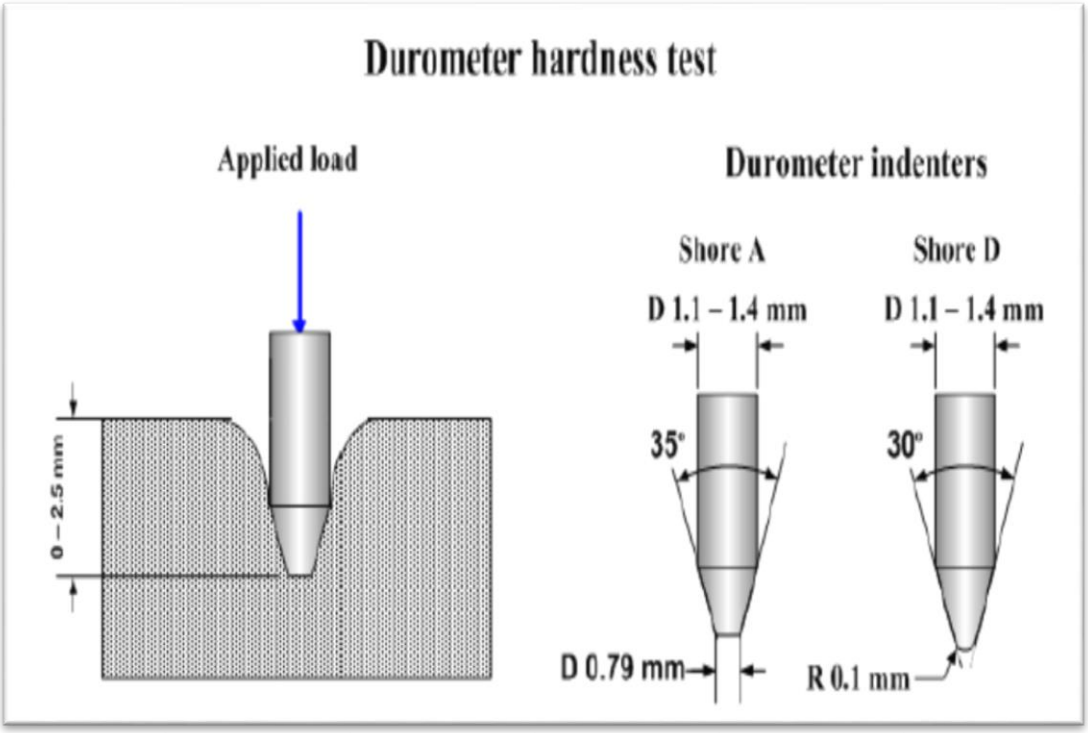

Figure(3 .12): Shore Durometer[89].

3. 6 Thermal properties:

3.6.1 Differential Scanning Calorimetry (DSC) Test:

A method which makes it possible for exploring Polymers' thermal behavior, The DSC system is made upp of two basic components, A chamber for measurements and a monitor, this makes it possible to regulate the temperature and to control the heat flow, Two pans are positioned in the measurement chamber :

1. The sample pan in which the examined sample is placed.

2. A reference pan that usually remains clean.

On the top of a heater, each pan is positioned. Via a computer interface, the heating rate of the two pans can be calculated ; it is normally set to 10 °C /min. In the two dishes, due to the different composition in the container, the adsorption of heat would be different. During the experiment, holding the temperature of the two pans steady. Either of the

two pans allows the machine more or less heat to provide. The DSC experiment's output is the extra amount of heat provided to keep the temperature of the two pans equal, to the pan. This test is used to calculate the physical properties of the thermos, including : melting temperature(Tm), glass transition (Tg) and crystallinity temperature Tc. The samples of (PEEK), (PEEK+20% CF), and (PEEK+30% CF) are prepared ASTM D3418-03and tested by using instrument (NETZSCH – model DSC F3Maia, pan Aluminum) as sown in Figure (3.13). The gas specification (N2 (50 ml /min) and heating levels 10ºC/min with heating range(20-380ºC).

Fig (3.13) DSC Test device.

The degree of crystallinity was calculated according to the following equation [90].

$$\chi c = \Delta H_{exp} / \Delta H^{*}. W_f \quad \textbf{(3.3)}$$

χc : The degree of crystallinity.

ΔH_{exp} : The experimental heat of fusion determined from DSC .

ΔH^{*} : The heat of fusion of fully crystalline PEEK 130J/g .

W_f : The weight fraction of PEEK in the blend.

Chapter Four

Results and Discussion

Chapter Four
Results and Discussion

4.1. Introduction

This chapter covers experimental findings, characterization test includes X-ray, FTIR, and SEM, where FTIR and XRD results show the chemical structure and nature of pure poly ether ether keton to note if a new peak appear when add 20% and 30%carbon fibers. Furthermore, there is a density test, This chapter also discusses mechanical results such as tensile, impact, and hardness, the emphasis of the thermal test is on (DSC) test to show the effect of 20% and 30% carbon fibers addition on crystallization level of pure PEEK, where Tg, Tm and Tc values of these materials that are calculated, mentioned later in this chapter.

4.2Characterization Test

4.2.1 FTIR Test

In general, the IR spectrum range (4000-400 cm^{1}) can be divided into two categories: The fingerprint area (1500-600 cm^{1}), as well as the functional groups region, which is divided into three sections: The triple-bond region (2500-2000 cm^{1}), and the double-bond region (2000-1500 cm^{1}), and the X–H stretching region (4000–2500 cm^{-1}). Figure 4.1 displays the FTIR spectrum and absorption band of virgin poly ether ether ketone. PEEK's main peak is C-O-C, which represents cyclic ether and has an absorption range of (900-1250), while C=O stretching represents ketone groups along the polymer backbone and has an absorption range of (900-1250). (1650-1740). The aromatic phenyl rings with absorption bands at (1497-1584) are defined by the C=C stretching, which agrees with Mizolo Ginette Kasiamat and B. Stuart [91,92].

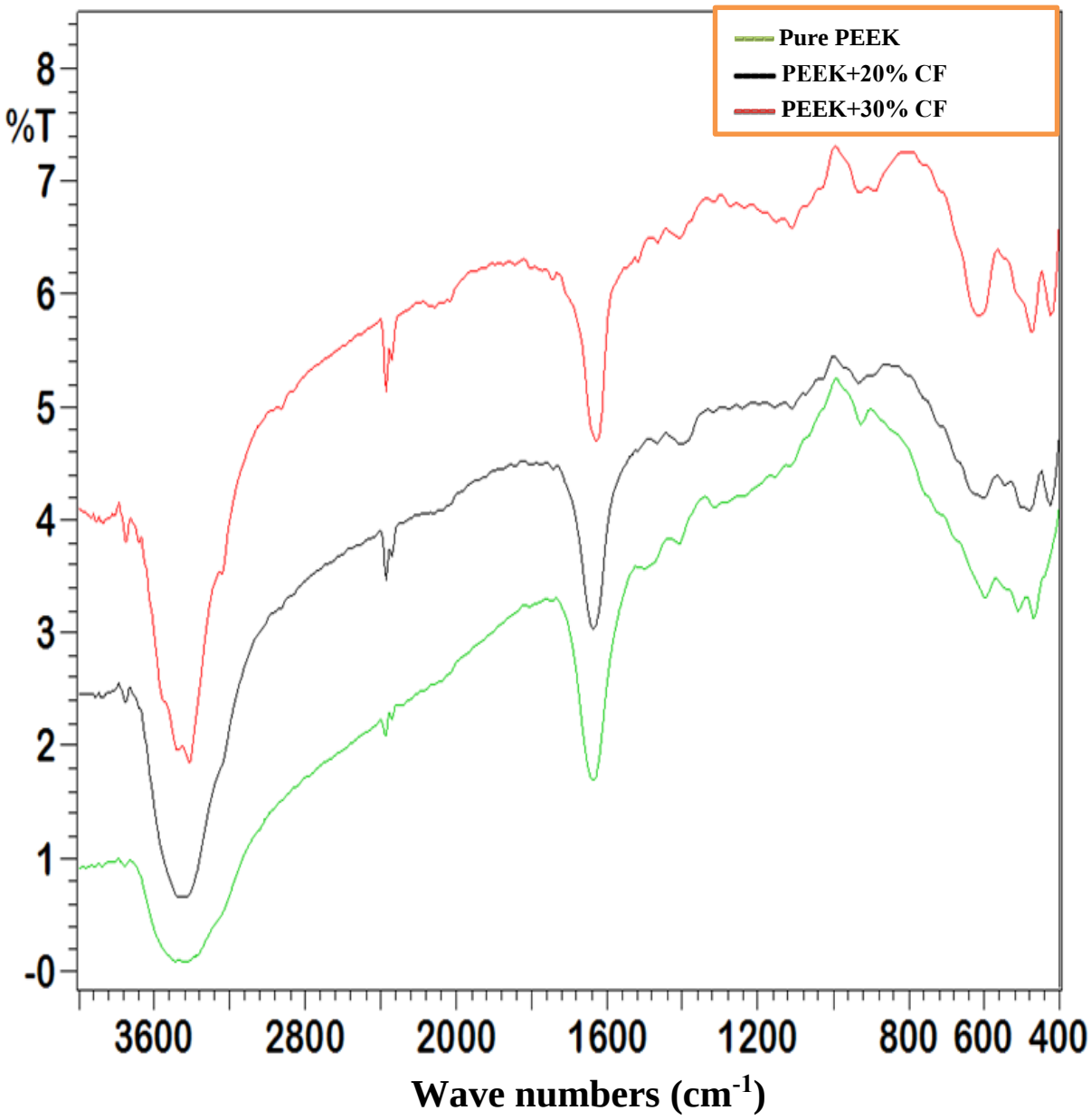

Figure(4.1): Show the FTIR Test for Pure PEEK and there composite

Figure (4.1) shows FTIR for (Pure) ,(PEEK+20% CF) and (PEEK+ 30% CF), respectively. It is found that the addition of 20% and 30% of carbon fiberss causes slightly shafting in peaks and does not result in the emergence of new peaks and this indicates that the fibers and the PEEK matrix do not react chemically, only physical reaction. Carbon fiber decreases the peak sharpness and it agrees with x-ray.

4.2.2 Density Test

For all samples, the density is measured using the Archimedes equation. The density of pure PEEK is 1.33 g / cm^{-3}, As PEEK is reinforced with carbon fiber with a different amount of weight, when reinforced by 20 % and 30 %, the density of PEEK will increase by 1.3375 g/cm^{-3} and 1.3838 g/cm^{-3} respectively. From equation (3.2), the degree of crystallinity χc is determined by understanding the theoretical density of the amorphous phase ρa and the crystalline phase ρ_c , respectively 1.263 g · cm^{-3} and 1.400 g .cm^{-3}, by considering Δρa and Δρc are theories values and tantamount to zero. The absolute uncertainty is 4 per cent. Crystallization for PEEK without carbon fiber addition was found to be about (35.9 percent), then the degree of crystallization will reach about (54.4 percent) when adding 20 percent carbon fiber, and more than 20 percent will reach about (54.4 percent) when adding 30 percent carbon fiber (88.2 percent). as shown in table (1).

Table (1) : Density and Calculated Crystallinity Degree by density for pure PEEK , PEEK+20% CF and PEEK+30%CF

Sample	Density (g/cm^{-3})	Xc
Pure PEEK	1.3122	35.9%
PEEK+20% CF	1.3375	54.4%
PEEK+30%CF	1.3838	88.2%

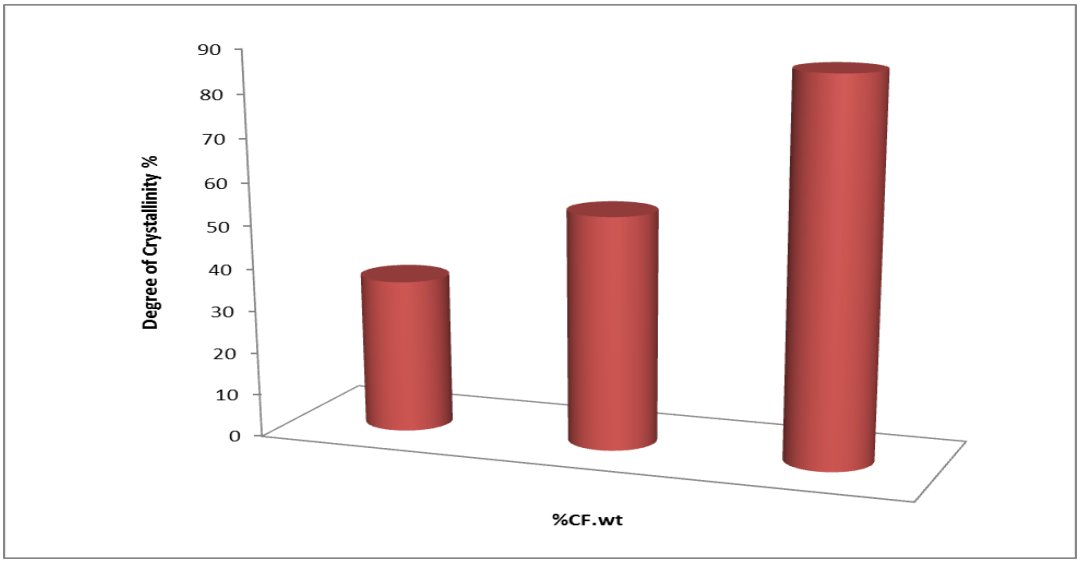

Figure (4.2): Show the degree of crystallinity of Pure PEEK , PEEK+20% CF, and PEEK+30% CF

4.2.3 DSC Test

It is necessary to understand the addition of fibers on the morphologyy of polymer matrix, DSC is used to show the effect of 20% and 30% of carbon fibers on pure poly ether ether ketone and thermal properties. Figure(4.3) shows thermal properties of pure poly ether ether ketone and the Figure (4.4),(4.5) show the polyetherether ketone filled with 20%,30% of carbon fiber respectively.

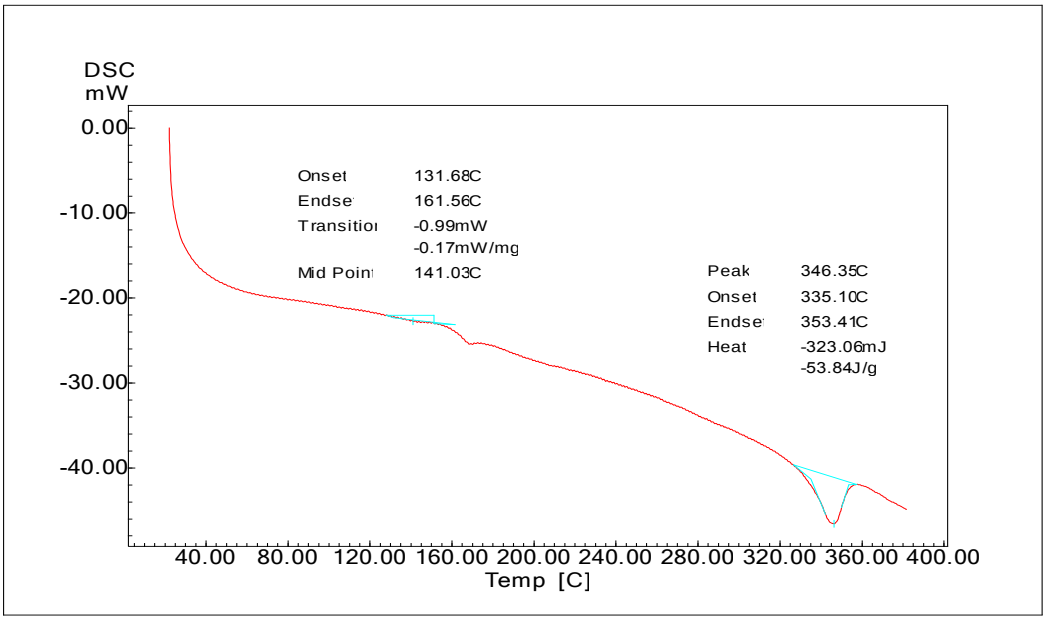

Fig (4.3) Show DSC for Pure PEEK

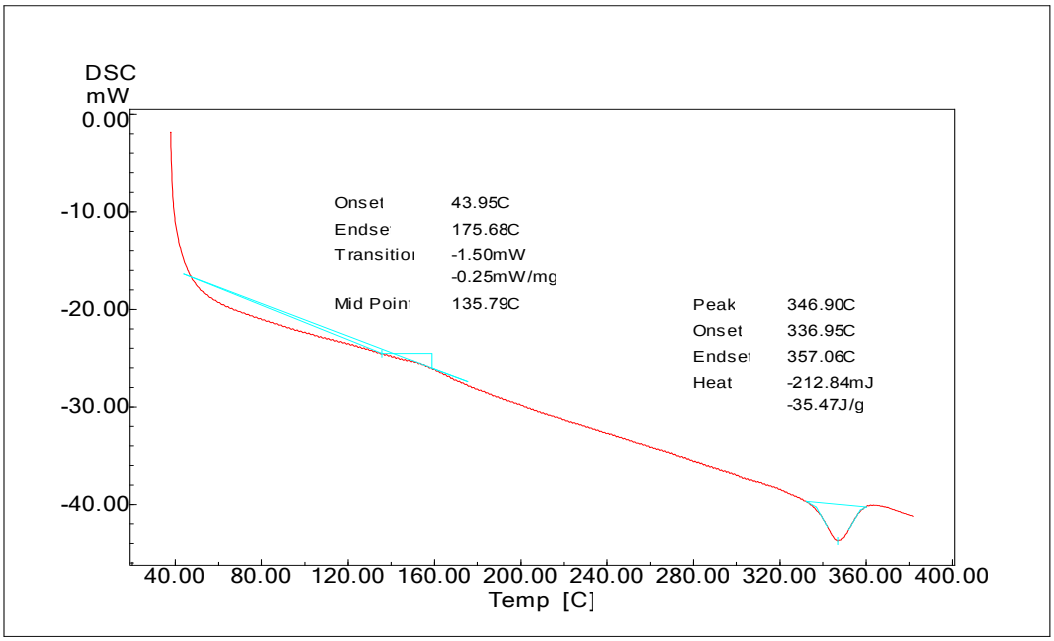

Fig (4.4) Show DSC for PEEK +20% CF

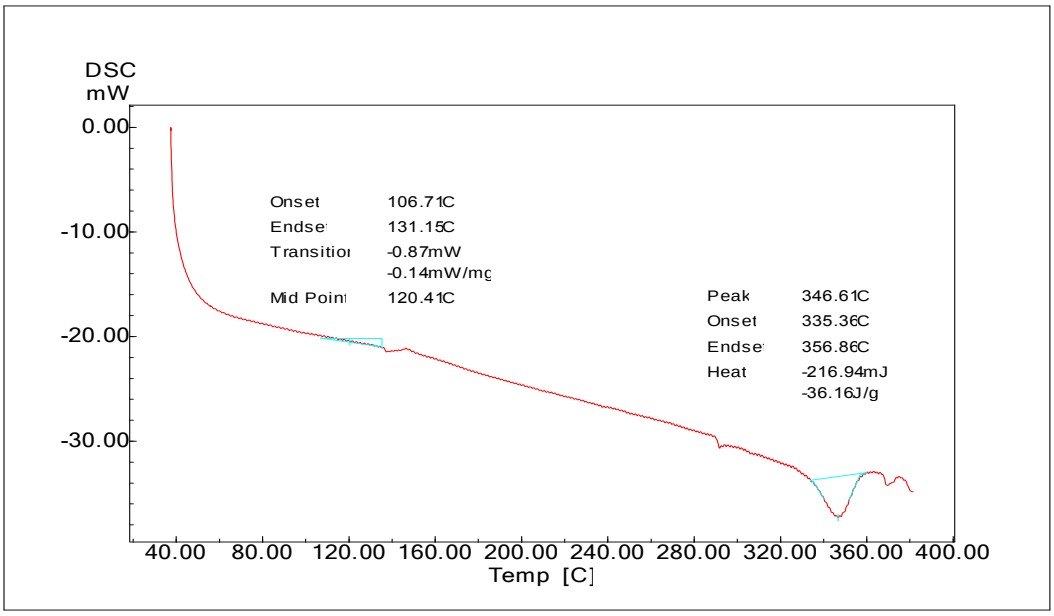

Figure(4.5) : Show DSC for PEEK+30%CF

Differential Scanning Calorimetry Characteristic temperatures , including the glass transition temperature , melting temperature ,hot crystallization temperature , and degree of crystallinity are measured by DSC for the sample as cleared in table (2).

Table(2):DSC for Pure PEEK,PEEK+20%CF,PEEK+30%CF

Sample	Tg(ºC)	Tm(ºC)	ΔH(mJ) (J/g)	Xc
Pure PEEK	141.03 ºC	346.35ºC	323.06 mJ 53.84 J/g	41.42 %
PEEK+20%CF	135.79 °C	346.90°C	212.84 mJ 35.47 J/g	21.83 %
PEEK+30%CF	120.41 °C	346.61°C	216.94 mJ 36.16 J/g	19.47 %

During the DSC examination, the degree of crystallinity decreased because the method of preparing the sample does not clearly show the effect of the fiber. The samples used in this test are small, fine particles which means that the sample is closer to the pure sample than the reinforced sample. Also, the heat cycle is not ideal for the PEEK sample it should be a complete heating and cooling cycle.

4.2.4 X-RAY test

X-ray test is used to show the chemical structure of virgin PEEK as shown in Figure (4.6), and to show if a new peak appears when 20% and 30% of carbon fibers are added .PEEK is a semi crystalline material and it is difficult to use X-ray to determine the crystallization of material therefor it is used to show the change in chemical structure and DSC is used to show the crystalline level of material. The results show that the addition20% and 30% of carbon fiber does not lead to the appearance of new peaks but only affects sharpness of peak where adding 20% and 30% of fiber increases peak sharpness as shown in figure (4.7) and (4.8),This is indicates that the occurrence of physical reaction causes this change in the peaks without the occurrence of chemical reaction and this

agrees with FTIR results. Note that in the pure PEEK polymer state, the degree of crystallinity is in proportion 61.9% , but when adding 20% of carbon fiber to pure polymer we will notice that the degree of crystalline will be equal to 76.8 % , And also the increase in the degree of crystallization continues to be 90% when adding of 30% carbon fiber to pure PEEK.

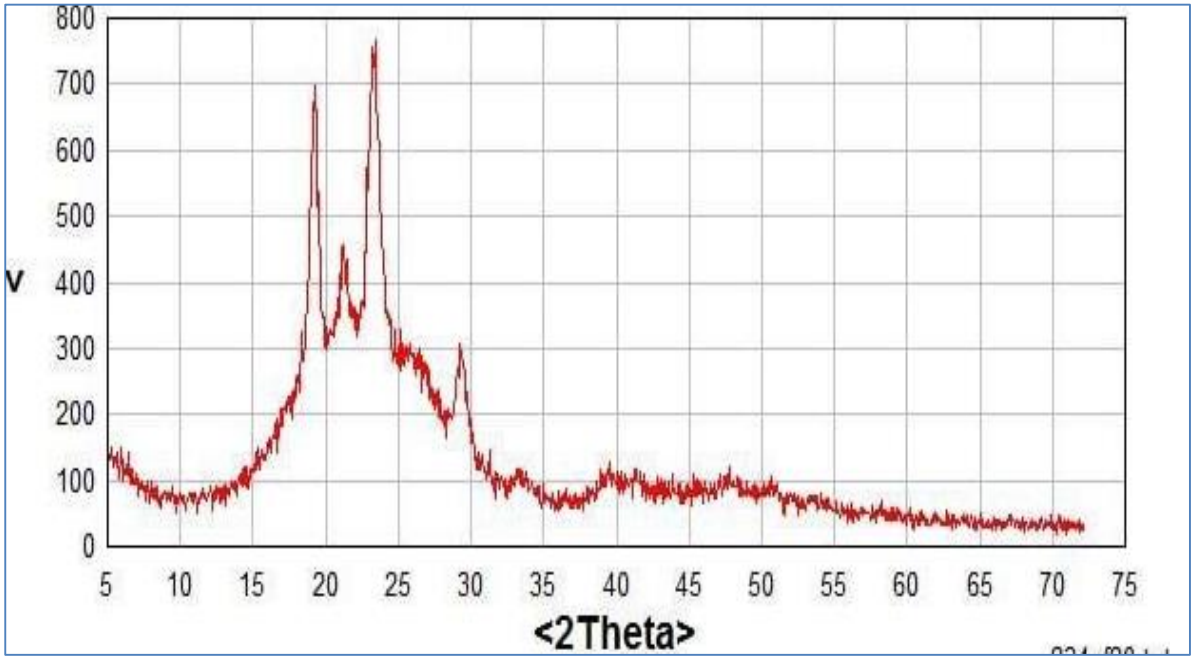

Figure (4.6) : Show the X-ray test for Pure PEEK

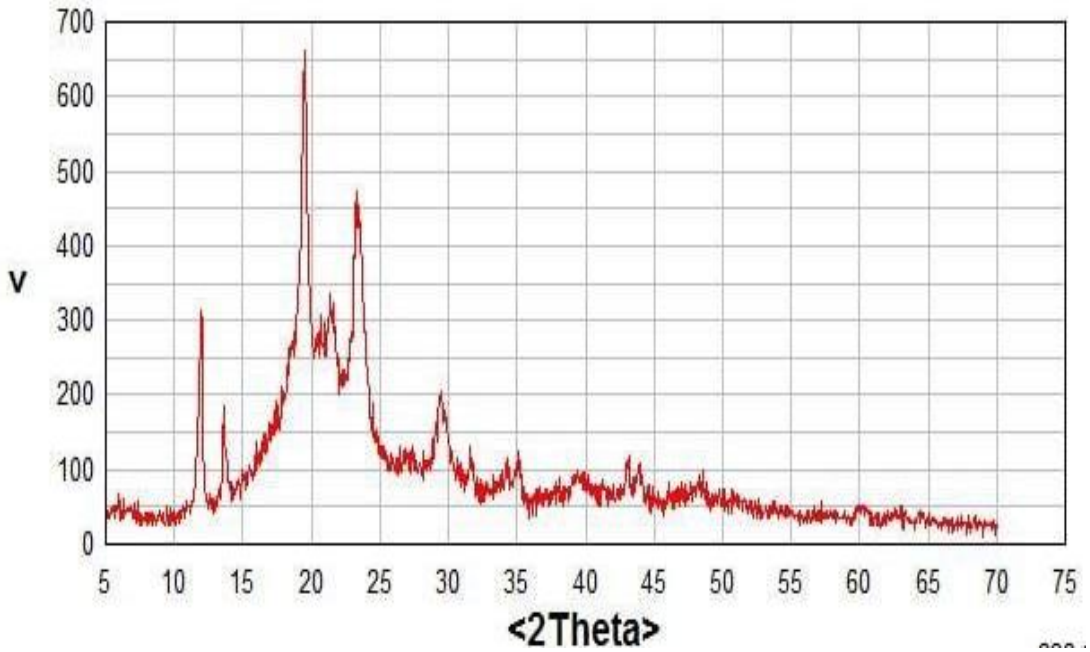

Figure (4.7) : Show the X-ray test for PEEK+20%CF

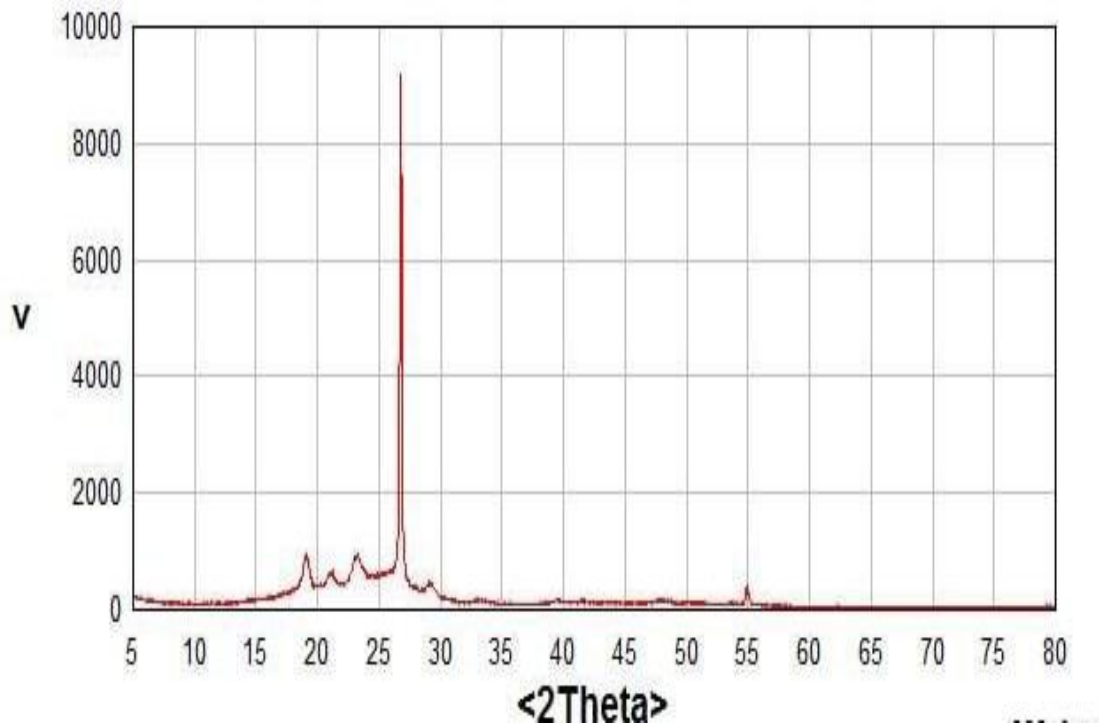

Figure (4.8) : Show the X-ray test for PEEK +30%CF

4.2.5 SEM Test

Figure(4.9),(4.10)and(4.11) represented SEM images in different magnification size (1micron),(100nm)and (200nm) for the different samples at the materials which were used in this study pure PEEK , PEEK+20%CF and PEEK+30%CF . the SEM is very important tools to evaluated the microstructure of the sample and its very accuracy to exam. The second phase or the phases inside of the materials and these phases with the pure materials. From the observe the three images of SEM for three different samples are (Pure PEEK ,PEEK+20%CF, and PEEK+30%CF). The images in the figure (4.11) it is very clear that the density of the second phase (fiber) is higher than the density in images at the Figures(4.9),(4.10).

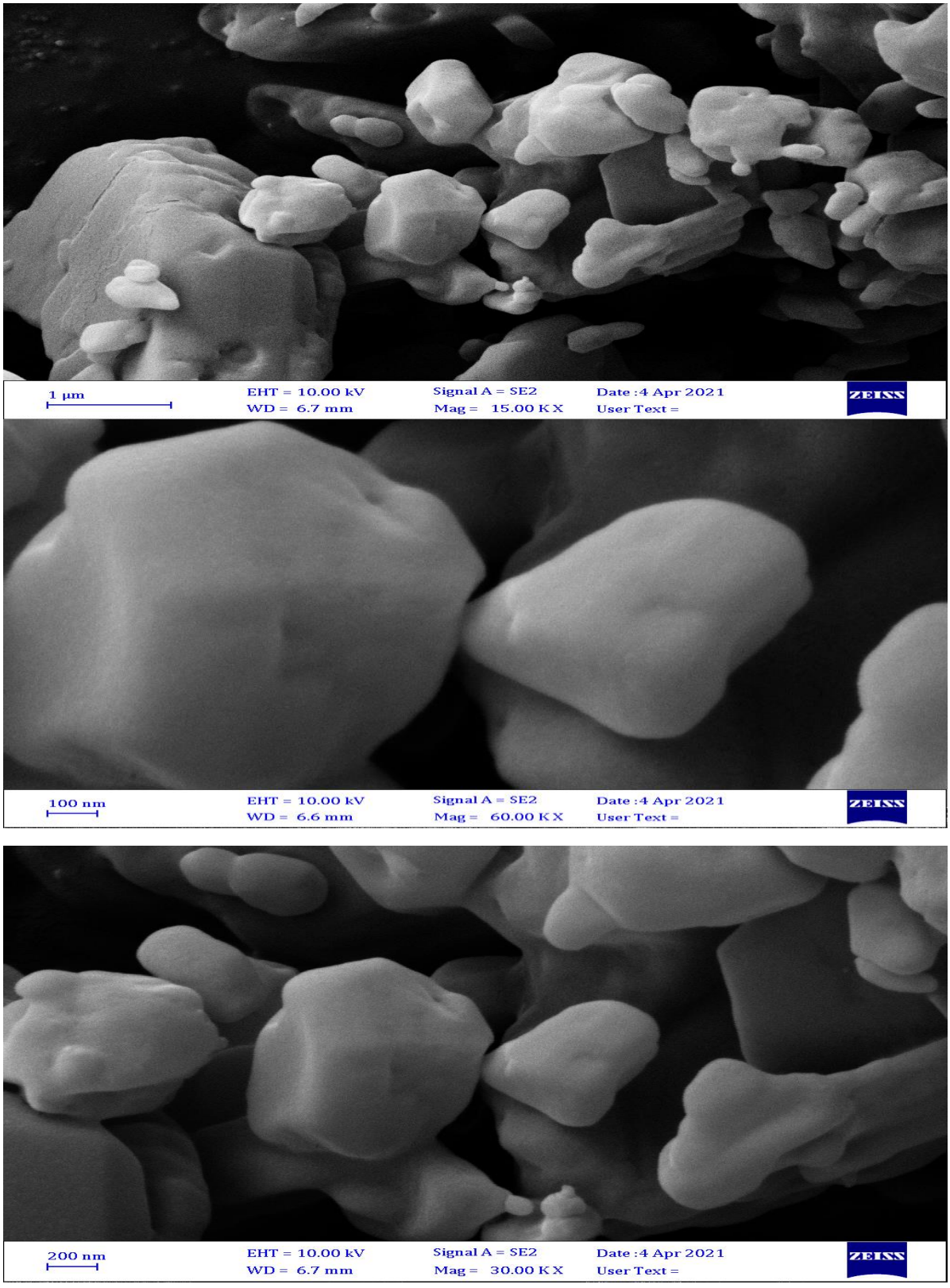

Figure(4.9):Show the SEM test for pure PEEK at different magnifications size

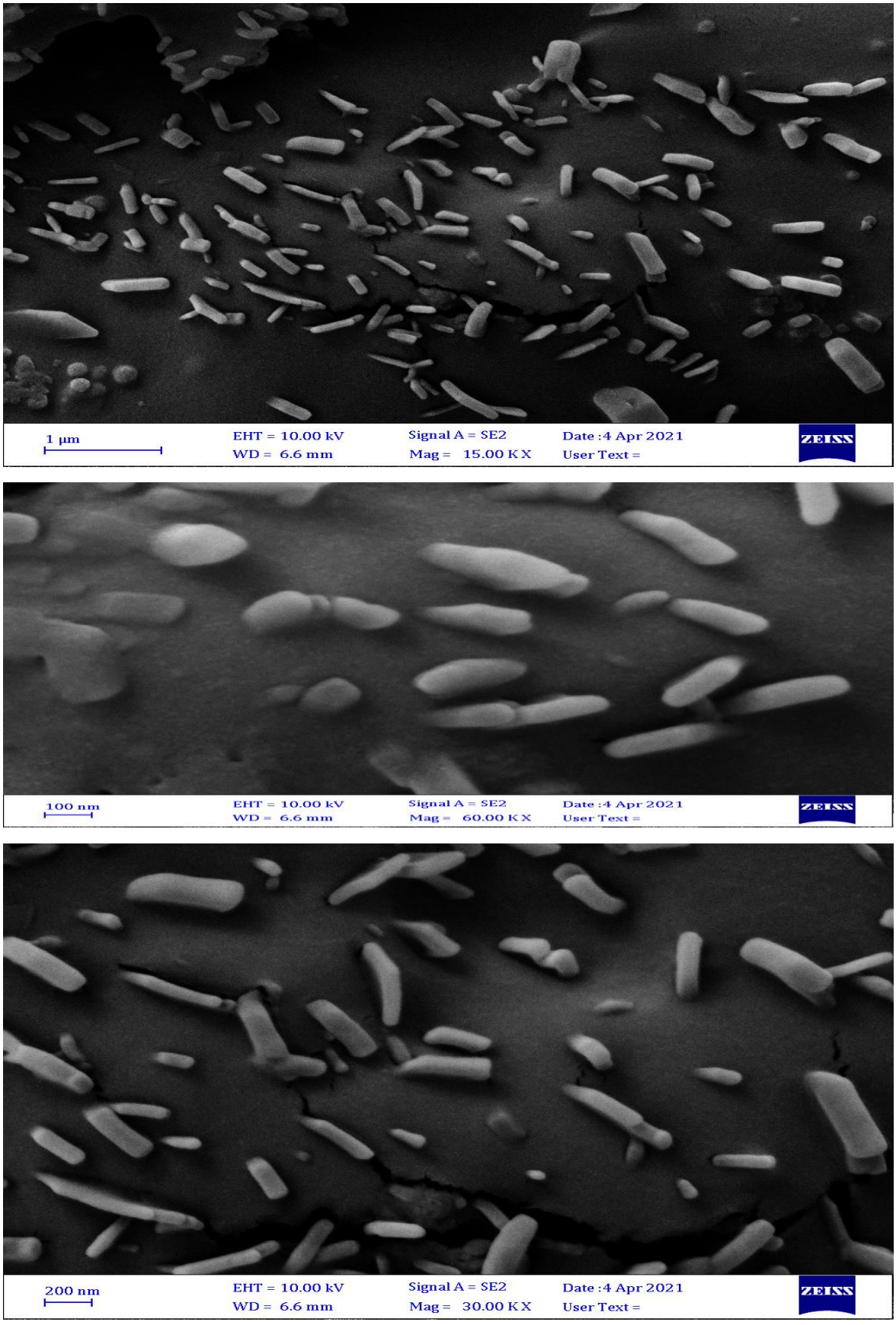

Figure (4.10) : Show the SEM test for pure PEEK+20%CF At different magnifications size

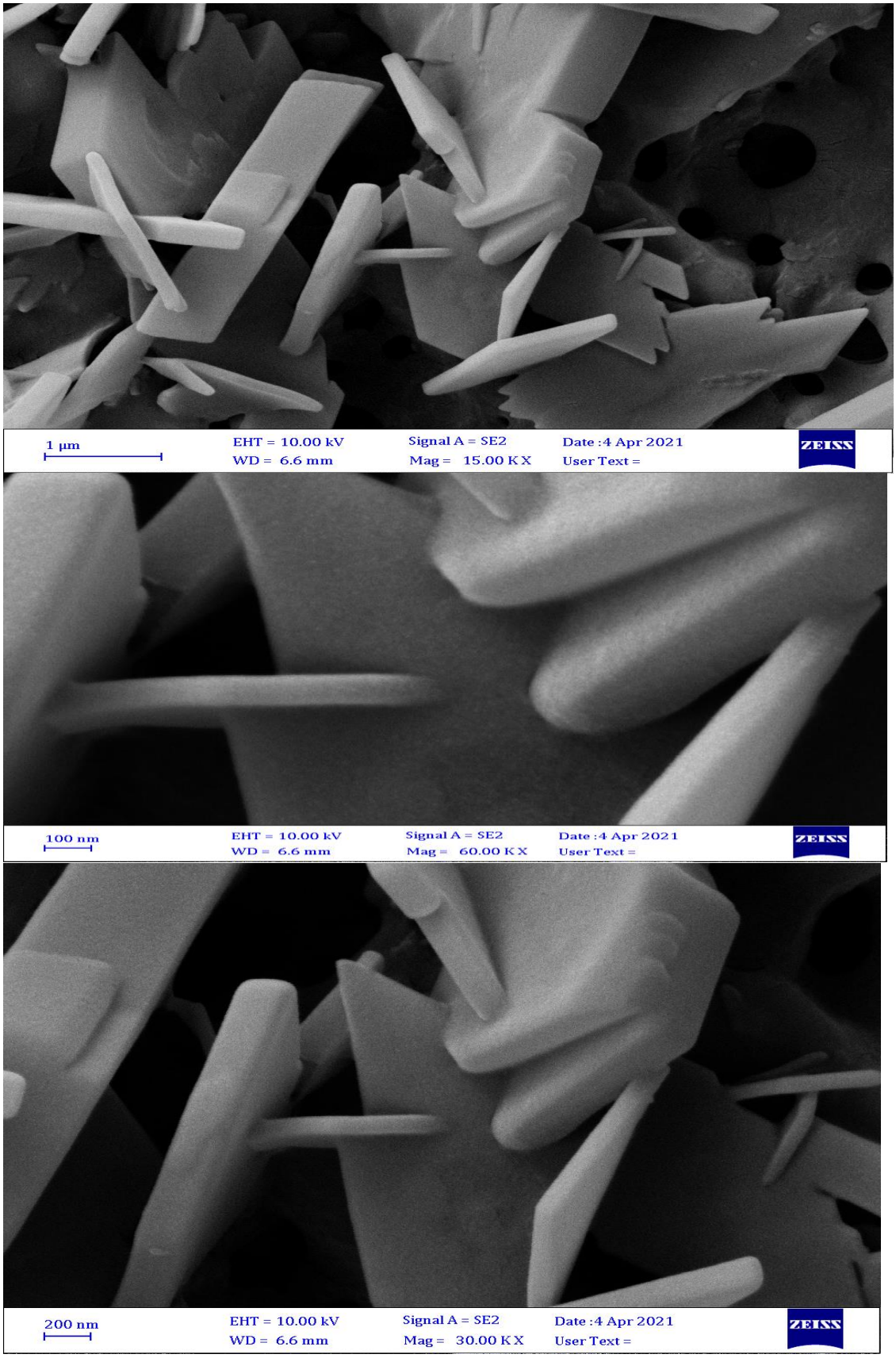

Figure (4.11) : Show the SEM test for pure PEEK+30%CF at different magnifications size

From the results , it can be conclusion that the crystallinity is higher in in Figure (4.11) which is (PEEK+30%CF) than the images (4.9),(4.10) which is that (Pure PEEK, and PEEK+20% CF) because of the increasing of carbon fiber content and it is very clear that the mixing of fiber in the matrix is very good , very uniform distribution , and that leads to uniformity at the crystallinity.

4.2.6 UV test

By following the results of the UV test , we note that the permeability increased with the increase in the percentage of carbon fibers, and this is definitely due to the presence of fibers inside the structure.

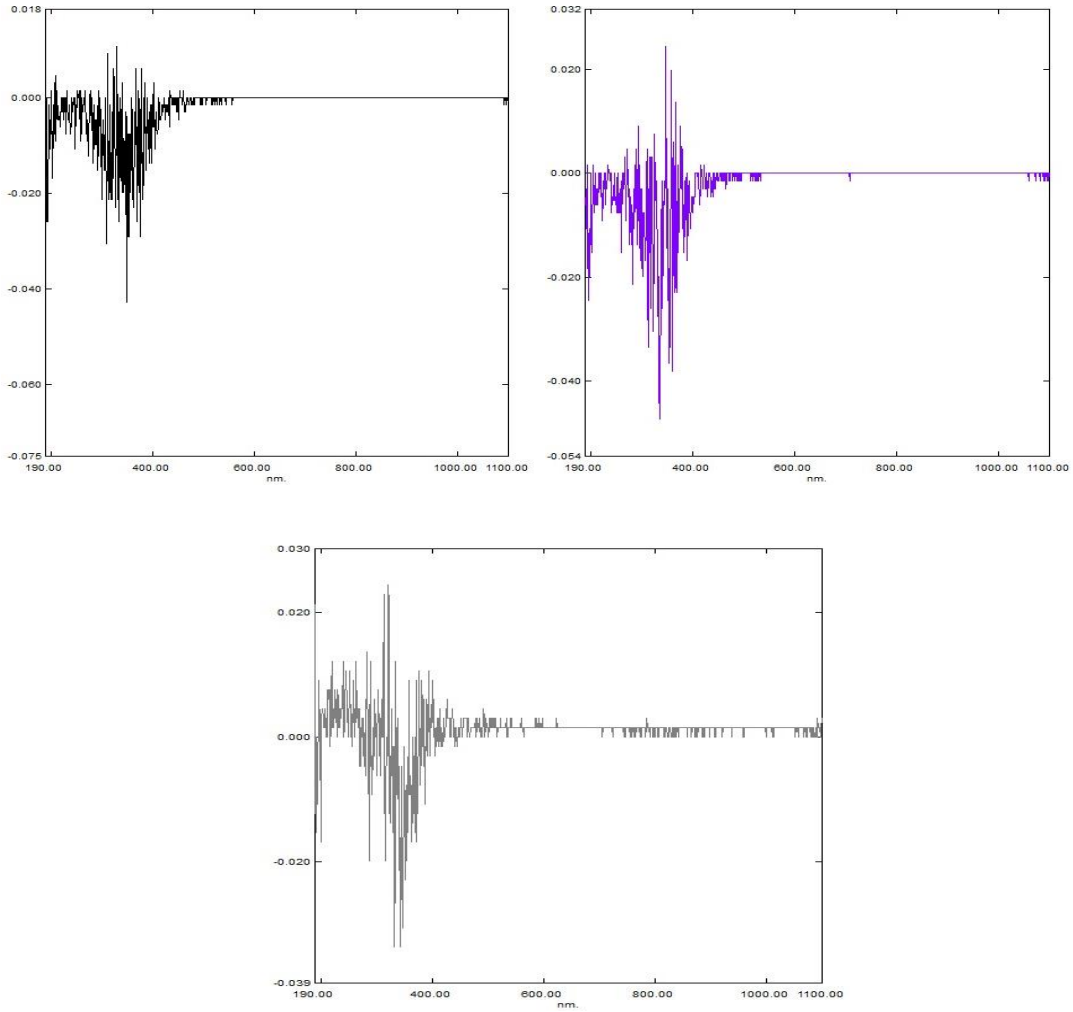

Figure(4.12): Show the UV test for Pure PEEK,PEEK+20%CF and PEEK+30%CF

The carbon fiber has a higher crystallinity than the crystalline of the base material,It means that it leads to the permeability in the interlayer regions, and thus the permeability increases for the sample as a whole . Therefore, the conclusion, that the examination of the UV can give a clear indication of the percentage of crystallization ; Because the percentage of crystallinity is a function of permeability, as the higher the permeability, the lower the crystallization rate. We can compare it with the previous methods IR ,DSC , X RAY and density where we note that it is consistent with the results DSC and FTIR .

4.3 Mechanical test

4.3.1 Tensile test

This test compares the pure PEEK and PEEK composites' tensile properties (tensile strength at Split in break, Young's modulus (E) and percentage of Elongation at break) reinforced with different weight percentages of 20% carbon fiber Percentage, 30 %. Percentage . Changing the proportion of the reinforcement weight, the tensile properties of composite substances under study are affected by many factors, such as the nature of the material for the matrix, type of reinforcement, volume fraction, and adherence between the matrix and the particles incorporated. The samples in the first part behave elastically from the above figures in the (stress-strain) curves (extension occurs in polymer chains without any bond rupture) and finally the behavior changes to plastic deformation (the deformation of polymeric material will lead to rupture in their bonding, and when the load stresses rise, growing cracks occur in polymer. The stress-strain curve of pure PEEK, 20wt. percent 30wt percent CF is represented in Figures (4.13),(4.14)and (4.15). From this figure, it can be noted that the increase in CF wt. The percentage contributes to an improvement in polymer composite tensile

strength values, so the neat PEEK transforms from (soft and strong) to (hard and strong) when the CF wt percent in the composite exceeds 30wt. percent.

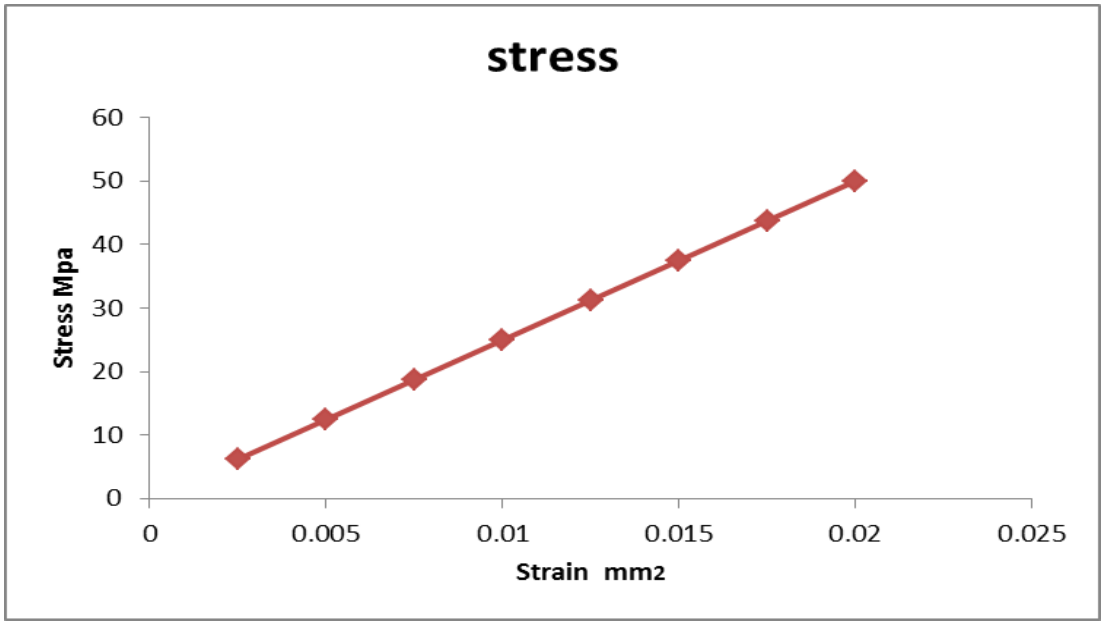

Figure (4.13): Curve of Stress –Strain for Pure PEEK

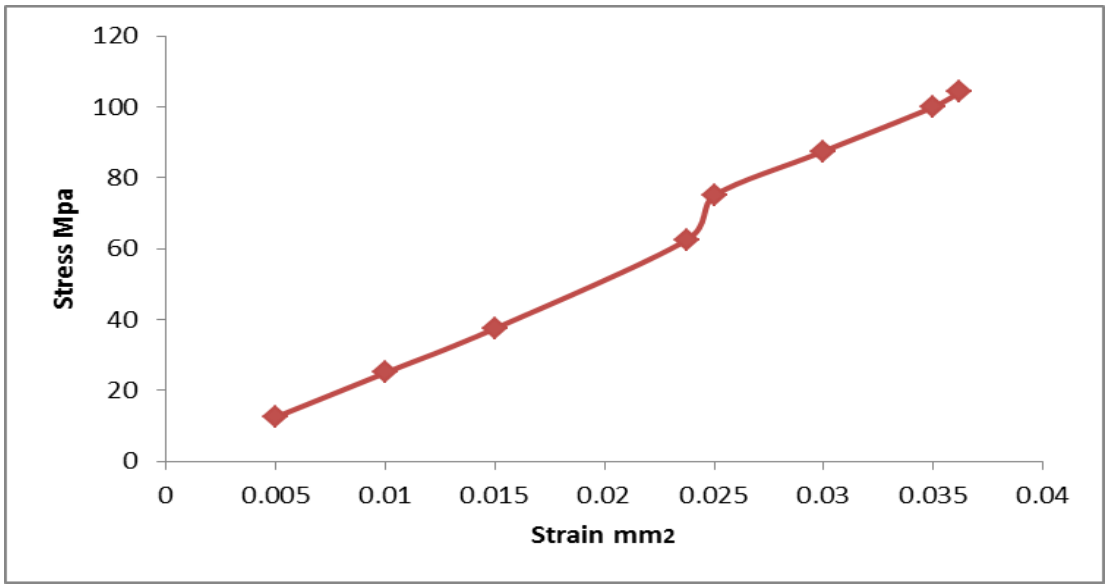

Figure (4.14): Curve of Stress-Strain for PEEK+20%CF

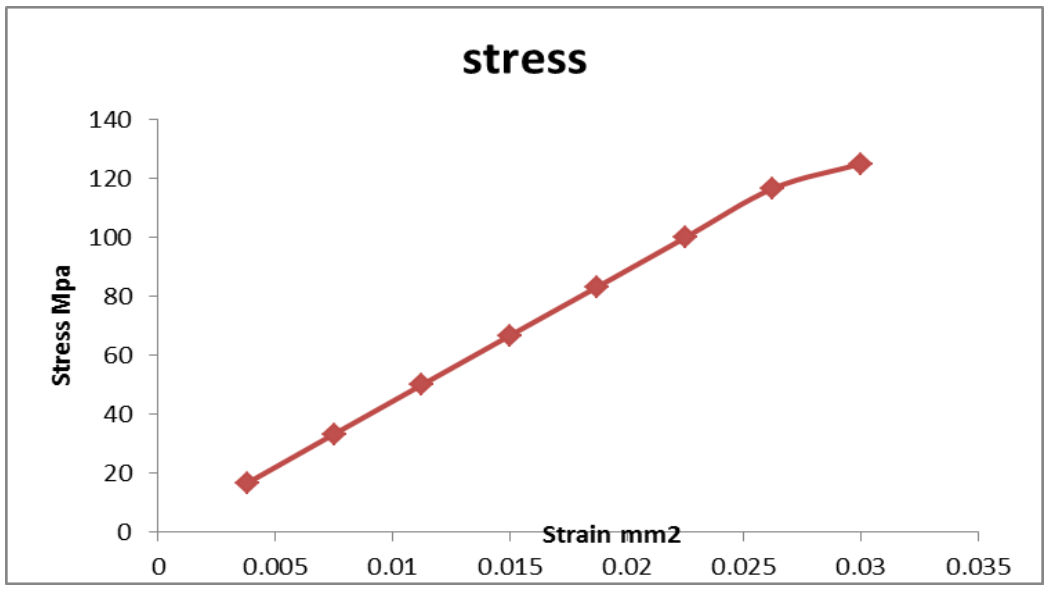

Figure (4.15): Curve of Stress-Strain for PEEK+30%CF

The average data from the results of the tensile tests, (tensile strength at break (σ), Young's modulus (E), and failure elongation (e) have been drawn. It appeared that the tensile strength and elastic modulus were increased with increasing the present of CF rising. For composites reinforced with 20% CF, the tensile strength 104.2 Mpa, for a composite reinforced with 30%, the addition of carbon fiber to polymer has increased the tensile strength and their value reached 124Mpa, and also the elastic modulus increase from 1.25 GPa for pure PEEK ,when reinforced with carbon fiber in 20% carbon fiber the elastic modulus increase to 2.8511GPa ,also increased with increase the percentage of carbon fiber to 30 % will be reaches to 4.4533 Gpa. The explanation for this outcome is owing to the successful bonding of the interface between the polymer matrix and carbon fibers, as well as the integration of strong fibers into the polymer matrix, resulting in limited polymer chain movement. This improves the stiffness of polymer composites, reduces plastic deformation and, for polymer composites, increases tensile strength and elastic modulus.

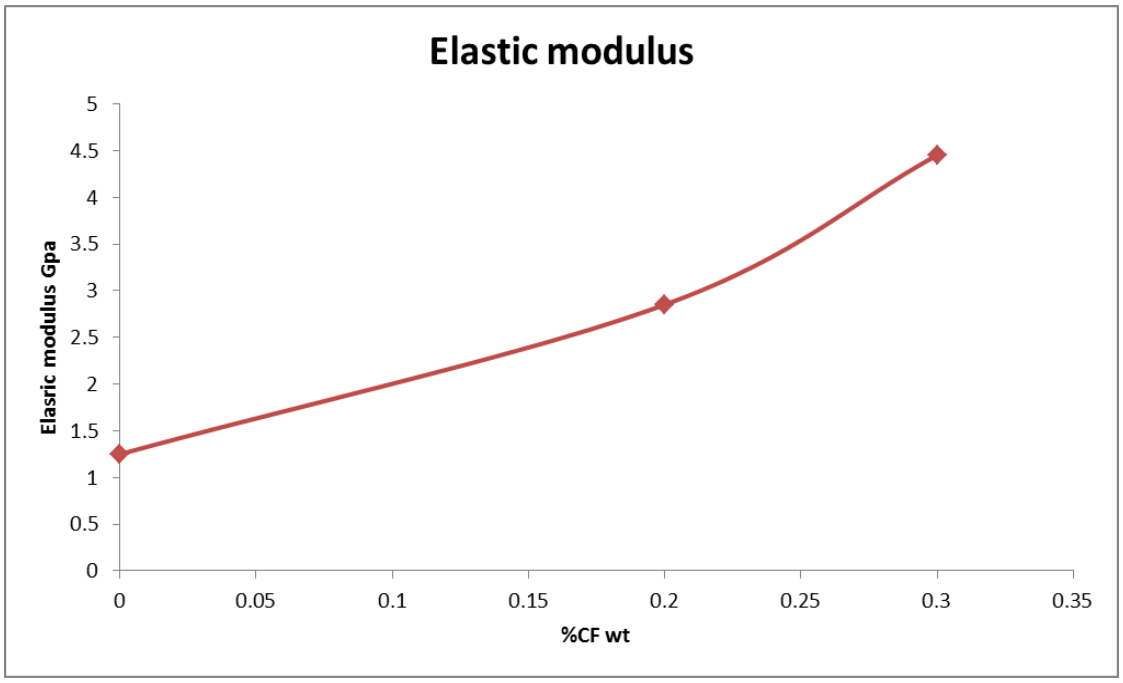

Figure (4.16): Show the Elastic modulus with Strengthening ratio for Pure PEEK,PEEK+20%CF ,PEEK+30%CF

4.3.2 Impact test

A resistance the material to the fracture under stresses that are applied at high velocity. Figure (4.17) shows the effect of percent of carbon fiber content on impact strength for PEEK . It can be observed from this figure, that impact strength of polymer composite has been increased with the addition of carbon fiber and reaching to the values (16.75) J/m^2 at 20% CF and reaching to the values (21.91) J/m^2 at 30% CF , when the impact strength for PEEK without Carbon fiber is about (9.180) J/m^2.

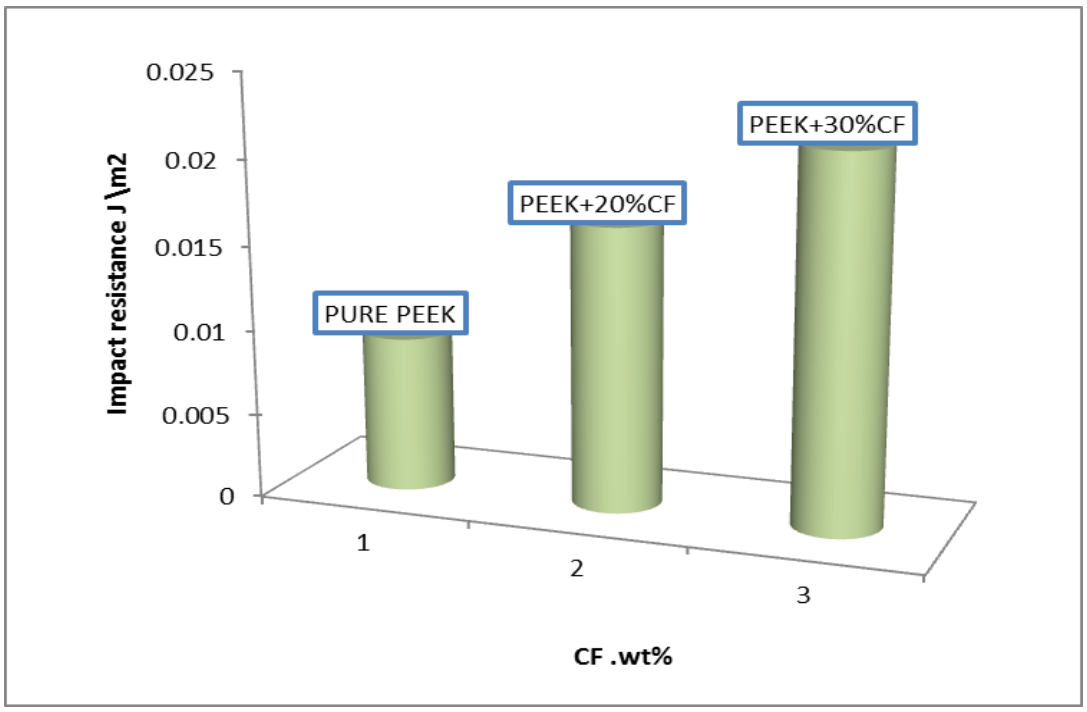

Fig (4.17) : Impact Strength of PEEK with different weight percentage of carbon fiber , for Pure PEEK,PEEK+20%CF, PEEK+30%CF

With the addition of the chosen carbon fiber weight percentage, a remarkable change in the impact strength of the polymer composites can be seen. So, the effect strength values have improved by 45.1 percent when 20 percent of carbon fiber content is compared to pure PEEK, and it also rises by 57.85 when it includes 30 percent carbon fiber.

4.3.3 Hardness test

As shown in figure (4.25), we observe that the reinforcement percentage by 20% carbon fiber for pure PEEK will lead to an increase in the hardness in the rate of 4.33% , and the continuity of the increase in hardness with 30% carbon fiber for pure PEEK also will lead to increase in the hardness in the rate of 5.6% . And that is attributed to homogeneous mixing and manufacturing method . The bonding between carbon fiber and poly ether ether ketone matrix is complex , carbon fiber is tough and overlapping within the polymeric matrix because it has greasy texture and thus results in stronger bonding and high hardness.

This means, that with the increase in the stiffening percentage, the strings describe with each other and be compact and their crystallinity is higher, and thus the voids decrease and the hardness increases.

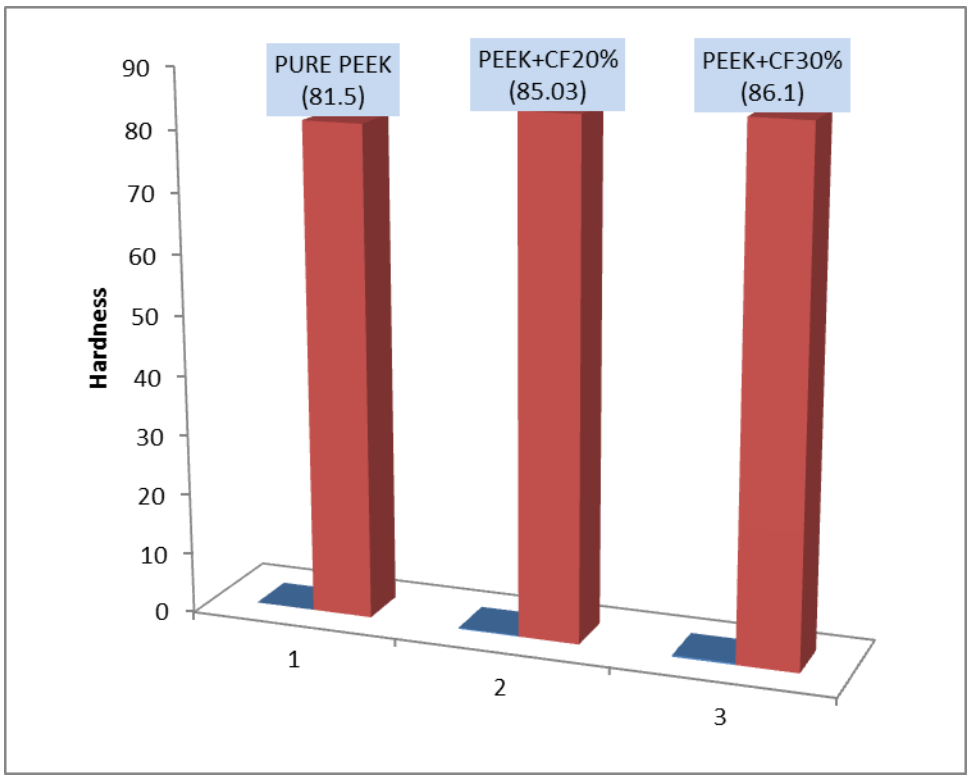

Fig (4.18) : Hardness of PEEK, PEEK+20%CF, and PEEK+30%CF

Chapter Five

Conclusions and Recommendations

Chapter Five

Conclusions and Recommendations

5.1 Introduction :

The most important conclusions and remarks which are obtained from this study are mentioned in this chapter, as well as some recommendations which are suggested , that may be useful for future research work.

5.2 Conclusions :

According to the results which were obtained and their discussion, the following conclusions were obtained regarding the effect of the reinforcement ratio on the crystallinity of the polymer, as well as other mechanical and physical properties:

1.Increase the percentage of crystallinity during examination x ray .

2. The mechanical properties (Tensile strength, Elastic modulus, Hardness and impact strength) increased clearly by 20% and 30% of carbon fiber reinforced composite .

3. Increase the degree of crystallinity during examination by using density for pure PEEK , PEEK+20% CF and PEEK+30%CF respectively.

4. Decrease in the degree of crystallinity of the composite material when increasing the percentage of carbon fibers during examination using DSC as well as UV test .

5. The permeability of the compounds was increased when increasing the percentage of reinforcement (carbon fiber), when examination by using UV Test.

5.3 Recommendations :

The recommendations for future work are:

1. Study the effect of another fibers in other ratios on the PEEK polymer and on the other polymers .

2. Studying the effect of shape and method of distribution for fibers and their effect on PEEK polymer and on their crystallization .

3. Studying crystalline behavior of other polymers , like PPS (Polyphenylene sulfide) and PEI (Polyethylenimine) with carbon fiber and another of fiber .

4. Manufacturing local composite material and study all properties that are used in this research and Comparison with the results as composite materials manufactured in China.

5. Studying the effect carbon fiber on the fatigue and wear behaviors for PEEK polymer.

6. Calculating the degree of crystallization in other tests , such as DTA Test.

Abstract

The aim of this work to study the effect of additives (fiber)on the crystallinity of Polyether ether ketone(PEEK) which is combined with carbon fiber as reinforcement because the degree of crystallinity plays an important role in semi-crystalline thermoplastics (such as toughness, stiffness and solvent resistance). Three sheets were used (pure PEEK, PEEK with 20% carbon fiber and PEEK with 30% carbon fiber).One of the most important tests used in this work is the density test, X-ray test, DSC and FTIR to investigate the different degrees of crystallization induced in PEEK composites reinforced with carbon fibers in different proportions. Density test results showed a rise in crystallization levels of (35.9%, 54.4%, 88.2%) respectively. X-Ray test results showed a rise in crystallization levels (61.9 % , 76.8 % 90 %) respectively. In FTIR test it is found that the addition 20% and 30% of carbon fibers causes slightly shift in peaks and does not result in the creation of new peaks and this indicates that the fibers and the PEEK matrix do not react chemically, only there is a physical reaction and the presence of carbon fiber decreases the peak sharpness . In the Mechanical properties such as tensile strength, Young's modulus, and Impact strength showed improvement in properties with an increase in reinforcement ratio with carbon fibers, but during the DSC examination, decrease in crystallinity when examined by DSC (41.42 %, 21.83 %, 19.47 %) respectively , the degree of crystallinity decreased because the method of preparing the sample does not clearly show the effect of the fiber, The samples used in this test are small, fine particles. which means that the sample is closer to the pure sample than the reinforced sample. Also the heat cycle is not ideal for the PEEK sample it should be a complete heating and cooling cycle.

List of Contents

Item	Title	Page
	Abstract	I
	List of contents	II
	List of English Symbols	V
	List of Greek symbols	VI
	List of Abbreviations	VII
	List of Figures	VII
	List of tables	X
Chapter One : Introduction		
1.1	General Introduction	1
1.2	The Aims of this work	3
Chapter Two: Theoretical Part and Literature Review		
2.1	Introduction	4
2.2	Morphology	5
2.2.1	Amorphous State	5
2.2.2	Crystalline state	5
2.2.3	Difference between amorphous and crystalline polymer	6
2.3	Crystallization Mechanisms	6
2.3.1	Solidification from the met	6
2.3.2	Crystal growth from the melt	7
2.3.3	Crystallization by stretching	7
2.3.4	Crystallization from solution	7
2.3.5	Confined Crystallization	7

2.4	Thermal and Mechanical properties	8
2.5	Optical property	8
2.6	Composite materials	9
2.6.1	Structure of composite material	9
2.6.1.1	Matrix Phase	10
2.6.1.2	Reinforcement phase	10
2.6.1.3	The Fiber –Matrix interfaced	10
2.6.2	Classification of Composite material	11
2.6.2.1	Polymer Matrix Composite (PMC)	11
2.6.2.2	Metal Matrix Composite (MMC)	11
2.6.2.3	Ceramic Matrix composite (CMC)	11
2.6.2.4	Carbone and Graphite Matrix	12
2.7	Polyetheretherketone(PEEK)	12
2.7.1	Introduction	12
2.7.2	Applications of Poly ether ether Ketone (PEEK)	14
2.7.2.1	PEEK Replaces Metal Tubing	14
2.7.2.2	Chemical Processing	15
2.7.2.3	Medical Applications	15
2.7.2.4	HPLC(High Performance Liquid Chromatography)	15
2.7.2.5	Aerospace application	16
2.7.3	Poly ether ether ketone Matrix	16
2.8	Reinforcing materials	16
2.8.1	Carbon fiber	16
2.8.2	Effects of fillers on structure and properties	17
2.9	Literatures Review	19
	Chapter three: Experimental Work	

3.1	Introduction	26
3.2	Materials Used in the study	26
3.3	Procedure of the work	26
3.4	Structural Properties	27
3.4.1	FTIR(Fourier Transform Infrared Spectrometry)	27
3.4.2	X-Ray Diffraction(XRD)Test	28
3.4.3	Density Test	30
3.4.4	SEM Test	31
3.4.5	UV Test	32
3.5	Mechanical properties	32
3.5.1	Tensile Test	32
3.5.2	Impact Test	34
3.5.3	Hardness(Shore D)	34
3.6	Thermal properties	38
3.6.1	DSC Test	38
	Chapter Four: Results and Discussion	
4.1	Introduction	41
4.2	Characterization test	41
4.2.1	FTIR test	41
4.2.2	Density test	43
4.2.3	DSC test	44
4.2.4	X-RAY test	46
4.2.5	SEM test	48
4.2.6	UV test	52
4.3	Mechanical test	53
4.3.1	Tensile test	53

4.3.2	Impact test	56
4.3.3	Hardness test	57
	Chapter Five: Conclusions and Recommendations	
	5.1 Conclusions	59
	5.2 Recommendations	60
	References	61

List English Symbols

Symbol	Description	Unit
A	Cross– sectional Area of specimen	m^2
Aa	The area of amorphous peaks of diffraction	
Ac	The area of Crystalline peaks of diffraction	
E	Modulus of Elasticity or Young's Modulus	Gpa
Gc	Impact Strength of Material	J/m^2
H	Hardness	--
Kc	Fracture Toughness of Material	$MPa.m^{1/2}$
Tc	Crystallization Temperature	^oC
Tg	Glass Transition Temperature	^oC
Tm	Melting Temperature	^oC
Uc	Impact Energy	J

List of Greek Symbols

Symbol	Description	Unit
χc	The degreee of crystallinity	%
ρ	Density	$g .cm^{-3}$
ρa	The amorphous phase density	$g . cm^{-3}$
ρc	The Crystalline phase density	$g .cm^{-3}$

List of Abbreviations

Character	Item
PEEK	Polyetheretherketon
ASTM	American Society for Testing Materials
CF	Carbon fiber
CMC	Ceramic Matrix Composite
DSC	Differential Scanning Calorimetry
HPLC	High Performance Liquid Chromatograph
PMC	Polymer Matrix Composites
SEM	Scanningg electron microscopy
MMC	Metal Matrix Composite
CGM	Carbon and Graphite Matrices
FTIR	Fourier transform infrared
UV	Ultraviolet
XRD	X-Ray Diffractionn
PPS	Polyphenylene sulfide
PEI	Polyethylenimine

List of Figures

Figure No.	Subject	
Chapter one	**Introdution**	
1.1	Offer a semi crystalline polymer structure	2
Chapter two	**Introdution**	
2.1	Composite Materials Structure	10
2.3	Poly(oxy-1,4-phenyleneoxy-1,4-phenylenecarbonyl-1,4 phenylene) (PEEK)	13
Chapter three	**Experimental Work**	
3.1	Shows Simple Schematic Procedure of the Experimental Work.	27
3.2	FTIR Instrument	28
3.3	XRD Instrument	29
3.4	Density measurement device	31
3.5	UV- Visible device	32
3.6	Tensile Schematic Specimen (ASTM D638)	33
3.7	Experimental Tensile Specimen	33
3.8	Tensile Instrument	34
3.9	Impact Schematic Specimen without Notch	35
3.10	Impact Machine Used in the Test	36
3.11	Hardness test device	37
3.12	Shore Durometer	38
3.13	DSC Test device	39
	Chapter Four Results and discussion	

4.1	Show the FTIR Test for Pure PEEK and there composite	42
4.2	Show the degree of crystallinity of Pure PEEK , PEEK+20% CF, and PEEK+30% CF	44
4.3	Show DSC for Pure PEEK	44
4.4	Show DSC for PEEK +20% CF	45
4.5	Show DSC for PEEK+30%CF	45
4.6	Show the X-ray test for Pure PEEK	47
4.7	Show the X-ray test for PEEK+20%CF	47
4.8	Show the X-ray test for PEEK +30%CF	48
4.9	Show the SEM test for pure PEEK at different magnifications size	49
4.10	Show the SEM test for pure PEEK+20%CF At different magnifications size	50
4.11	Show the SEM test for pure PEEK+30%CF at different magnifications size	51
4.12	Show the UV test for Pure PEEK,PEEK+20%CF and PEEK+30%CF	52
4.13	Curve of Stress –Strain for Pure PEEK	54
4.14	Curve of Stress-Strain for PEEK+20%CF	54
4.15	Curve of Stress-Strain for PEEK+30%CF	55
4.16	Show the Elastic modulus with Strengthening ratio for Pure PEEK,PEEK+20%CF ,PEEK+30%CF	56
4.17	Impact Strength of PEEK with different weight percentage of carbon fiber , for Pure PEEK,PEEK+20%CF, PEEK+30%CF	57
4.22	Hardness of PEEK, PEEK+20%CF, and PEEK+30%CF	58

List of Tables

Table No.	Subject	
(1)	Density and Calculated Crystallinity Degree by density for pure PEEK , PEEK+20% CF and PEEK+30%CF	43
(2)	DSC for PurePEEK,PEEK+20%CF,PEEK+30%CF	46

A comparative study of the crystallinity of Polyetheretherketone by using density, DSC, XRD, and Raman spectroscopy techniques

M. Doumeng, L. Makhlouf, Florentin Berthet, O. Marsan, K. Delbé, Jean Denape, F. Chabert

Polymer Testing 93 (2021) 106878

Contents lists available at ScienceDirect

Polymer Testing

journal homepage: http://www.elsevier.com/locate/polytest

A comparative study of the crystallinity of polyetheretherketone by using density, DSC, XRD, and Raman spectroscopy techniques

M. Doumeng [a], L. Makhlouf [a], F. Berthet [c], O. Marsan [b], K. Delbé [a,*], J. Denape [a], F. Chabert [a]

[a] Laboratoire Génie de Production (LGP), Université de Toulouse, INP-ENIT, Tarbes, France
[b] CIRIMAT, Université de Toulouse, INP-ENSIACET, Toulouse, France
[c] Institut Clément Ader (ICA), Université de Toulouse, École des Mines, Albi, France

ARTICLE INFO

Keywords:
PEEK
Degree of crystallinity
Density
DSC
XRD
Raman spectroscopy

ABSTRACT

A comparative study of the crystallinity of Polyetheretherketone by using density, DSC, XRD, and Raman spectroscopy techniques.

In this work, the microstructure of Polyetheretherketone is first analyzed with usual techniques such as density, Differential Scanning Calorimetry, X-ray Diffraction, and secondly, compared with Raman Spectroscopy. Assessing the degree of crystallinity of PEEK is challenging because of the different interpretation of the crystallinity according to each technique. The density measurement gives the highest most trusted absolute uncertainty for the degree of crystallinity, around 4%, compared to the other techniques. The Differential Scanning Calorimetry, usually used by the polymer community, overestimates up to 18% the degree of crystallinity due to a competitive phenomenon between crystallization and melting of PEEK over the same temperature range, and a fast crystallization. When Analyzing the X-ray Diffraction data, the degree of crystallinity is underestimated up to 11% as a consequence of the broad amorphous halo. Lastly, our investigation proves that Raman microspectroscopy is appropriate to determine the local crystallinity on the sample surface and compares 18 indicators in the same study. The 1651 cm^{-1} band shift has the highest correlation coefficient of 0.92 with the degree of crystallinity determined by density. This work attempts to correlate the results of degree of crystallinity of PEEK obtained by these four techniques in order to establish the best evaluation of this fundamental property for numerous applications.

1. Introduction

Polyetheretherketone (PEEK) is a high-performance thermoplastic widely used as a matrix in the growing thermoplastic composite industry. Launched in the '80s by Imperial Chemical Industries, PEEK is still a promising material because of its inert response to chemical reagents and heat resistance, highly elastic modulus and durability in thermo-oxidative conditions. PEEK is synthesized from biphenyl (hydroquinone) and fluorinated aromatic compound in a polar aprotic solvent (diphenyl sulfone). The fluorinated derivatives are privileged for this synthesis for their better reactivity and higher electronegativity than chlorinated derivatives [1]. The chemical reaction is a nucleophilic substitution obtained by polycondensation between 200 °C and 400 °C. The resulting compound, PEEK, is a copolymer composed of ether and ketone groups, as seen in Fig. 1. The ether/ketone ratio units remain equal to two, even if the order of appearance of monomers in the macromolecular chain differs [1]. The molecular weight varies between 3500 and 50 000 $g.^{-1}$ [2]. Short molecular chains have higher molecular mobility which favors the crystallization [3].

Dawson and Blundell [4] were the first ones to describe an orthorhombic crystalline unit cell of PEEK from X-ray data. The *a*- and *b*-axis in the radial direction and the *c*-axis in the lamellae thickness direction are determined with the position of stronger peaks corresponding to plan (110), (111), (200) and (211). The cell parameter *c*-axis coincides to 2/3 of the elementary pattern, as indicated by the crystal structure unit cell which is presented by Kumar et al. [5] and Jin et al. [6]. Two estimations are proposed for this value. Dawson et al. [4] and Hay et al. [7] described it by 2/3 repeat unit of about 1 nm. Ji et al. [8] and Wakelyn et al. [9] reported a *c*-axis with two repeat units, with the sum of two repeat units amounting to around 3 nm. The crystallographic plane (110) appears to be a preferential growth plan. Dawson and Blundell [4] and Hay et al. [7,10] measured the unit cell dimensions of a

* Corresponding author.
E-mail address: karl.delbe@enit.fr (K. Delbé).

https://doi.org/10.1016/j.polymertesting.2020.106878
Received 27 May 2020; Received in revised form 24 August 2020; Accepted 25 September 2020
Available online 2 October 2020

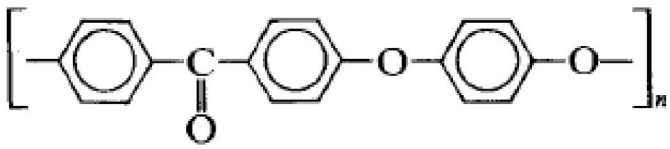

Fig. 1. Chemical formula of PEEK.

Table 1
Extremum of unit cell dimensions of PEEK.

References	Unit cell dimensions (nm)		
	a	*b*	*c*
Dawson et al. [4]	0.763–0.775	0.585–0.596	1.000
Rueda et al. [11]	0.775	0.589	0.988
Hay et al. [10]	0.778	0.592	1.006
Shimizu et al. [12]	0.780	0.592	1.000
Fratini et al. [13]	0.783	0.594	0.986
Kumar et al. [5]	0.779–0.783	0.591–0.592	1.000–1.007
Wakelyn et al. [9]	0.773–0.784	0.584–0.593	2.985–3.037
Hay et al. [7]	0.771–0.786	0.587–0.592	0.990–0.998
Pisani et al. [14]	0.743	0.592	3.009

disoriented polymer, while Rueda et al. [11] used drawn material. All three denote different values for the unit cell dimensions, which are mentioned in Table 1.

Later, Hay et al. [10] noticed the same dimensions for oriented and disoriented PEEK specimens. The molecular orientation does not affect the cell parameters. The cell volume is 0.463 ± 0.1nm^3. Based on four equivalent monomer units per unit cell, the crystalline density is calculated at 1.378 ± 0.005 $g.^{-3}$ and the amorphous density for quenched PEEK is measured as 1.262 ± 0.001$g.^{-3}$. The density increases linearly with the crystalline rate between these two values.

Wakelyn et al. [9] observed that the unit cell dimensions of PEEK decrease systematically with increasing crystallization temperature from amorphous specimens for annealing time of 1 h. When increasing the annealing temperature, there is a progressive change of diffractogram toward higher and narrower peaks. A closer look reveals a progressive change of the angular position of the major diffraction reflections toward higher angles, and an increase in crystalline perfection in the sense of a more tightly packed assembling of macromolecular chains. The a-, b-, c-axis for each temperature specimen were calculated using the orthorhombic relation and the appropriate (110), (113), and (213) data. The a-axis remains constant from 189 °C to 241 °C then regularly decreases with increasing annealing temperature. There is a general decrease in the b-axis with increasing temperature. The c-axis is not affected. The unit cell parameters were used to calculate the crystallographic density values that rises with increasing annealing temperature. It appears to agree with a more densely packed assembling of macromolecular chains.

Hay et al. [7] explained that PEK does not exhibit any dependence between unit cell volume and temperature. A change in crystallite size is not correlated with crystallization temperature. These variations are related to higher disorder in the lateral packing of the molecular chains, specifically the increased torsional angle of the phenylene groups along

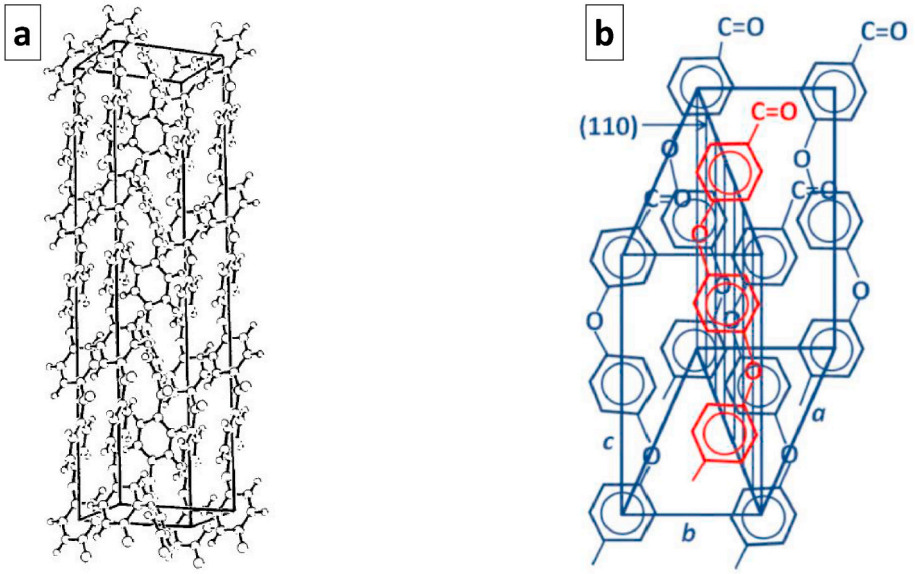

Fig. 2. Unit cell of PEEK reported by a) Fratini [13] and b) Jin [6].

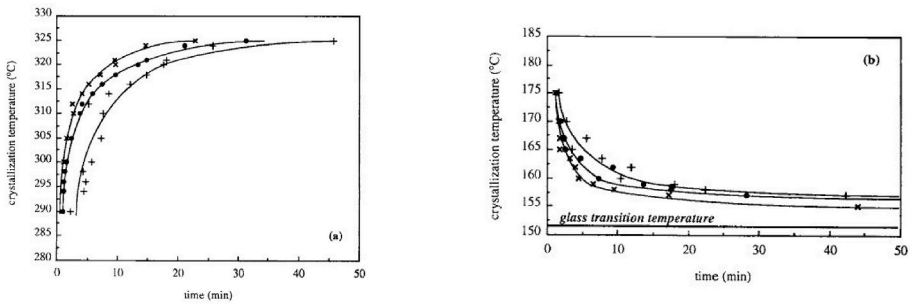

Fig. 3. Time-Temperature-Transformation diagrams: a) from melted state; b) from glassy state. Different relative crystallinity ratios: (×) 5%, (·) 50%, (+) 95% [15].

the c-axis. Steric effects of the adjacent ortho-hydrogen atoms increase the carbonyl and ether chain angles and widen the c-axis dimension.

Recently, Pisani et al. [14] modeled the optimized structure of PEEK with density functional theory, the density reported being 1.450 $g.^{-3}$. To deepen the structure of the PEEK, two organizations of the unit cell are found in the literature. Fratini et al. [13] define the unit cell with a subcell of a two-ring unit repeated three times inside the unit cell, as seen in Fig. 2-a. The crystal density of a subcell is 1.392 $g.^{-3}$. Jin et al. [6] define the unit cell with a three-ring repeat unit, as seen in Fig. 2-b. The organization of the lamella is different according to the cooling conditions. The lamellar stacks and individual lamellae of 10 nm when the sample crystallized isothermally at 315 °C and only lamellar stacks when the sample is cooled down to ambient temperature.

Unit cell parameters depend on the annealing temperature. Crystallization kinetic is deduced from the unit cell parameters. Bas [15] established Time-Temperature-Transformation (TTT) diagrams representing the relative amount of crystallized material according to the crystallization temperature and the time at this temperature (see Fig. 3). Bas defines the relative crystallinity as the relative amount of crystallized material over the final value at the end of the test. The TTT diagram highlights that a sample cooled at 320 °C from the melted state, reached 5%, 50%, 95% of relative crystallinity for test time of 10, 14, 18 min.

Kemmish et al. [16] evaluate the crystallization kinetic of PEEK with the Avrami model. During its crystallization, two competitive mechanisms occur, with two constants of Avrami [17]. For example, the experimental exponent value of 2.5 corresponds to spherulitic, diffusion-controlled growth, with thermal nucleation, and the exponent value of 1.5 corresponds to rod-shaped, diffusion-controlled growth, with thermal nucleation. Rod-shaped crystals emerge from fiber surface, and spherulitic crystals emerge in the bulk. The crystallized volume fraction depends on the rate of temperature descent and remains relatively high ($>$ 20%) as long as the rate of temperature descent does not exceed 10 $K{\cdot}s^{-1}$.

Wang et al. [18] also highlight the influence of melting temperature and pre-crystallization conditions on the crystallization behaviour of PEEK.

The properties of PEEK are unanimously recognized to rival those of metals and could replace them in some applications. However its processing and assembling are still serious challenges that need to be overcome, before a widespread utilization in the industry. For a better understanding of PEEK properties and PEEK based composites, a deep knowledge of its crystalline structure is crucial. Mechanical properties are directly related to the degree of crystallinity and crystalline morphology. Kemmish et al. [16] observed a progressive increase in yield stress under tensile tests at room temperature from 59 MPa for quenched PEEK to 75 MPa for 32% crystalline PEEK. Similarly, as shown by Cebe et al. [19], the elastic modulus is measured at 1.5 GPa and 2.0 GPa for the 22% and the 32% degree of crystalline respectively, also at ambient temperature. The crystalline phase is considered as a reinforcement in the amorphous phase. Pisani [14] modeled molecular dynamics: the elastic modulus of PEEK increases from 3.62 GPa to 4.50 GPa for degrees of crystallinity of 0% and 70% respectively.

Measuring the degree of crystallinity χ_c is a challenging task for industrial quality control. It also gives information about material properties it is also related to material intrinsic properties. The main techniques are Differential Scanning Calorimetry (DSC), Small Angle X-ray Scattering (SAXS) and density measurement. However, the degree of crystallinity differs according to the technique as each has its limitations.

Mehmet et al. [20] measured the density of PEEK samples and calculated the weight fraction of the degree of crystallinity, using a value for the amorphous density of 1.261 $g.^{-3}$. Mehmet compared it with the weight fraction calculated by Wide Angle X-ray Scattering (WAXS) and the melting enthalpy obtained by DSC. Wide differences were observed between similar samples, and with the values obtained by other methods. When Mehmet examined the crystalline PEEK samples by the light microscope, he observed that polishing reveals extensive amounts of voids within the specimens. Since the PEEK had been extensively dried, the voids were attributed to trapped air or inserted solvent residue.

Table 2
Raman's assignment of band for PEEK [23]. γ: out-of-plane bending; δ: bending or scissoring; ν: stretching.

Wavenumber	Assignment
808 cm^{-1}	γ_{C-H}
882 cm^{-1}	Ring mode
1146 cm^{-1}	δ_{C-CO-C} or Ring stretching mode or ν_{C-CO-C}
1201 cm^{-1}	$\nu_{\varphi-O}$
1499 cm^{-1}	Ring stretching mode
1575 cm^{-1}	$\nu_{C=C}$
1595 cm^{-1}	$\nu_{C=C}$
1607 cm^{-1}	$\nu_{C=C}$
1644 cm^{-1}	$\nu_{C=O}$ crystalline
1651 cm^{-1}	$\nu_{C=O}$ amorphous

More recently, Wang et al. [21] performed measurements on injection-moulded PEEK and PEEK reinforced with fullerene nanoparticles and graphene nanoparticles. From their Wide angle X-ray diffraction (WAXD) measurements, they concluded that the process and the nanoparticles do not affect the crystal structure and crystallinity of PEEK.

Thermal analysis with DSC is also used to calculate the degree of crystallinity of PEEK and its composites, but account must be taken for melting and recrystallization that simultaneously occur when heating. Mehmet-Alkan and Hay advice direct measurement of the overall enthalpy change must be performed [22]. Bas et al. [15] note that the double peak observed on the PEEK is linked to two different crystalline structures. Between 175 °C and 290 °C, the crystallization is fast - it takes place in a few seconds -, which explains that recrystallization occurs when heating during the DSC scan. As a result, the melting enthalpy is a sum of simultaneous melting-recrystallization effects.

Raman spectroscopy is used to investigate the crystallinity of semi-crystalline polymers since 80s. The position and indexation of each peak are reported in Table 2. Only the most intense peaks are identified. All the peaks were identified by Ellis [23].

Conventional dispersive Raman spectroscopy establishes spectra with high fluorescence [24] and a low signal-to-noise that avoid high-precision calculation of the intensity ratio. Agbenyega et al. [25] used Fourier transform Raman spectroscopy to circumvent this negative effect. Briscoe et al. [26] thoroughly analyzed PEEK spectra and identified the strongest peaks at 808, 1146, 1201, 1595, 1606, 1644 and 3068cm^{-1}. Agbenyega et al. [25] and Stuart et al. [27] determined that the band at 1644 cm^{-1} is divided into two bands at 1644 cm^{-1} and 1651 cm^{-1} which are assigned to the $\nu_{C=O}$ modes for the crystalline part and to the amorphous part respectively. These authors proposed to calculate the degree of crystallinity by using the ratio intensity of these bands normalized with the band at 1595cm^{-1}. Because they assumed this band is less sensitive to the environment and the crystallinity [26]. The ratio of relative intensities between bands 1595 cm^{-1} over 1607 cm^{-1} [23,25,26] and 1146 cm^{-1} over 1595 cm^{-1} [24,26,27] are used to calculate the degree of crystallinity without destroying the sample.

The degree of crystallinity and crystalline structure depend on processing conditions similarly to any semi-crystalline polymer. However, for PEEK, the processing temperature has a huge impact on the structure. Numerous authors highlight crystallinity differences depending on whether PEEK is crystallized from the glassy state or from the molten state [15,28–31].

From glassy state, for the different annealing conditions, the increase in crystallinity leads to a decrease in the width at half height in XRD. An

Table 3
Degree of crystallinity calculated by density and DSC of the PEEK glassy samples. The absolute uncertainties of density and crystallinity are noted in the table. The enthalpy variations are presented with relative uncertainties.

Holding	Density		DSC - Sample 1			DSC - Sample 2		
time	ρ	χ_c	ΔH_{cc}	ΔH_m	χ_c	ΔH_{cc}	ΔH_m	χ_c
(minute)	($g.^{-1}$)	(%)	($J.g^{-1}$)	($J.g^{-1}$)	(%)	($J.g^{-1}$)	($J.g^{-1}$)	(%)
	$\pm$ 0.005	$\pm$ 4	1%	1%	$\pm$ 0.4	1%	1%	$\pm$ 0.4
0	1.263	0	25.5	39.5	10.8	25.1	35.9	8.3
5	1.264	1	25.3	49.8	18.9	24.4	43.5	14.7
10	1.262	0	23.3	43.8	15.7	24.0	48.0	18.4
15	1.258	−4	23.1	39.5	12.6	20.1	39.6	15.0
20	1.279	11	0.0	39.1	30.0	0.0	37.0	28.4
28	1.282	14	0.0	61.4	47.2	0.0	37.9	29.1
36	1.283	15	0.0	34.2	26.3	0.0	44.9	34.6
44	1.281	13	0.0	37.2	28.6	0.0	40.2	30.9
56	1.282	14	0.0	31.4	24.2	0.0	45.1	34.7

improvement of the primary lamellae would, therefore, be running during the isothermal treatment [32]. Using small-angle XRD analysis, Fougnies et al. [2] quantify the thickness of the crystalline lamellae of PEEK and follow its evolution during an anisothermal cold crystallization. Their results also seem to show a refinement of the crystal morphology with time after the growth of the main crystalline network.

From the melted state, this morphology appears to be different than the one established on a sample crystallized from the melted state then annealed. By thermal analysis, Ko and Woo [33] showed that annealing from the melted state results in one melting peak for each annealing condition on the thermogram. According to them, each peak corresponds to a population of lamellae with their thickness. Being confident in the study of Tardif et al. [34], the minor peak, closest to the main peak, is the consequence of a reorganization.

The paper presented hereby aims to compare the degree of crystallinity of a commercial PEEK using four techniques: density, DSC, XRD and Raman spectroscopy. It is the first time these techniques are compared on the same PEEK samples. Our work highlights the benefits and drawbacks of the techniques and the specificity of the measurement of PEEK crystallinity. Besides, with Raman spectroscopy, we wanted to propose new criteria characteristic of crystallinity. This analysis has the advantage of being local, whereas the other methods are global. By comparing mode shifts or intensity ratios with the crystallinity obtained by density, we underline the strong correlation of these news parameters with the crystallinity of PEEK.

2. Materials and methods

2.1. Materials

The film of PEEK *Aptiv 2000* used in this study was manufactured by Victrex, 250 μm thick. Two experiments were performed: from the glassy state and from the melted state. Based on Martineau's work [35], films are annealed at 156 °C, above the glassy transition temperature, during 5, 10, 15, 20, 28, 36, 44 and 56 min in the oven of a rheometer to ensure the temperature with the accuracy of 0.1 K. Then, samples are quenched with nitrogen for 1 min and stored at ambient temperature. Crystallization kinetic is thermo-dependent. Tardif and Boyard have shown that no crystallization occurs with a cooling rate of 2000 K/s from the melted state [34]. PEEK is heated at 380 °C, then cooled for 5 min at different temperatures 320, 300, 280, 260 °C, about the temperature of crystallization of PEEK at 300 °C. The crystallization is stopped by cooling it rapidly in nitrogen.

2.2. Density

The density is calculated by an immersion method according to the standard ISO 1183–1:2019. Before weighting, samples are dipped in a mix of water and wetting agent to prevent air bubbles formation on the sample surfaces. Each sample is weighted three times for reproducibility.

2.3. Differential Scanning Calorimetry

Differential scanning calorimetry - TA Instruments DSC, Q200 - is performed for each sample to estimate the glass transition T_g, melting T_m, cold crystallization T_{cc}, hot crystallization T_{hc} temperatures and the degree of crystallinity χ_c. Samples weighing approximately 10 mg are encapsulated in hermetic aluminum pans, heated with a temperature ramp of 10 K·min^{-1} from 80 °C to 380 °C, then cooled from 380 °C to 80 °C and finally heated from 80 °C to 380 °C under nitrogen flow of 50 mL·min^{-1}. Between each step, the temperature is maintained for 1 min. Each analysis is performed twice.

2.4. X-ray diffraction

X-ray diffraction - Philips, X'Pert Panalytical - is performed to calculate the degree of crystallinity χ_c of PEEK films. The diffraction angular 2θ is ranged from 5° to 40° with an increment of 0.01°. The diffractometer system uses Cu tube as an X-ray source with an intensity of 40 mA and a tension of 45 kV. The calculation of the degree of crystallinity is obtained by a deconvolution in Gaussian curves, and is performed with 9 curves for the crystalline part and 5 curves for the amorphous part. The degree of crystallinity is the ratio of the sum of the deconvoluted crystalline part over the sum of the crystalline and the amorphous deconvoluted parts. A supplementary data presents the deconvoluted curves for all samples.

2.5. Raman spectroscopy

Raman microspectroscopy provides chemical and structural characterizations of the samples. The spectrometer is a Horiba LabRAM HR 800 with a continue He/Ne source laser that emits at 633 nm The analyses are performed with a magnification of 100 with a numerical aperture of 0.9. Consequently, the spot diameter, the axial resolution and the spectral resolution are 858 nm, 2.8 μm and 3 cm^{-1} respectively. No surface degradation or debris is detected under these conditions. A confocal hole of 30–35 μm and a holographic network of 600 lines · /mm are used for spectrum profiles. Mappings of 60 μm × 60 μm are obtained for samples annealed from glassy state. More than 400 spectra were recorded to study statistically the evolution of the PEEK main vibration modes. For samples cooled from melted state, 10 spectra were performed on the material surface. Spectra profiles were performed with Fourier Transform Raman spectroscopy, given similar profiles. Then, we considered that polarization unaffected the results.

Table 4
Degree of crystallinity calculated by density and DSC of the PEEK melted samples.The absolute uncertainties of density and crystallinity are noted in the table. The enthalpy variations are presented with relative uncertainties.

Holding	Density		DSC - Sample 1			DSC - Sample 2		
temp.	ρ	χ_c	ΔH_{cc}	ΔH_m	χ_c	ΔH_{cc}	ΔH_m	χ_c
(°C)	($g.cm^{-3}$)	(%)	($J.g^{-1}$)	($J.g^{-1}$)	(%)	($J.g^{-1}$)	($J.g^{-1}$)	(%)
	± 0.005	± 4	1%	1%	± 0.4	1%	1%	± 0.4
260	1.300	27	0.0	53.7	40.6	0.0	38.5	29.6
280	1.303	29	0.0	40.0	30.8	0.0	61.8	47.5
300	1.307	32	0.0	39.9	30.7	0.0	45.0	38.4
320	1.259	−3	25.6	37.8	9.4	26.4	50.4	18.4

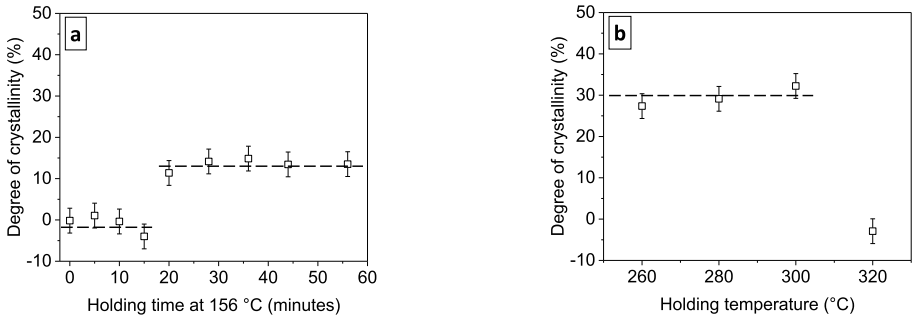

Fig. 4. Degree of crystallinity calculated from density for PEEK samples obtained: a) from glassy state; b) from melted state. The absolute uncertainty is 4%. Dashed lines are guides to the eyes.

3. Results

3.1. Density

Density is calculated for all samples by an Archimede's method (Tables 3 and 4). The density of untreated film PEEK is 1.263 $g.^{-3}$, the same as Blundell [36]. When PEEK is heated at 156 °C, no significant density change is detected until 15 min of annealing. The density of the sample annealed during 15 min is 1.258 $g.^{-3}$ and lower than the untreated sample, but the value is in the absolute uncertainty which is 0.005 $g.^{-3}$. From 20 min, the density increases around 1.279–1.283 $g.^{-3}$ and does not evolve until an annealing time of 56 min. For the sample cooled from the melted state, the density evolves between 1.300 $g.^{-3}$ and 1.307 $g.^{-3}$ for the temperature 260 °C, 280 °C and 300 °C. The density of 1.259 $g.^{-3}$, lower than the untreated sample, is determined for the sample cooled at 320 °C.

The degree of crystallinity χ_c is calculated from equation (1) by knowing the theoretical density of the amorphous phase ρ_a and the crystalline phase ρ_c, 1.263 $g.^{-3}$ and 1.400 $g.^{-3}$ respectively [36]. The absolute uncertainty is 4% by considering $\Delta\rho_a$ and $\Delta\rho_c$ are theories values and equal to zero.

$$\chi_c = \frac{\rho - \rho_a}{\rho_c - \rho_a} \quad (1)$$

The degree of crystallinity evolves similarly to the density as detailed previously (Fig. 4). For the samples annealed at 156 °C, the crystallization does not begin before 20 min and the degree of crystallinity is around 0%. After 20 min of annealing, the crystallization process begins, and increases until 13.5% for 56 min of annealing. According to the Time-Temperature-Transformation TTT diagram [15], the crystallization reaches only 50% of the relative crystallinity. For the sample cooled to 320 °C from the melted state, the degree of crystallization is 0% and the same as the unheated film PEEK. When the cooling temperatures are lower, the degrees of crystallization reach 30%. The experiment duration is 5 min, according to the TTT diagram, the crystallization starts around 316 °C. Below this temperature, the degree of crystallinity increases and the crystallization achieves more than 95% of the relative crystallinity, two-times higher than for glassy samples.

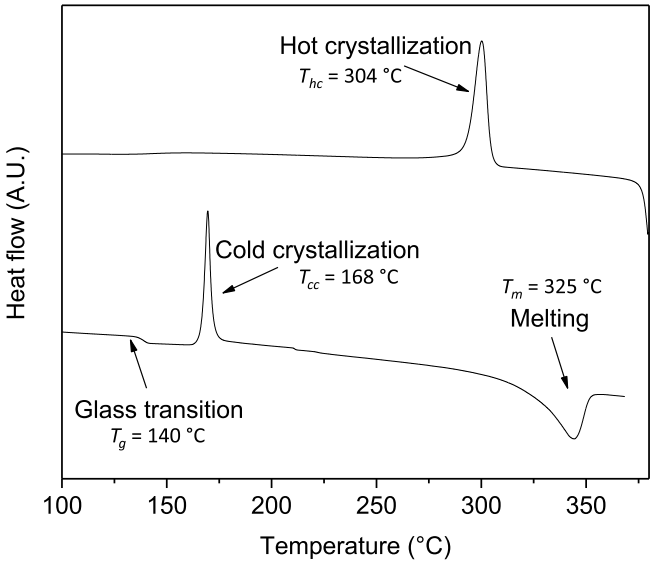

Fig. 5. Thermogram for the untreated sample of PEEK: 1st heating and cooling.

3.2. Differential Scanning Calorimetry

The characteristic temperatures, respectively the glass temperature, the cold crystallization temperature, the melting temperature and the hot crystallization temperature, are evaluated by DSC for the untreated sample (Fig. 5): $T_g = 140$ °C, $T_{cc} = 168$ °C, $T_m = 325$ °C and $T_{hc} = 304$ °C.

The melting enthalpy ΔH_m and the cold crystallization enthalpy ΔH_{cc} during the first heating are used to calculate the degrees of crystallinity from equation (2). The melting enthalpy of an ideal crystal of PEEK $\Delta H_m^{100\%}$ is 130 $J.g^{-1}$ [36].

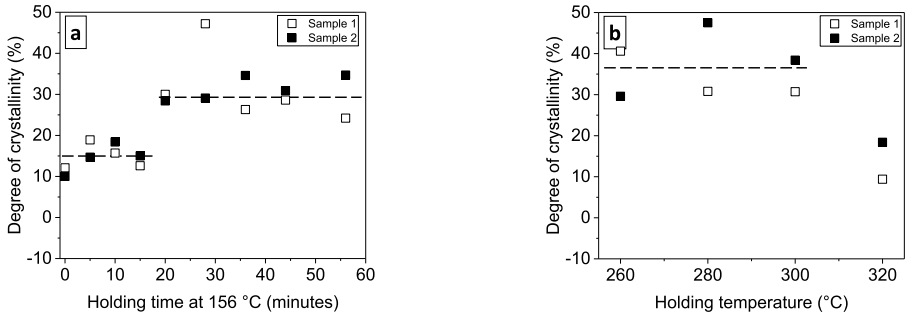

Fig. 6. Degree of crystallinity calculated by DSC for PEEK sample obtained: a) from glassy state; b) from melted state. Each analysis were performed two times. The absolute uncertainty is lower than 0.4% and not represented on the graphic. Dashed lines are guides to the eyes.

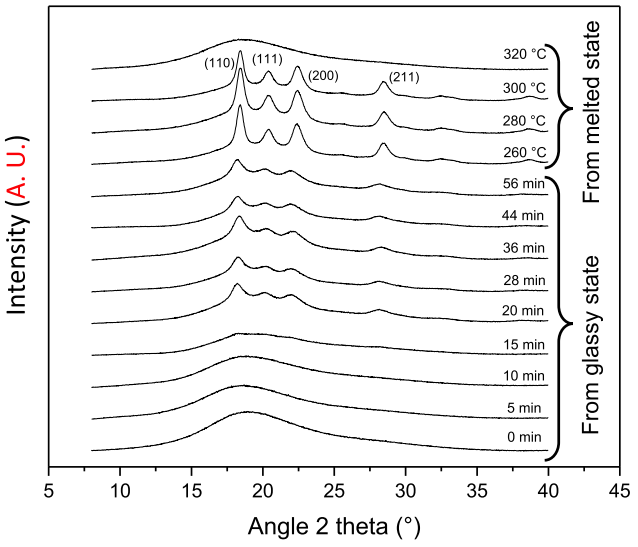

Fig. 7. Diffractogram for PEEK sample obtained from glassy state and from melted state.

$$\chi_c = \frac{\Delta H_m - \Delta H_{cc}}{\Delta H_m^{100\%}} \quad (2)$$

For the glassy samples, a cold crystallization occurs at 168 °C during the first heating for samples annealed until 15 min and evolves between 20.1 and 25.5 J.g^{-1} (Table 3). The evolution of the melting enthalpy is not linear according to the holding time. The degree of crystallinity evolves between 8.3% and 18.9% for a holding time from 0 to 15 min. Then, a second level between 24.2% and 47.2% appears for higher holding time (Fig. 6). No cold crystallization occurs after 20 min of annealing.

Table 5
Values calculated from XRD of the PEEK glassy samples. The relative and absolute uncertainty are noticed in the table.

Holding time	χ_c	a	b	c	$V_{unitcell}$	ρ_c
(minute)	(%)	(nm)	(nm)	(nm)	(nm^3)	(g.cm^{-3})
	± 0.5	2%	2%	2%	6%	6%
20	7.92	0.798	0.587	0.978	0.458	1.392
28	8.33	0.789	0.586	1.004	0.464	1.375
36	7.28	0.785	0.587	0.966	0.445	1.434
44	7.34	0.787	0.584	0.990	0.455	1.403
56	8.02	0.792	0.585	0.989	0.458	1.392

For the melted samples, during the cooling until 320 °C, the hot crystallization temperature at 304 °C is not achieved (Table. 4). The degree of crystallinity, 9.4% and 18.4%, is in a similar order of magnitude of the untreated sample. For temperatures lower than 300 °C, the crystallization occurs, and the degree of crystallization increases up to almost 50%.

3.3. X-ray diffraction (XRD)

Fig. 7 gathers the X-ray diffractogram for every studied samples with the indexation of crystalline peaks [4]. When the degree of crystallinity is low, no crystalline peak appears. The intensity of crystalline peaks increases and crystalline peaks refine with an increase of χ_c.

The degree of crystallinity is calculated from the area of crystalline peaks of diffraction A_c and the area of amorphous peaks of diffraction A_a from equation (3).

$$\chi_c = \frac{A_c}{A_c + A_a} \quad (3)$$

The crystallinity change is similar to those calculated by density: two levels of crystallinity can be detected and there is a factor of two between the degree of crystallinity of glassy samples and melted samples

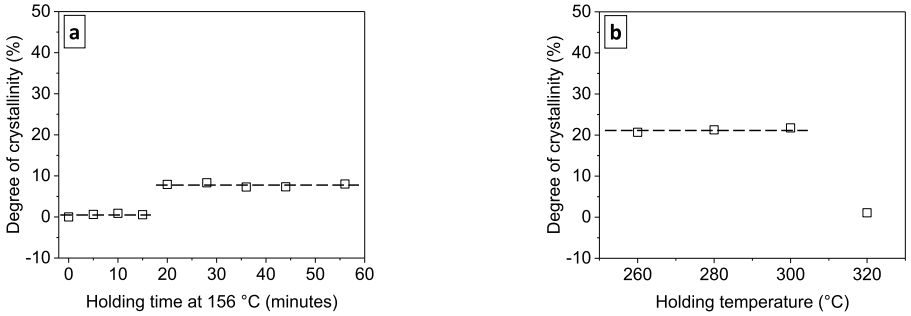

Fig. 8. Degree of crystallinity calculated by XRD for PEEK samples obtained a) from glassy state; b) from melted state. The absolute uncertainty is lower than 0.5% and not represented on the graphic. Dashed lines are guides to the eyes.

Table 6
Values calculated from XRD of the PEEK melted samples. The relative and absolute uncertainty are noticed in the table.

Holding temperature	χ_c	a	b	c	$V_{unitcell}$	ρ_c
(minute)	(%)	(nm)	(nm)	(nm)	(nm^3)	($.^{-3}$)
	± 0.5	2%	2%	2%	6%	6%
260	20.67	0.781	0.593	1.008	0.466	1.374
280	21.27	0.781	0.592	1.004	0.464	1.381
300	21.74	0.781	0.591	1.006	0.445	1.378

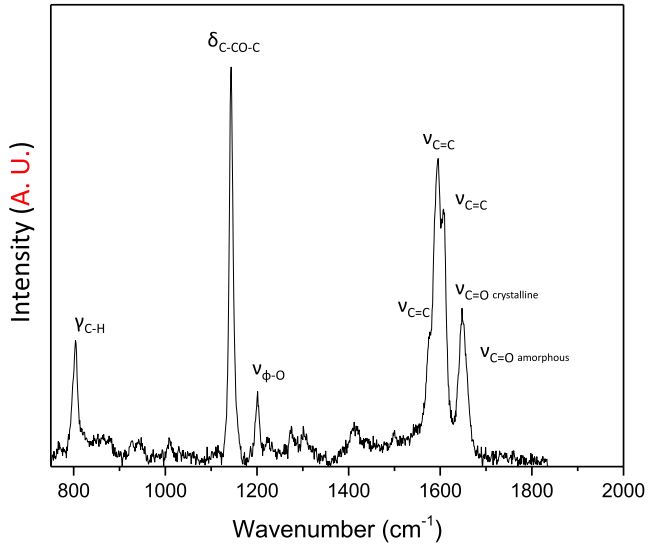

Fig. 9. Spectrum of the PEEK untreated sample. γ: out-of-plane bending; δ: bending or scissoring; ν: stretching.

(Fig. 8). The crystallinity of the sample annealed until 15 min is almost 0% as there is no crystalline peak in the spectra (Table 5). The detection limit of crystallinity with XRD is reached: this technique is not sensitive for samples with low degrees of crystallinity. On the sample spectra cooled at 320 °C from the melted state, no crystallinity peaks appear. The holding time of 5 min was not long enough for crystallinity formation.

The crystallinity of a polymer could be identified with another method based on the crystalline density calculated from the cell parameters, as Hay et al. did for an amorphous PEEK [7]. This method is possible only when peaks are detectable. In the following, the untreated film of PEEK, glassy samples annealed during 5, 10 and 15 min, and melted sample cooling at 320 °C are not studied. In the present study, parameters *a* and *b* are close to the values calculated by Hay for samples performed from a glassy state (Table. 5). Parameters *c* are dispersed, and the standard deviation is around 0.05 nm. For samples cooled from a melted state, the evolution of parameters is linear and the values of parameters *a*, *b* and *c* are respectively 0.781 nm, 0.593 nm and 1.008 nm for the sample cooled at 260 °C (Table. 6), close to the values calculated by Hay et al.

Then, cell parameters are used to calculate the volume of the orthorhombic cell only for samples with crystalline peaks on the spectrum (Tables 5 and 6). For the glassy samples annealed during 36–56 min, the unit cell volume evolves between 0.445 ^{3}nm and 0.464 ^{3}nm. For the melted samples, unit cell volume is constant, 0.464–0.466 ^{3}nm, regardless the holding temperature ranged from 260 °C to 300 °C. No difference appears during a test of 5 min. Hay et al. [7] apply a correction for the unit cell volume. The transparency of the material influences this value and induces asymmetrical deformation of the peak because of the peak at low diffraction angle.

Finally, the density of the crystalline phase ρ_c is calculated by dividing the mass by the volume of the unit cell (Tables 5 and 6). Models of Fratini [13] and Jin [6] give similar crystallographic density. For the glassy sample, crystalline density is between 1.398 $g.^{-3}$ and 1.408 $g.^{-3}$, no substantial evolution occurs when the holding time increases up to 56 min, except for the sample annealed during 36 min. For the melted sample, crystalline density is 1.368–1.375 $g.^{-3}$at 260 °C, 280 °C and 300 °C and lower than the density of the crystalline phase ρ_c. Wakelyn et al. [9] found that crystallographic density increases when the temperature of annealing increases. In this study, the annealing time was shorter than in Wakelyn's study, only 5 min compared to 1 h. Consequently, the crystallization did not have enough time to occur, especially at 320 °C.

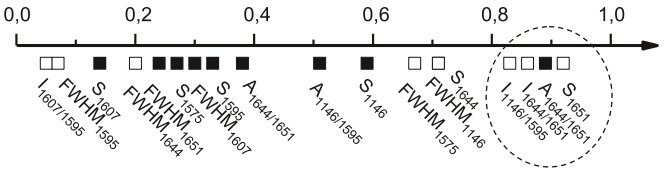

Fig. 10. Absolute values of correlation coefficient of Raman's indicator with the degree of crystallinity determined by density: positive value (■) and negative value (□).

3.4. Raman spectroscopy

Fig. 9 shows the spectrum of the untreated sample obtained by Raman spectroscopy. Mappings were performed on each glassy sample to calculate spatial statistics.

Four characteristics are studied by analyzing Raman spectra: band shift (S), full width at half maximum (FWHM), band intensity (I) and band area (A). We use the wavenumber in agreement with the Ellis assignment (Table 2) [23] to name the indicator with its vibrational mode. For example, S_{1595} and $FWHM_{1595}$ denote the band shift and the full width at half maximum of the $\nu_{C=C}$ mode at 1595 cm^{-1}, respectively. $I_{1607/1595}$ signifies the intensity ratio of the $\nu_{C=C}$ mode at 1607 cm^{-1} on the one at 1595 cm^{-1}. In the same way, $A_{1607/1595}$ symbolizes the area ratio of these two modes. For the six most intense bands, band shift and band full width at half maximum are determined. The mode at 1595 cm^{-1} is less sensitive to the environment and less change occurs. We paid attention to the band at 1146 cm^{-1}, given its dichroic response according to Everall [37]. Intensity and area ratios are determined for the mode at 1146 cm^{-1} over mode at 1595 cm^{-1}, mode at 1575 cm^{-1} over mode at 1595 cm^{-1} and mode at 1644 cm^{-1} over mode at 1651 cm^{-1}. Eighteen Raman indicators are calculated. A correlation coefficient *r* is determined with a linear regression between Raman indicators and the degree of crystallinity deduced from the density. *r* is calculated according to the Pearson's formula and represents for each indicator in Fig. 10). First results reveal a low Pearson's coefficient *r* with all samples. At the scale of our mapping and the size of the probe used to record our spectra, we assume that the crystallinity is heterogeneous. To limit the effect of this heterogeneity, we select samples with low crystallinity - annealed at 156 °C during 0, 5, 10 and 15 min- and high crystallinity - cooled from melted state at 260, 280 and 300 °C - are used for the correlation.

Among the 18 indicators calculated, 4 of them have a correlation with the degree of crystallinity determined by density, superior to the absolute value of 0.8: S_{1651}, $A_{1644/1651}$, $I_{1644/1651}$ and $I_{1146/1595}$ (Fig. 12). The results concerning the FWHM reveal a low correlation coefficient with the degree of crystallinity. S_{1651}, the band shift of the band $\nu_{C=O\ Amor.}$ which is the amorphous part of the band C=O, has the highest correlation coefficient at −0.92. This band moves until 10 cm^{-1} towards lower wavenumber as the degree of crystallinity increases. Louden [24], Everall [37], Stuart [38] found similar evolution. The shift of the bands

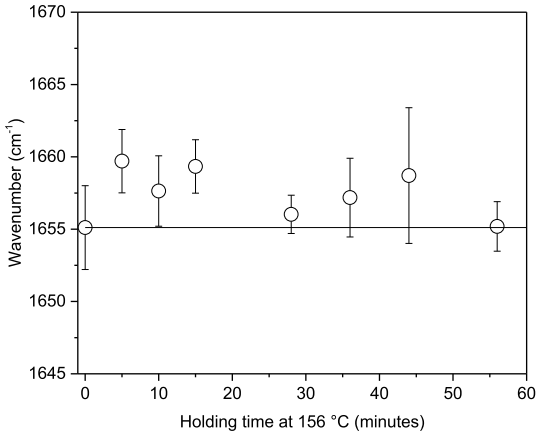

Fig. 11. The band shift δ_{C-CO-C} for glassy samples. The line indicates the values of the untreated film PEEK. Error bars represented the standard deviation.

provides information on the local stresses and information of environment. If the band shifts towards lower wavenumber, the measured area of the material can be under tensile stress. Otherwise, the area can be in compression, like the band at 1651 /cm. During the annealing, the degree of crystallinity increases, therefore the unit cell lengthens, a network of crystallinity grows. The system, and the constraints are released. When glassy samples are annealed, the shift towards higher wavenumber is noticeable (Fig. 11). During the initial forming of PEEK film, macromolecules are in tensile, the annealing relieves stresses in the material.

Concerning area ratios, $A_{1607/1595}$ has the better correlation coefficient at 0.89. When the degree of crystallinity increases, this indicator increases.

Two intensity ratios give high an absolute value of the correlation coefficients: $I_{1644/1651}$, $I_{1146/1595}$ have correlation coefficient of - 0.86 and - 0.83 respectively. $I_{1146/1595}$ corresponds to the C═O band, crystalline and amorphous phase are indexed at 1644 and 1651 /cm respectively. When this ratio increases, the crystalline phase is less important. Ellis [23] found a different result. However, the bands $\nu_{C=O\ Crist.}$ and $\nu_{C=O\ Amor.}$ are close; the deconvolution of these two bands is difficult and may explain this difference with Ellis's previous studies (See Supplementary Data). Moreover, when the degree of crystallinity increases, the ratio $I_{1146/1595}$ decreases, which is in good agreement with Louden [24] and Stuart [27] works.

4. Discussion and conclusion

In this work, a comparison of the degrees of crystallinity of PEEK is performed as a function of the thermal history undergone by the material. For the same thermal history, the degree of crystallinity is measured with four different techniques: density, DSC, XRD and Raman microspectrometry. The benefits and drawbacks of the techniques were highlighted as well as the specificity of the measurement of PEEK crystallinity. Fig. 13 represents, as a function of crystallinity measured by density, the crystallinity obtained by the other techniques (density, XRD and DSC). The best performing indicator calculated by Raman spectroscopy, S_{1651}, has been added.

DSC overestimates degrees of crystallinity of PEEK and gives the highest values, up to 40%. At low degrees of crystallinity, the overestimation comparing density is around 10%–18%, and more important than at high degrees of crystallinity which is around 2%–10%. This technique is based on the heat exchanges measured during the thermal transitions of the material. The sample is subjected to a temperature ramp causing the crystalline zones to melt. However, the crystallization and melting temperature windows overlap for PEEK. When it is heated, the macromolecules of the amorphous phase have more mobility, which leads to the crystallization before they melt. The measured enthalpy of fusion is thus increased, the sample is heated to measure its fusion enthalpy.

DSC is a destructive method. On the contrary, XRD is non-destructive

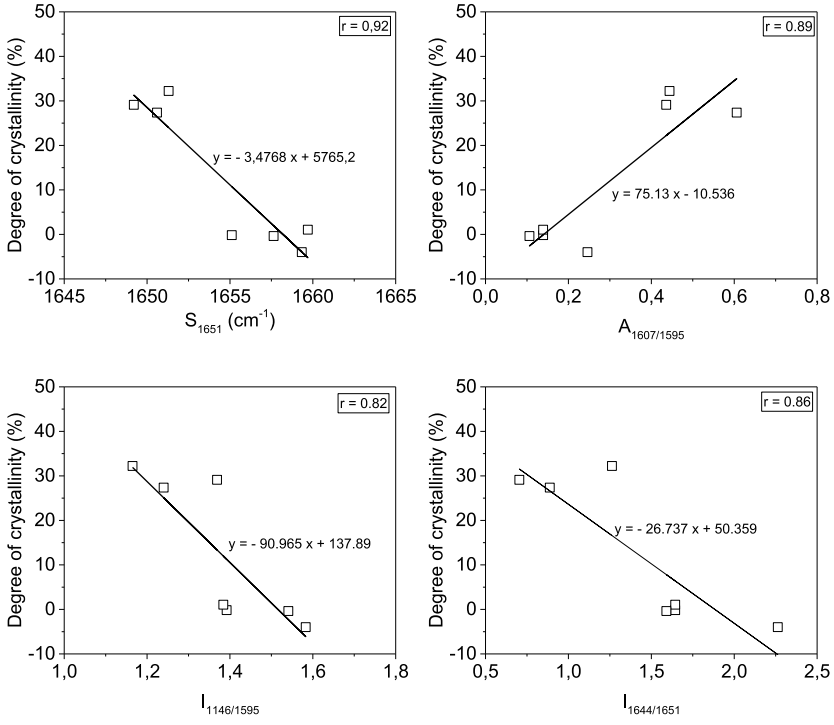

Fig. 12. Value of Raman's indicator according to the degree of crystallinity determined by density; Line: linear regression of the values; r: coefficient of correlation.

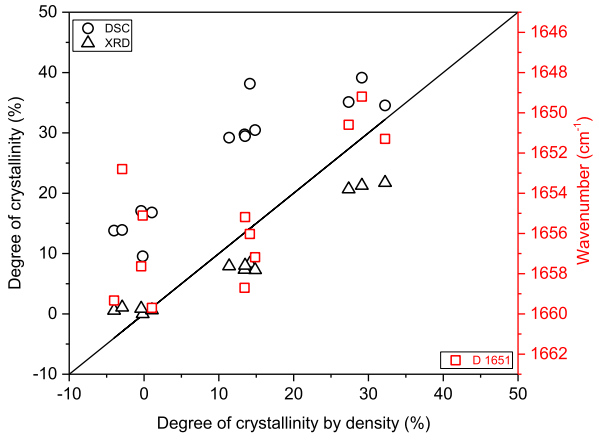

Fig. 13. Degree of crystallinity according to the technique. S_{1651}: wavenumber of the band 1651 cm^{-1}. The line indicates the ratio conservation. S_{1651}: wavenumber of the band 1651 cm^{-1}.

measurement. The XRD underestimates the degrees of crystallinity which are lower than the values determined by density at high degrees of crystallinity. On the one hand, it is difficult, for low crystallinity rates, to extract the crystalline part hidden by the halo from the amorphous phase. On the other hand, the quantity of amorphous phase is difficult to estimate on the samples of which the crystalline part is important. The degree of crystallinity is possibly lowered. The underestimation is negligible for low degrees of crystallinity and around 7% and 11% for high values.

Raman spectroscopy seems to be a good technique to determine the local crystallinity on the sample surface. A link between crystallinity and Raman spectroscopy was highlighted by Louden [24], Briscoe [26], Stuart [27], Ellis [23] and Everall [37]. They proposed several indicators and they didn't compare those to each other. Several reasons can be advanced concerning the indicators having a low Pearson's coefficient. Specifically, Ellis [23] shows that the response of some bands can be affected by polarization effects for the isotropic sample. We note that the low sensitivity of the $\nu_{C=C}$ modes at 1644 /cm and 1651 / cm affects the estimation of the FWHM and its intensity. Our investigation compares 18 indicators in the same study and proves that the 1651 / cm band shift, S_{1651}, has the highest correlation coefficient with the degree of crystallinity determined by density. Three other indicators, $A_{1607/1595}$, $I_{1644/1651}$ and $I_{1146/1595}$, have a correlation coefficient with an absolute value superior to 0.8. Thus, we propose four indicators to determine locally on the PEEK surface the degree of crystallinity with Raman spectroscopy.

CRediT authorship contribution statement

M. Doumeng: Investigation, Methodology, Formal analysis, Writing - original draft. **L. Makhlouf:** Investigation, Formal analysis. **F. Berthet:** Validation, Funding acquisition, Writing - review & editing. **O. Marsan:** Investigation, Writing - review & editing. **K. Delbé:** Project administration, Supervision, Conceptualization, Methodology, Validation, Resources, Funding acquisition, Writing - review & editing. **J. Denape:** Project administration, Validation, Funding acquisition, Writing - review & editing. **F. Chabert:** Validation, Funding acquisition, Writing - review & editing.

Declaration of competing interest

The authors declare that they have no known competing financial interests or personal relationships that could have appeared to influence the work reported in this paper.

Acknowledgments

The Occitanie country fund this research in the context a University of Toulouse thesis (APR n^o ALDOC-000185-2017 001834).

Appendix A. Supplementary data

Supplementary data to this article can be found online at https://doi.org/10.1016/j.polymertesting.2020.106878.

References

[1] T.E. Attwood, P.C. Dawson, J.L. Freeman, L.R.J. Hoy, J.B. Rose, P.A. Staniland, Synthesis and properties of polyarylетherketones, Polymer 22 (1981) 1096–1103.
[2] C. Fougnies, M. Dosière, M.H.J. Koch, J. Roovers, Cold crystallization of narrow molecular weight fractions of PEEK, Macromolecules 32 (1999) 8133–8138.
[3] M. Yuan, J.A. Galloway, R.J. Hoffman, S. Bhatt, Influence of molecular weight on rheological, thermal, and mechanical properties of PEEK, Polym. Eng. Sci. 51 (2011) 94–102.
[4] P.C. Dawson, D.J. Blundell, X-ray data for poly(aryl ether ketones), Polymer 21 (1980) 577–578.
[5] S. Kumar, D.P. Anderson, W.W. Adams, Crystallization and morphology of poly (aryl-ether-ether-ketone), Polymer 27 (1986) 329–336.
[6] L. Jin, J. Ball, T. Bremner, H.J. Sue, Crystallization behavior and morphological characterization of poly(ether ether ketone), Polymer 55 (2014) 5255–5265.
[7] J.N. Hay, J.I. Langford, J.R. Lloyd, Variation in unit cell parameters of aromatic polymers with crystallization temperature, Polymer 30 (1989) 489–493.
[8] X.L. Ji, X.F. Qiu, W.J. Zhang, Z.S. Mo, H.F. Zhang, Z.W. Wu, Variation in unit cell parameters with crystallization temperature in poly(ether diphenyl ether ketone), Polym. J. 30 (1998) 601–603.
[9] N.T. Wakelyn, Variation of unit cell parameters of poly(arylene ether ether ketone) film with annealing temperature, J. Polym. Sci., Part C 25 (1987) 25–28.
[10] J.N. Hay, D.J. Kemmish, J.I. Langford, A.I.M. Rae, The structure of crystalline PEEK, Polym. Commun. 25 (1984) 175–178.
[11] D.R. Rueda, F. Ania, A. Richardson, I.M. Ward, F.J. Balta Calleja, X-Ray diffraction study of die drawn poly(aryletherketone)(PEEK), Polym. Commun. 24 (1983) 258–260.
[12] J. Shimizu, T. Kikutani, Y. Ookoshi, A. Takaku, The crystal structure and the refractive index of drawn and annealed poly(ether-ether-ketone) (PEEK) fibers, Seni Gakkai Shi 41 (1985) T461–T467.
[13] A.V. Fratini, E.M. Cross, R.B. Whitaker, W.W. Adams, Refinement of the structure of PEEK fibre in an orthorhombic unit cell, Polymer 27 (1986) 861–865.
[14] W.A. Pisani, M.S. Radue, S. Chinkanjanarot, B.A. Bednarcyk, E.J. Pineda, K. Waters, R. Pandey, J.A. King, G.M. Odegard, Multiscale modeling of PEEK using reactive molecular dynamics modeling and micromechanics, Polymer 163 (2019) 96–105.
[15] C. Bas, P. Battesti, N.D. Albérola, Crystallization and melting behaviors of poly (aryletheretherketone)(PEEK) on origin of double melting peaks, J. Appl. Polym. Sci. 53 (1994) 1745–1757.
[16] D.J. Kemmish, J.N. Hay, The effect of physical ageing on the properties of amorphous PEEK, Polymer 26 (1985) 905–912.
[17] C.N. Velisaris, J.C. Seferis, Crystallization kinetics of polyetheretherketone (peek) matrices, Polym. Eng. Sci. 26 (1986) 1574–1581.
[18] Y. Wang, Y. Wang, Q. Lin, W. Cao, C. Liu, C. Shen, Crystallization behavior of partially melted poly (ether ether ketone), J. Therm. Anal. Calorim. 129 (2017) 1021–1028.
[19] P. Cebe, S.Y. Chung, S.D. Hong, Effect of thermal history on mechanical properties of polyetheretherketone below the glass transition temperature, J. Appl. Polym. Sci. 33 (1987) 487–503.
[20] A.A. Mehmet-Alkan, J.N. Hay, The crystallinity of poly(ether ether ketone), Polymer 33 (1992) 3527–3530.
[21] P. Wang, R. Ma, Y. Wang, W. Cao, C. Liu, C. Shen, Comparative study of fullerenes and graphene nanoplatelets on the mechanical and thermomechanical properties of poly(ether ether ketone), Mater. Lett. 249 (2019) 180–184.
[22] A.A. Mehmet-Alkan, J.N. Hay, The crystallinity of PEEK composites, Polymer 34 (1993) 3529–3531.
[23] G. Ellis, M. Naffakh, C. Marco, P.J. Hendra, Fourier transform Raman spectroscopy in the study of technological polymers Part 1: poly(aryl ether ketones), their composites and blends, Spectrochim. Acta A 53 (1997) 2279–2294.
[24] J.D. Louden, Crystallinity in poly(aryl ether ketone) films studied by Raman spectroscopy, Polym. Commun. 27 (1986) 82–84.
[25] J.K. Agbenyega, G. Ellis, P.J. Hendra, W.F. Maddams, C. Passingham, H.A. Willis, J. Chalmers, Applications of Fourier Transform Raman spectroscopy in the synthetic polymer field, Spectrochim. Acta A 46 (1990) 197–216.
[26] B.J. Briscoe, B.H. Stuart, P.S. Thomas, D.R. Williams, A comparison of thermal- and solvent-induced relaxation of poly(ether ether ketone) using Fourier transform Raman spectroscopy, Spectrochim. Acta A 47 (1991) 1299–1303.
[27] B.H. Stuart, B.J. Briscoe, A Fourier transform Raman spectroscopy study of poly (ether ether ketone)/polytetrafluoroethylene (PEEK/PTFE) blends, Spectrochim. Acta A 50 (1994) 2005–2009.

[28] C. Bas, Crystallization kinetics of poly(aryl ether ether ketone) Time-temperature-transformation and continuous-cooling-transformation diagrams, Eur. Polym. J. 31 (1995) 911–921.
[29] P. Cebe, S.D. Hong, Crystallization behaviour of poly(ether-ether-ketone), Polymer 27 (1986) 1183–1192.
[30] C. Fougnies, P. Damman, D. Villers, M. Dosière, M.H.J. Koch, Time-resolved SAXS, WAXS, and DSC study of the annealing of poly(aryl ether ether ketone) (PEEK) from the glassy state, Macromolecules 30 (1997) 1385–1391.
[31] C. Fougnies, P. Damman, M. Dosière, M.H.J. Koch, Time-resolved SAXS, WAXS, and DSC study of melting of poly(aryl ether ether ketone) (PEEK) annealed from the amorphous state, Macromolecules 30 (1997) 1392–1399.
[32] L. Martineau, F. Chabert, G. Bernhart, T. Djilali, Mechanical behavior of amorphous PEEK in the rubbery state, in: Proceedings of the 17th European Conference on Composite Materials ECCM17, vol. 17, Germany, Munich, 2016, p. 10.
[33] T.Y. Ko, E.M. Woo, Changes and distribution of lamellae in the spherulites of poly (ether ether ketone) upon stepwise crystallization, Polymer 37 (1996) 1167–1175.
[34] X. Tardif, B. Pignon, N. Boyard, J.W.P. Schmelzer, V. Sobotka, D. Delaunay, C. Schick, Experimental study of crystallization of PolyEtherEtherKetone (PEEK) over a large temperature range using a nano-calorimeter, Polym. Test. 36 (2014) 10–19.
[35] L. Martineau, F. Chabert, B. Boniface, G. Bernhart, Effect of interfacial crystalline growth on autohesion of PEEK, Int. J. Adhesion Adhes. 89 (2019) 82–87.
[36] D.J. Blundell, B.N. Osborn, The morphology of poly(aryl-ether-ether-ketone), Polymer 24 (1983) 953–958.
[37] N.J. Everall, J.M. Chalmers, R. Ferwerda, J.H. van der Maas, P.J. Hendra, Measurement of poly(aryl ether ether ketone) crystallinity in isotropic and uniaxial samples using Fourier transform-Raman spectrocopy: a comparison of univariate and partial least-squares calibrations, J. Raman Spectrosc. 25 (1994) 43–51.
[38] B.H. Stuart, Polymer crystallinity studied using Raman spectroscopy, Vib. Spectrosc. 10 (1996) 79–87.

A comparative study of the crystallinity of Polyetheretherketone by using density, DSC, XRD, and Raman spectroscopy techniques

M. Doumeng, L. Makhlouf, Florentin Berthet, O. Marsan, K. Delbé, Jean Denape, F. Chabert

Polymer Testing 93 (2021) 106878

Contents lists available at ScienceDirect

Polymer Testing

journal homepage: http://www.elsevier.com/locate/polytest

A comparative study of the crystallinity of polyetheretherketone by using density, DSC, XRD, and Raman spectroscopy techniques

M. Doumeng [a], L. Makhlouf [a], F. Berthet [c], O. Marsan [b], K. Delbé [a,*], J. Denape [a], F. Chabert [a]

[a] Laboratoire Génie de Production (LGP), Université de Toulouse, INP-ENIT, Tarbes, France
[b] CIRIMAT, Université de Toulouse, INP-ENSIACET, Toulouse, France
[c] Institut Clément Ader (ICA), Université de Toulouse, École des Mines, Albi, France

ARTICLE INFO

Keywords:
PEEK
Degree of crystallinity
Density
DSC
XRD
Raman spectroscopy

ABSTRACT

A comparative study of the crystallinity of Polyetheretherketone by using density, DSC, XRD, and Raman spectroscopy techniques.

In this work, the microstructure of Polyetheretherketone is first analyzed with usual techniques such as density, Differential Scanning Calorimetry, X-ray Diffraction, and secondly, compared with Raman Spectroscopy. Assessing the degree of crystallinity of PEEK is challenging because of the different interpretation of the crystallinity according to each technique. The density measurement gives the highest most trusted absolute uncertainty for the degree of crystallinity, around 4%, compared to the other techniques. The Differential Scanning Calorimetry, usually used by the polymer community, overestimates up to 18% the degree of crystallinity due to a competitive phenomenon between crystallization and melting of PEEK over the same temperature range, and a fast crystallization. When Analyzing the X-ray Diffraction data, the degree of crystallinity is underestimated up to 11% as a consequence of the broad amorphous halo. Lastly, our investigation proves that Raman microspectroscopy is appropriate to determine the local crystallinity on the sample surface and compares 18 indicators in the same study. The 1651 cm^{-1} band shift has the highest correlation coefficient of 0.92 with the degree of crystallinity determined by density. This work attempts to correlate the results of degree of crystallinity of PEEK obtained by these four techniques in order to establish the best evaluation of this fundamental property for numerous applications.

1. Introduction

Polyetheretherketone (PEEK) is a high-performance thermoplastic widely used as a matrix in the growing thermoplastic composite industry. Launched in the '80s by Imperial Chemical Industries, PEEK is still a promising material because of its inert response to chemical reagents and heat resistance, highly elastic modulus and durability in thermo-oxidative conditions. PEEK is synthesized from biphenyl (hydroquinone) and fluorinated aromatic compound in a polar aprotic solvent (diphenyl sulfone). The fluorinated derivatives are privileged for this synthesis for their better reactivity and higher electronegativity than chlorinated derivatives [1]. The chemical reaction is a nucleophilic substitution obtained by polycondensation between 200 °C and 400 °C. The resulting compound, PEEK, is a copolymer composed of ether and ketone groups, as seen in Fig. 1. The ether/ketone ratio units remain equal to two, even if the order of appearance of monomers in the macromolecular chain differs [1]. The molecular weight varies between 3500 and 50 000 $g.^{-1}$ [2]. Short molecular chains have higher molecular mobility which favors the crystallization [3].

Dawson and Blundell [4] were the first ones to describe an orthorhombic crystalline unit cell of PEEK from X-ray data. The *a*- and *b*-axis in the radial direction and the *c*-axis in the lamellae thickness direction are determined with the position of stronger peaks corresponding to plan (110), (111), (200) and (211). The cell parameter *c*-axis coincides to 2/3 of the elementary pattern, as indicated by the crystal structure unit cell which is presented by Kumar et al. [5] and Jin et al. [6]. Two estimations are proposed for this value. Dawson et al. [4] and Hay et al. [7] described it by 2/3 repeat unit of about 1 nm. Ji et al. [8] and Wakelyn et al. [9] reported a *c*-axis with two repeat units, with the sum of two repeat units amounting to around 3 nm. The crystallographic plane (110) appears to be a preferential growth plan. Dawson and Blundell [4] and Hay et al. [7,10] measured the unit cell dimensions of a

* Corresponding author.
E-mail address: karl.delbe@enit.fr (K. Delbé).

https://doi.org/10.1016/j.polymertesting.2020.106878
Received 27 May 2020; Received in revised form 24 August 2020; Accepted 25 September 2020
Available online 2 October 2020

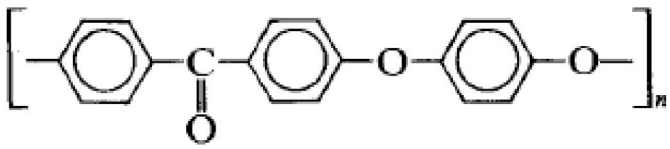

Fig. 1. Chemical formula of PEEK.

Table 1
Extremum of unit cell dimensions of PEEK.

References	Unit cell dimensions (nm)		
	a	*b*	*c*
Dawson et al. [4]	0.763–0.775	0.585–0.596	1.000
Rueda et al. [11]	0.775	0.589	0.988
Hay et al. [10]	0.778	0.592	1.006
Shimizu et al. [12]	0.780	0.592	1.000
Fratini et al. [13]	0.783	0.594	0.986
Kumar et al. [5]	0.779–0.783	0.591–0.592	1.000–1.007
Wakelyn et al. [9]	0.773–0.784	0.584–0.593	2.985–3.037
Hay et al. [7]	0.771–0.786	0.587–0.592	0.990–0.998
Pisani et al. [14]	0.743	0.592	3.009

disoriented polymer, while Rueda et al. [11] used drawn material. All three denote different values for the unit cell dimensions, which are mentioned in Table 1.

Later, Hay et al. [10] noticed the same dimensions for oriented and disoriented PEEK specimens. The molecular orientation does not affect the cell parameters. The cell volume is 0.463 ± 0.1nm^3. Based on four equivalent monomer units per unit cell, the crystalline density is calculated at 1.378 ± 0.005 $g.^{-3}$ and the amorphous density for quenched PEEK is measured as 1.262 ± 0.001$g.^{-3}$. The density increases linearly with the crystalline rate between these two values.

Wakelyn et al. [9] observed that the unit cell dimensions of PEEK decrease systematically with increasing crystallization temperature from amorphous specimens for annealing time of 1 h. When increasing the annealing temperature, there is a progressive change of diffractogram toward higher and narrower peaks. A closer look reveals a progressive change of the angular position of the major diffraction reflections toward higher angles, and an increase in crystalline perfection in the sense of a more tightly packed assembling of macromolecular chains. The a-, b-, c-axis for each temperature specimen were calculated using the orthorhombic relation and the appropriate (110), (113), and (213) data. The a-axis remains constant from 189 °C to 241 °C then regularly decreases with increasing annealing temperature. There is a general decrease in the b-axis with increasing temperature. The c-axis is not affected. The unit cell parameters were used to calculate the crystallographic density values that rises with increasing annealing temperature. It appears to agree with a more densely packed assembling of macromolecular chains.

Hay et al. [7] explained that PEK does not exhibit any dependence between unit cell volume and temperature. A change in crystallite size is not correlated with crystallization temperature. These variations are related to higher disorder in the lateral packing of the molecular chains, specifically the increased torsional angle of the phenylene groups along

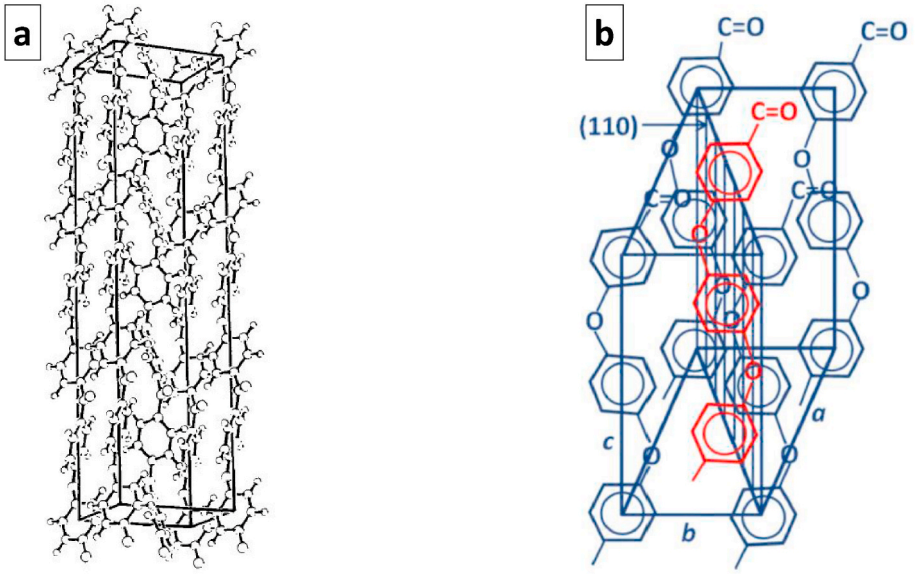

Fig. 2. Unit cell of PEEK reported by a) Fratini [13] and b) Jin [6].

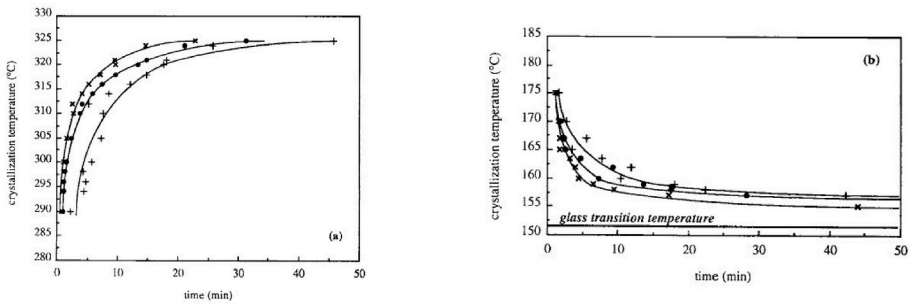

Fig. 3. Time-Temperature-Transformation diagrams: a) from melted state; b) from glassy state. Different relative crystallinity ratios: (×) 5%, (·) 50%, (+) 95% [15].

the c-axis. Steric effects of the adjacent ortho-hydrogen atoms increase the carbonyl and ether chain angles and widen the c-axis dimension.

Recently, Pisani et al. [14] modeled the optimized structure of PEEK with density functional theory, the density reported being 1.450 $g.^{-3}$. To deepen the structure of the PEEK, two organizations of the unit cell are found in the literature. Fratini et al. [13] define the unit cell with a subcell of a two-ring unit repeated three times inside the unit cell, as seen in Fig. 2-a. The crystal density of a subcell is 1.392 $g.^{-3}$. Jin et al. [6] define the unit cell with a three-ring repeat unit, as seen in Fig. 2-b. The organization of the lamella is different according to the cooling conditions. The lamellar stacks and individual lamellae of 10 nm when the sample crystallized isothermally at 315 °C and only lamellar stacks when the sample is cooled down to ambient temperature.

Unit cell parameters depend on the annealing temperature. Crystallization kinetic is deduced from the unit cell parameters. Bas [15] established Time-Temperature-Transformation (TTT) diagrams representing the relative amount of crystallized material according to the crystallization temperature and the time at this temperature (see Fig. 3). Bas defines the relative crystallinity as the relative amount of crystallized material over the final value at the end of the test. The TTT diagram highlights that a sample cooled at 320 °C from the melted state, reached 5%, 50%, 95% of relative crystallinity for test time of 10, 14, 18 min.

Kemmish et al. [16] evaluate the crystallization kinetic of PEEK with the Avrami model. During its crystallization, two competitive mechanisms occur, with two constants of Avrami [17]. For example, the experimental exponent value of 2.5 corresponds to spherulitic, diffusion-controlled growth, with thermal nucleation, and the exponent value of 1.5 corresponds to rod-shaped, diffusion-controlled growth, with thermal nucleation. Rod-shaped crystals emerge from fiber surface, and spherulitic crystals emerge in the bulk. The crystallized volume fraction depends on the rate of temperature descent and remains relatively high ($>$ 20%) as long as the rate of temperature descent does not exceed 10 $K{\cdot}s^{-1}$.

Wang et al. [18] also highlight the influence of melting temperature and pre-crystallization conditions on the crystallization behaviour of PEEK.

The properties of PEEK are unanimously recognized to rival those of metals and could replace them in some applications. However its processing and assembling are still serious challenges that need to be overcome, before a widespread utilization in the industry. For a better understanding of PEEK properties and PEEK based composites, a deep knowledge of its crystalline structure is crucial. Mechanical properties are directly related to the degree of crystallinity and crystalline morphology. Kemmish et al. [16] observed a progressive increase in yield stress under tensile tests at room temperature from 59 MPa for quenched PEEK to 75 MPa for 32% crystalline PEEK. Similarly, as shown by Cebe et al. [19], the elastic modulus is measured at 1.5 GPa and 2.0 GPa for the 22% and the 32% degree of crystalline respectively, also at ambient temperature. The crystalline phase is considered as a reinforcement in the amorphous phase. Pisani [14] modeled molecular dynamics: the elastic modulus of PEEK increases from 3.62 GPa to 4.50 GPa for degrees of crystallinity of 0% and 70% respectively.

Measuring the degree of crystallinity χ_c is a challenging task for industrial quality control. It also gives information about material properties it is also related to material intrinsic properties. The main techniques are Differential Scanning Calorimetry (DSC), Small Angle X-ray Scattering (SAXS) and density measurement. However, the degree of crystallinity differs according to the technique as each has its limitations.

Mehmet et al. [20] measured the density of PEEK samples and calculated the weight fraction of the degree of crystallinity, using a value for the amorphous density of 1.261 $g.^{-3}$. Mehmet compared it with the weight fraction calculated by Wide Angle X-ray Scattering (WAXS) and the melting enthalpy obtained by DSC. Wide differences were observed between similar samples, and with the values obtained by other methods. When Mehmet examined the crystalline PEEK samples by the light microscope, he observed that polishing reveals extensive amounts of voids within the specimens. Since the PEEK had been extensively dried, the voids were attributed to trapped air or inserted solvent residue.

Table 2
Raman's assignment of band for PEEK [23]. γ: out-of-plane bending; δ: bending or scissoring; ν: stretching.

Wavenumber	Assignment
808 cm^{-1}	γ_{C-H}
882 cm^{-1}	Ring mode
1146 cm^{-1}	δ_{C-CO-C} or Ring stretching mode or ν_{C-CO-C}
1201 cm^{-1}	$\nu_{\varphi-O}$
1499 cm^{-1}	Ring stretching mode
1575 cm^{-1}	$\nu_{C=C}$
1595 cm^{-1}	$\nu_{C=C}$
1607 cm^{-1}	$\nu_{C=C}$
1644 cm^{-1}	$\nu_{C=O}$ crystalline
1651 cm^{-1}	$\nu_{C=O}$ amorphous

More recently, Wang et al. [21] performed measurements on injection-moulded PEEK and PEEK reinforced with fullerene nanoparticles and graphene nanoparticles. From their Wide angle X-ray diffraction (WAXD) measurements, they concluded that the process and the nanoparticles do not affect the crystal structure and crystallinity of PEEK.

Thermal analysis with DSC is also used to calculate the degree of crystallinity of PEEK and its composites, but account must be taken for melting and recrystallization that simultaneously occur when heating. Mehmet-Alkan and Hay advice direct measurement of the overall enthalpy change must be performed [22]. Bas et al. [15] note that the double peak observed on the PEEK is linked to two different crystalline structures. Between 175 °C and 290 °C, the crystallization is fast - it takes place in a few seconds -, which explains that recrystallization occurs when heating during the DSC scan. As a result, the melting enthalpy is a sum of simultaneous melting-recrystallization effects.

Raman spectroscopy is used to investigate the crystallinity of semi-crystalline polymers since 80s. The position and indexation of each peak are reported in Table 2. Only the most intense peaks are identified. All the peaks were identified by Ellis [23].

Conventional dispersive Raman spectroscopy establishes spectra with high fluorescence [24] and a low signal-to-noise that avoid high-precision calculation of the intensity ratio. Agbenyega et al. [25] used Fourier transform Raman spectroscopy to circumvent this negative effect. Briscoe et al. [26] thoroughly analyzed PEEK spectra and identified the strongest peaks at 808, 1146, 1201, 1595, 1606, 1644 and 3068cm^{-1}. Agbenyega et al. [25] and Stuart et al. [27] determined that the band at 1644 cm^{-1} is divided into two bands at 1644 cm^{-1} and 1651 cm^{-1} which are assigned to the $\nu_{C=O}$ modes for the crystalline part and to the amorphous part respectively. These authors proposed to calculate the degree of crystallinity by using the ratio intensity of these bands normalized with the band at 1595cm^{-1}. Because they assumed this band is less sensitive to the environment and the crystallinity [26]. The ratio of relative intensities between bands 1595 cm^{-1} over 1607 cm^{-1} [23,25,26] and 1146 cm^{-1} over 1595 cm^{-1} [24,26,27] are used to calculate the degree of crystallinity without destroying the sample.

The degree of crystallinity and crystalline structure depend on processing conditions similarly to any semi-crystalline polymer. However, for PEEK, the processing temperature has a huge impact on the structure. Numerous authors highlight crystallinity differences depending on whether PEEK is crystallized from the glassy state or from the molten state [15,28–31].

From glassy state, for the different annealing conditions, the increase in crystallinity leads to a decrease in the width at half height in XRD. An

Table 3
Degree of crystallinity calculated by density and DSC of the PEEK glassy samples. The absolute uncertainties of density and crystallinity are noted in the table. The enthalpy variations are presented with relative uncertainties.

Holding	Density		DSC - Sample 1			DSC - Sample 2		
time	ρ	χ_c	ΔH_{cc}	ΔH_m	χ_c	ΔH_{cc}	ΔH_m	χ_c
(minute)	($g.^{-1}$)	(%)	($J.g^{-1}$)	($J.g^{-1}$)	(%)	($J.g^{-1}$)	($J.g^{-1}$)	(%)
	$\pm$ 0.005	$\pm$ 4	1%	1%	$\pm$ 0.4	1%	1%	$\pm$ 0.4
0	1.263	0	25.5	39.5	10.8	25.1	35.9	8.3
5	1.264	1	25.3	49.8	18.9	24.4	43.5	14.7
10	1.262	0	23.3	43.8	15.7	24.0	48.0	18.4
15	1.258	−4	23.1	39.5	12.6	20.1	39.6	15.0
20	1.279	11	0.0	39.1	30.0	0.0	37.0	28.4
28	1.282	14	0.0	61.4	47.2	0.0	37.9	29.1
36	1.283	15	0.0	34.2	26.3	0.0	44.9	34.6
44	1.281	13	0.0	37.2	28.6	0.0	40.2	30.9
56	1.282	14	0.0	31.4	24.2	0.0	45.1	34.7

improvement of the primary lamellae would, therefore, be running during the isothermal treatment [32]. Using small-angle XRD analysis, Fougnies et al. [2] quantify the thickness of the crystalline lamellae of PEEK and follow its evolution during an anisothermal cold crystallization. Their results also seem to show a refinement of the crystal morphology with time after the growth of the main crystalline network.

From the melted state, this morphology appears to be different than the one established on a sample crystallized from the melted state then annealed. By thermal analysis, Ko and Woo [33] showed that annealing from the melted state results in one melting peak for each annealing condition on the thermogram. According to them, each peak corresponds to a population of lamellae with their thickness. Being confident in the study of Tardif et al. [34], the minor peak, closest to the main peak, is the consequence of a reorganization.

The paper presented hereby aims to compare the degree of crystallinity of a commercial PEEK using four techniques: density, DSC, XRD and Raman spectroscopy. It is the first time these techniques are compared on the same PEEK samples. Our work highlights the benefits and drawbacks of the techniques and the specificity of the measurement of PEEK crystallinity. Besides, with Raman spectroscopy, we wanted to propose new criteria characteristic of crystallinity. This analysis has the advantage of being local, whereas the other methods are global. By comparing mode shifts or intensity ratios with the crystallinity obtained by density, we underline the strong correlation of these news parameters with the crystallinity of PEEK.

2. Materials and methods

2.1. Materials

The film of PEEK *Aptiv 2000* used in this study was manufactured by Victrex, 250 μm thick. Two experiments were performed: from the glassy state and from the melted state. Based on Martineau's work [35], films are annealed at 156 °C, above the glassy transition temperature, during 5, 10, 15, 20, 28, 36, 44 and 56 min in the oven of a rheometer to ensure the temperature with the accuracy of 0.1 K. Then, samples are quenched with nitrogen for 1 min and stored at ambient temperature. Crystallization kinetic is thermo-dependent. Tardif and Boyard have shown that no crystallization occurs with a cooling rate of 2000 K/s from the melted state [34]. PEEK is heated at 380 °C, then cooled for 5 min at different temperatures 320, 300, 280, 260 °C, about the temperature of crystallization of PEEK at 300 °C. The crystallization is stopped by cooling it rapidly in nitrogen.

2.2. Density

The density is calculated by an immersion method according to the standard ISO 1183–1:2019. Before weighting, samples are dipped in a mix of water and wetting agent to prevent air bubbles formation on the sample surfaces. Each sample is weighted three times for reproducibility.

2.3. Differential Scanning Calorimetry

Differential scanning calorimetry - TA Instruments DSC, Q200 - is performed for each sample to estimate the glass transition T_g, melting T_m, cold crystallization T_{cc}, hot crystallization T_{hc} temperatures and the degree of crystallinity χ_c. Samples weighing approximately 10 mg are encapsulated in hermetic aluminum pans, heated with a temperature ramp of 10 K·min^{-1} from 80 °C to 380 °C, then cooled from 380 °C to 80 °C and finally heated from 80 °C to 380 °C under nitrogen flow of 50 mL·min^{-1}. Between each step, the temperature is maintained for 1 min. Each analysis is performed twice.

2.4. X-ray diffraction

X-ray diffraction - Philips, X'Pert Panalytical - is performed to calculate the degree of crystallinity χ_c of PEEK films. The diffraction angular 2θ is ranged from 5° to 40° with an increment of 0.01°. The diffractometer system uses Cu tube as an X-ray source with an intensity of 40 mA and a tension of 45 kV. The calculation of the degree of crystallinity is obtained by a deconvolution in Gaussian curves, and is performed with 9 curves for the crystalline part and 5 curves for the amorphous part. The degree of crystallinity is the ratio of the sum of the deconvoluted crystalline part over the sum of the crystalline and the amorphous deconvoluted parts. A supplementary data presents the deconvoluted curves for all samples.

2.5. Raman spectroscopy

Raman microspectroscopy provides chemical and structural characterizations of the samples. The spectrometer is a Horiba LabRAM HR 800 with a continue He/Ne source laser that emits at 633 nm The analyses are performed with a magnification of 100 with a numerical aperture of 0.9. Consequently, the spot diameter, the axial resolution and the spectral resolution are 858 nm, 2.8 μm and 3 cm^{-1} respectively. No surface degradation or debris is detected under these conditions. A confocal hole of 30–35 μm and a holographic network of 600 lines · /mm are used for spectrum profiles. Mappings of 60 μm × 60 μm are obtained for samples annealed from glassy state. More than 400 spectra were recorded to study statistically the evolution of the PEEK main vibration modes. For samples cooled from melted state, 10 spectra were performed on the material surface. Spectra profiles were performed with Fourier Transform Raman spectroscopy, given similar profiles. Then, we considered that polarization unaffected the results.

Table 4
Degree of crystallinity calculated by density and DSC of the PEEK melted samples.The absolute uncertainties of density and crystallinity are noted in the table. The enthalpy variations are presented with relative uncertainties.

Holding	Density		DSC - Sample 1			DSC - Sample 2		
temp.	ρ	χ_c	ΔH_{cc}	ΔH_m	χ_c	ΔH_{cc}	ΔH_m	χ_c
(°C)	($g.cm^{-3}$)	(%)	($J.g^{-1}$)	($J.g^{-1}$)	(%)	($J.g^{-1}$)	($J.g^{-1}$)	(%)
	± 0.005	± 4	1%	1%	± 0.4	1%	1%	± 0.4
260	1.300	27	0.0	53.7	40.6	0.0	38.5	29.6
280	1.303	29	0.0	40.0	30.8	0.0	61.8	47.5
300	1.307	32	0.0	39.9	30.7	0.0	45.0	38.4
320	1.259	−3	25.6	37.8	9.4	26.4	50.4	18.4

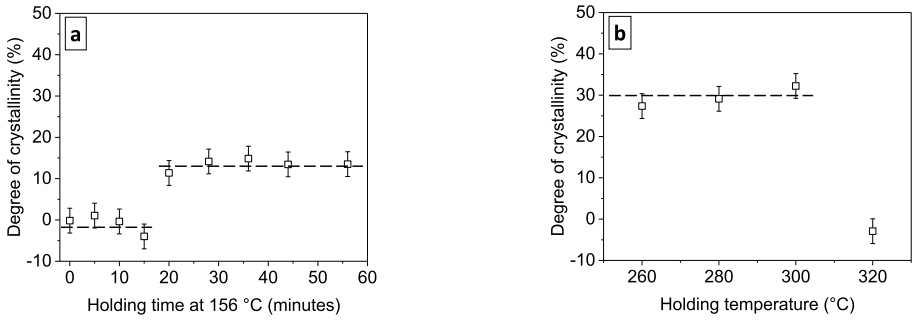

Fig. 4. Degree of crystallinity calculated from density for PEEK samples obtained: a) from glassy state; b) from melted state. The absolute uncertainty is 4%. Dashed lines are guides to the eyes.

3. Results

3.1. Density

Density is calculated for all samples by an Archimede's method (Tables 3 and 4). The density of untreated film PEEK is 1.263 $g.^{-3}$, the same as Blundell [36]. When PEEK is heated at 156 °C, no significant density change is detected until 15 min of annealing. The density of the sample annealed during 15 min is 1.258 $g.^{-3}$ and lower than the untreated sample, but the value is in the absolute uncertainty which is 0.005 $g.^{-3}$. From 20 min, the density increases around 1.279–1.283 $g.^{-3}$ and does not evolve until an annealing time of 56 min. For the sample cooled from the melted state, the density evolves between 1.300 $g.^{-3}$ and 1.307 $g.^{-3}$ for the temperature 260 °C, 280 °C and 300 °C. The density of 1.259 $g.^{-3}$, lower than the untreated sample, is determined for the sample cooled at 320 °C.

The degree of crystallinity χ_c is calculated from equation (1) by knowing the theoretical density of the amorphous phase ρ_a and the crystalline phase ρ_c, 1.263 $g.^{-3}$ and 1.400 $g.^{-3}$ respectively [36]. The absolute uncertainty is 4% by considering $\Delta\rho_a$ and $\Delta\rho_c$ are theories values and equal to zero.

$$\chi_c = \frac{\rho - \rho_a}{\rho_c - \rho_a} \quad (1)$$

The degree of crystallinity evolves similarly to the density as detailed previously (Fig. 4). For the samples annealed at 156 °C, the crystallization does not begin before 20 min and the degree of crystallinity is around 0%. After 20 min of annealing, the crystallization process begins, and increases until 13.5% for 56 min of annealing. According to the Time-Temperature-Transformation TTT diagram [15], the crystallization reaches only 50% of the relative crystallinity. For the sample cooled to 320 °C from the melted state, the degree of crystallization is 0% and the same as the unheated film PEEK. When the cooling temperatures are lower, the degrees of crystallization reach 30%. The experiment duration is 5 min, according to the TTT diagram, the crystallization starts around 316 °C. Below this temperature, the degree of crystallinity increases and the crystallization achieves more than 95% of the relative crystallinity, two-times higher than for glassy samples.

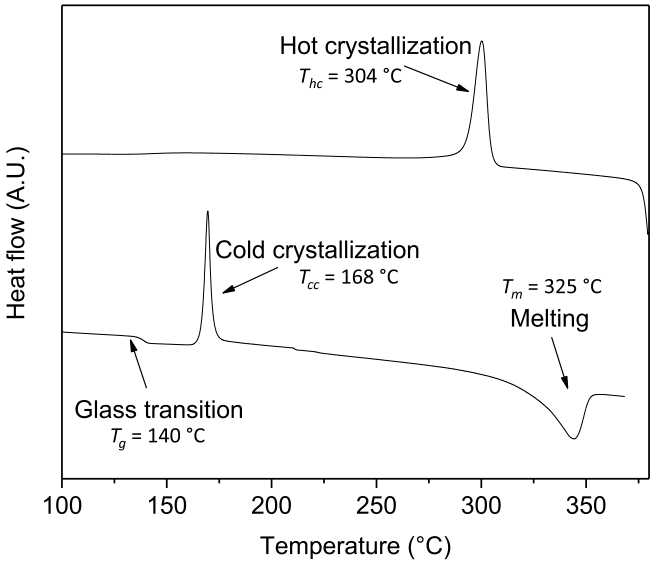

Fig. 5. Thermogram for the untreated sample of PEEK: 1st heating and cooling.

3.2. Differential Scanning Calorimetry

The characteristic temperatures, respectively the glass temperature, the cold crystallization temperature, the melting temperature and the hot crystallization temperature, are evaluated by DSC for the untreated sample (Fig. 5): $T_g = 140$ °C, $T_{cc} = 168$ °C, $T_m = 325$ °C and $T_{hc} = 304$ °C.

The melting enthalpy ΔH_m and the cold crystallization enthalpy ΔH_{cc} during the first heating are used to calculate the degrees of crystallinity from equation (2). The melting enthalpy of an ideal crystal of PEEK $\Delta H_m^{100\%}$ is 130 $J.g^{-1}$ [36].

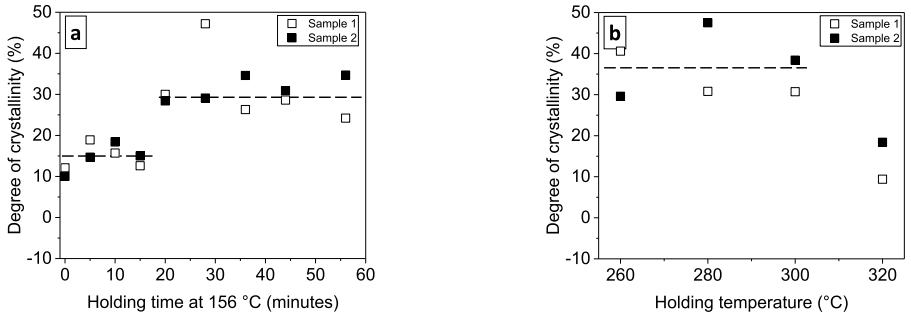

Fig. 6. Degree of crystallinity calculated by DSC for PEEK sample obtained: a) from glassy state; b) from melted state. Each analysis were performed two times. The absolute uncertainty is lower than 0.4% and not represented on the graphic. Dashed lines are guides to the eyes.

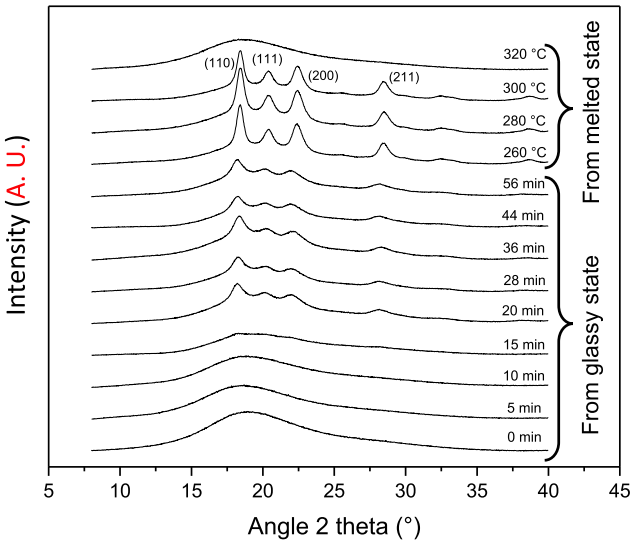

Fig. 7. Diffractogram for PEEK sample obtained from glassy state and from melted state.

$$\chi_c = \frac{\Delta H_m - \Delta H_{cc}}{\Delta H_m^{100\%}} \quad (2)$$

For the glassy samples, a cold crystallization occurs at 168 °C during the first heating for samples annealed until 15 min and evolves between 20.1 and 25.5 J.g^{-1} (Table 3). The evolution of the melting enthalpy is not linear according to the holding time. The degree of crystallinity evolves between 8.3% and 18.9% for a holding time from 0 to 15 min. Then, a second level between 24.2% and 47.2% appears for higher holding time (Fig. 6). No cold crystallization occurs after 20 min of annealing.

Table 5
Values calculated from XRD of the PEEK glassy samples. The relative and absolute uncertainty are noticed in the table.

Holding time	χ_c	a	b	c	$V_{unitcell}$	ρ_c
(minute)	(%)	(nm)	(nm)	(nm)	(nm^3)	(g.cm^{-3})
	± 0.5	2%	2%	2%	6%	6%
20	7.92	0.798	0.587	0.978	0.458	1.392
28	8.33	0.789	0.586	1.004	0.464	1.375
36	7.28	0.785	0.587	0.966	0.445	1.434
44	7.34	0.787	0.584	0.990	0.455	1.403
56	8.02	0.792	0.585	0.989	0.458	1.392

For the melted samples, during the cooling until 320 °C, the hot crystallization temperature at 304 °C is not achieved (Table. 4). The degree of crystallinity, 9.4% and 18.4%, is in a similar order of magnitude of the untreated sample. For temperatures lower than 300 °C, the crystallization occurs, and the degree of crystallization increases up to almost 50%.

3.3. X-ray diffraction (XRD)

Fig. 7 gathers the X-ray diffractogram for every studied samples with the indexation of crystalline peaks [4]. When the degree of crystallinity is low, no crystalline peak appears. The intensity of crystalline peaks increases and crystalline peaks refine with an increase of χ_c.

The degree of crystallinity is calculated from the area of crystalline peaks of diffraction A_c and the area of amorphous peaks of diffraction A_a from equation (3).

$$\chi_c = \frac{A_c}{A_c + A_a} \quad (3)$$

The crystallinity change is similar to those calculated by density: two levels of crystallinity can be detected and there is a factor of two between the degree of crystallinity of glassy samples and melted samples

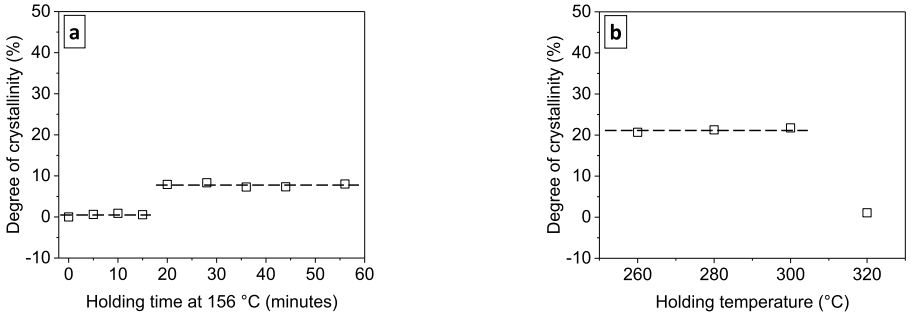

Fig. 8. Degree of crystallinity calculated by XRD for PEEK samples obtained a) from glassy state; b) from melted state. The absolute uncertainty is lower than 0.5% and not represented on the graphic. Dashed lines are guides to the eyes.

Table 6
Values calculated from XRD of the PEEK melted samples. The relative and absolute uncertainty are noticed in the table.

Holding temperature	χ_c	a	b	c	$V_{unitcell}$	ρ_c
(minute)	(%)	(nm)	(nm)	(nm)	(nm^3)	($.^{-3}$)
	± 0.5	2%	2%	2%	6%	6%
260	20.67	0.781	0.593	1.008	0.466	1.374
280	21.27	0.781	0.592	1.004	0.464	1.381
300	21.74	0.781	0.591	1.006	0.445	1.378

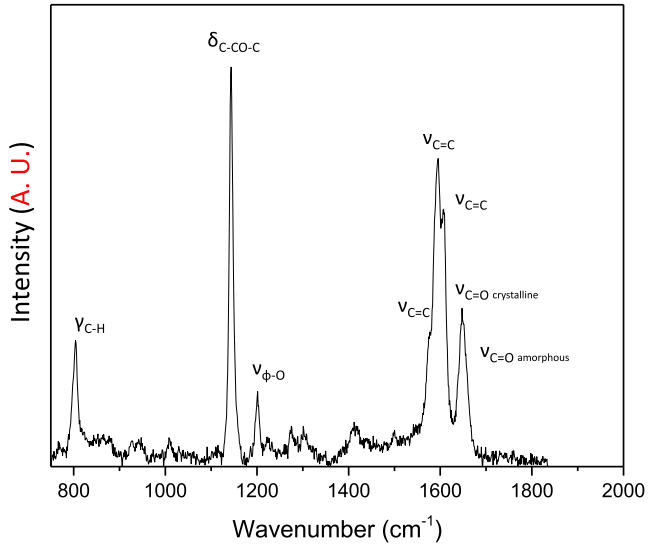

Fig. 9. Spectrum of the PEEK untreated sample. γ: out-of-plane bending; δ: bending or scissoring; ν: stretching.

(Fig. 8). The crystallinity of the sample annealed until 15 min is almost 0% as there is no crystalline peak in the spectra (Table 5). The detection limit of crystallinity with XRD is reached: this technique is not sensitive for samples with low degrees of crystallinity. On the sample spectra cooled at 320 °C from the melted state, no crystallinity peaks appear. The holding time of 5 min was not long enough for crystallinity formation.

The crystallinity of a polymer could be identified with another method based on the crystalline density calculated from the cell parameters, as Hay et al. did for an amorphous PEEK [7]. This method is possible only when peaks are detectable. In the following, the untreated film of PEEK, glassy samples annealed during 5, 10 and 15 min, and melted sample cooling at 320 °C are not studied. In the present study, parameters *a* and *b* are close to the values calculated by Hay for samples performed from a glassy state (Table. 5). Parameters *c* are dispersed, and the standard deviation is around 0.05 nm. For samples cooled from a melted state, the evolution of parameters is linear and the values of parameters *a*, *b* and *c* are respectively 0.781 nm, 0.593 nm and 1.008 nm for the sample cooled at 260 °C (Table. 6), close to the values calculated by Hay et al.

Then, cell parameters are used to calculate the volume of the orthorhombic cell only for samples with crystalline peaks on the spectrum (Tables 5 and 6). For the glassy samples annealed during 36–56 min, the unit cell volume evolves between 0.445 ^{3}nm and 0.464 ^{3}nm. For the melted samples, unit cell volume is constant, 0.464–0.466 ^{3}nm, regardless the holding temperature ranged from 260 °C to 300 °C. No difference appears during a test of 5 min. Hay et al. [7] apply a correction for the unit cell volume. The transparency of the material influences this value and induces asymmetrical deformation of the peak because of the peak at low diffraction angle.

Finally, the density of the crystalline phase ρ_c is calculated by dividing the mass by the volume of the unit cell (Tables 5 and 6). Models of Fratini [13] and Jin [6] give similar crystallographic density. For the glassy sample, crystalline density is between 1.398 $g.^{-3}$ and 1.408 $g.^{-3}$, no substantial evolution occurs when the holding time increases up to 56 min, except for the sample annealed during 36 min. For the melted sample, crystalline density is 1.368–1.375 $g.^{-3}$at 260 °C, 280 °C and 300 °C and lower than the density of the crystalline phase ρ_c. Wakelyn et al. [9] found that crystallographic density increases when the temperature of annealing increases. In this study, the annealing time was shorter than in Wakelyn's study, only 5 min compared to 1 h. Consequently, the crystallization did not have enough time to occur, especially at 320 °C.

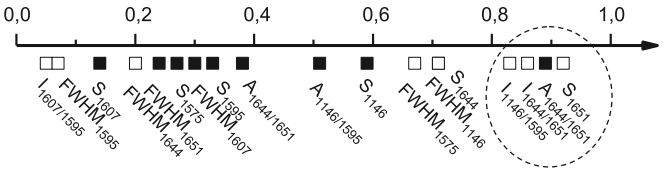

Fig. 10. Absolute values of correlation coefficient of Raman's indicator with the degree of crystallinity determined by density: positive value (■) and negative value (□).

3.4. Raman spectroscopy

Fig. 9 shows the spectrum of the untreated sample obtained by Raman spectroscopy. Mappings were performed on each glassy sample to calculate spatial statistics.

Four characteristics are studied by analyzing Raman spectra: band shift (S), full width at half maximum (FWHM), band intensity (I) and band area (A). We use the wavenumber in agreement with the Ellis assignment (Table 2) [23] to name the indicator with its vibrational mode. For example, S_{1595} and $FWHM_{1595}$ denote the band shift and the full width at half maximum of the $\nu_{C=C}$ mode at 1595 cm^{-1}, respectively. $I_{1607/1595}$ signifies the intensity ratio of the $\nu_{C=C}$ mode at 1607 cm^{-1} on the one at 1595 cm^{-1}. In the same way, $A_{1607/1595}$ symbolizes the area ratio of these two modes. For the six most intense bands, band shift and band full width at half maximum are determined. The mode at 1595 cm^{-1} is less sensitive to the environment and less change occurs. We paid attention to the band at 1146 cm^{-1}, given its dichroic response according to Everall [37]. Intensity and area ratios are determined for the mode at 1146 cm^{-1} over mode at 1595 cm^{-1}, mode at 1575 cm^{-1} over mode at 1595 cm^{-1} and mode at 1644 cm^{-1} over mode at 1651 cm^{-1}. Eighteen Raman indicators are calculated. A correlation coefficient *r* is determined with a linear regression between Raman indicators and the degree of crystallinity deduced from the density. *r* is calculated according to the Pearson's formula and represents for each indicator in Fig. 10). First results reveal a low Pearson's coefficient *r* with all samples. At the scale of our mapping and the size of the probe used to record our spectra, we assume that the crystallinity is heterogeneous. To limit the effect of this heterogeneity, we select samples with low crystallinity - annealed at 156 °C during 0, 5, 10 and 15 min- and high crystallinity - cooled from melted state at 260, 280 and 300 °C - are used for the correlation.

Among the 18 indicators calculated, 4 of them have a correlation with the degree of crystallinity determined by density, superior to the absolute value of 0.8: S_{1651}, $A_{1644/1651}$, $I_{1644/1651}$ and $I_{1146/1595}$ (Fig. 12). The results concerning the FWHM reveal a low correlation coefficient with the degree of crystallinity. S_{1651}, the band shift of the band $\nu_{C=O\ Amor.}$ which is the amorphous part of the band C=O, has the highest correlation coefficient at −0.92. This band moves until 10 cm^{-1} towards lower wavenumber as the degree of crystallinity increases. Louden [24], Everall [37], Stuart [38] found similar evolution. The shift of the bands

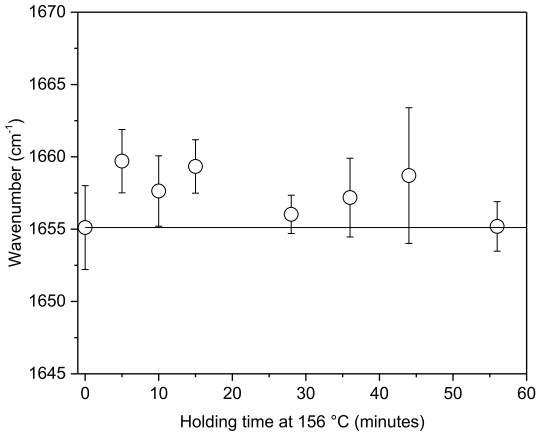

Fig. 11. The band shift δ_{C-CO-C} for glassy samples. The line indicates the values of the untreated film PEEK. Error bars represented the standard deviation.

provides information on the local stresses and information of environment. If the band shifts towards lower wavenumber, the measured area of the material can be under tensile stress. Otherwise, the area can be in compression, like the band at 1651 /cm. During the annealing, the degree of crystallinity increases, therefore the unit cell lengthens, a network of crystallinity grows. The system, and the constraints are released. When glassy samples are annealed, the shift towards higher wavenumber is noticeable (Fig. 11). During the initial forming of PEEK film, macromolecules are in tensile, the annealing relieves stresses in the material.

Concerning area ratios, $A_{1607/1595}$ has the better correlation coefficient at 0.89. When the degree of crystallinity increases, this indicator increases.

Two intensity ratios give high an absolute value of the correlation coefficients: $I_{1644/1651}$, $I_{1146/1595}$ have correlation coefficient of - 0.86 and - 0.83 respectively. $I_{1146/1595}$ corresponds to the C═O band, crystalline and amorphous phase are indexed at 1644 and 1651 /cm respectively. When this ratio increases, the crystalline phase is less important. Ellis [23] found a different result. However, the bands $\nu_{C=O\ Crist.}$ and $\nu_{C=O\ Amor.}$ are close; the deconvolution of these two bands is difficult and may explain this difference with Ellis's previous studies (See Supplementary Data). Moreover, when the degree of crystallinity increases, the ratio $I_{1146/1595}$ decreases, which is in good agreement with Louden [24] and Stuart [27] works.

4. Discussion and conclusion

In this work, a comparison of the degrees of crystallinity of PEEK is performed as a function of the thermal history undergone by the material. For the same thermal history, the degree of crystallinity is measured with four different techniques: density, DSC, XRD and Raman microspectrometry. The benefits and drawbacks of the techniques were highlighted as well as the specificity of the measurement of PEEK crystallinity. Fig. 13 represents, as a function of crystallinity measured by density, the crystallinity obtained by the other techniques (density, XRD and DSC). The best performing indicator calculated by Raman spectroscopy, S_{1651}, has been added.

DSC overestimates degrees of crystallinity of PEEK and gives the highest values, up to 40%. At low degrees of crystallinity, the overestimation comparing density is around 10%–18%, and more important than at high degrees of crystallinity which is around 2%–10%. This technique is based on the heat exchanges measured during the thermal transitions of the material. The sample is subjected to a temperature ramp causing the crystalline zones to melt. However, the crystallization and melting temperature windows overlap for PEEK. When it is heated, the macromolecules of the amorphous phase have more mobility, which leads to the crystallization before they melt. The measured enthalpy of fusion is thus increased, the sample is heated to measure its fusion enthalpy.

DSC is a destructive method. On the contrary, XRD is non-destructive

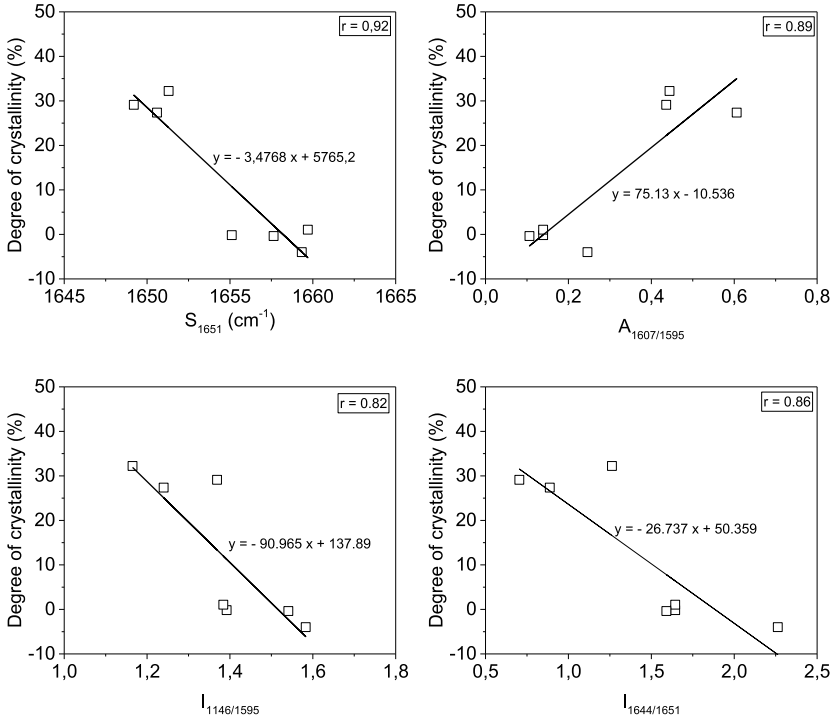

Fig. 12. Value of Raman's indicator according to the degree of crystallinity determined by density; Line: linear regression of the values; r: coefficient of correlation.

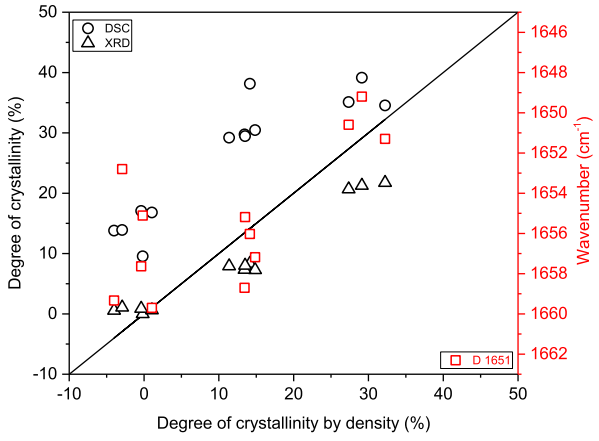

Fig. 13. Degree of crystallinity according to the technique. S_{1651}: wavenumber of the band 1651 cm^{-1}. The line indicates the ratio conservation. S_{1651}: wavenumber of the band 1651 cm^{-1}.

measurement. The XRD underestimates the degrees of crystallinity which are lower than the values determined by density at high degrees of crystallinity. On the one hand, it is difficult, for low crystallinity rates, to extract the crystalline part hidden by the halo from the amorphous phase. On the other hand, the quantity of amorphous phase is difficult to estimate on the samples of which the crystalline part is important. The degree of crystallinity is possibly lowered. The underestimation is negligible for low degrees of crystallinity and around 7% and 11% for high values.

Raman spectroscopy seems to be a good technique to determine the local crystallinity on the sample surface. A link between crystallinity and Raman spectroscopy was highlighted by Louden [24], Briscoe [26], Stuart [27], Ellis [23] and Everall [37]. They proposed several indicators and they didn't compare those to each other. Several reasons can be advanced concerning the indicators having a low Pearson's coefficient. Specifically, Ellis [23] shows that the response of some bands can be affected by polarization effects for the isotropic sample. We note that the low sensitivity of the $\nu_{C=C}$ modes at 1644 /cm and 1651 / cm affects the estimation of the FWHM and its intensity. Our investigation compares 18 indicators in the same study and proves that the 1651 / cm band shift, S_{1651}, has the highest correlation coefficient with the degree of crystallinity determined by density. Three other indicators, $A_{1607/1595}$, $I_{1644/1651}$ and $I_{1146/1595}$, have a correlation coefficient with an absolute value superior to 0.8. Thus, we propose four indicators to determine locally on the PEEK surface the degree of crystallinity with Raman spectroscopy.

CRediT authorship contribution statement

M. Doumeng: Investigation, Methodology, Formal analysis, Writing - original draft. **L. Makhlouf:** Investigation, Formal analysis. **F. Berthet:** Validation, Funding acquisition, Writing - review & editing. **O. Marsan:** Investigation, Writing - review & editing. **K. Delbé:** Project administration, Supervision, Conceptualization, Methodology, Validation, Resources, Funding acquisition, Writing - review & editing. **J. Denape:** Project administration, Validation, Funding acquisition, Writing - review & editing. **F. Chabert:** Validation, Funding acquisition, Writing - review & editing.

Declaration of competing interest

The authors declare that they have no known competing financial interests or personal relationships that could have appeared to influence the work reported in this paper.

Acknowledgments

The Occitanie country fund this research in the context a University of Toulouse thesis (APR n^o ALDOC-000185-2017 001834).

Appendix A. Supplementary data

Supplementary data to this article can be found online at https://doi.org/10.1016/j.polymertesting.2020.106878.

References

[1] T.E. Attwood, P.C. Dawson, J.L. Freeman, L.R.J. Hoy, J.B. Rose, P.A. Staniland, Synthesis and properties of polyarylетherketones, Polymer 22 (1981) 1096–1103.
[2] C. Fougnies, M. Dosière, M.H.J. Koch, J. Roovers, Cold crystallization of narrow molecular weight fractions of PEEK, Macromolecules 32 (1999) 8133–8138.
[3] M. Yuan, J.A. Galloway, R.J. Hoffman, S. Bhatt, Influence of molecular weight on rheological, thermal, and mechanical properties of PEEK, Polym. Eng. Sci. 51 (2011) 94–102.
[4] P.C. Dawson, D.J. Blundell, X-ray data for poly(aryl ether ketones), Polymer 21 (1980) 577–578.
[5] S. Kumar, D.P. Anderson, W.W. Adams, Crystallization and morphology of poly (aryl-ether-ether-ketone), Polymer 27 (1986) 329–336.
[6] L. Jin, J. Ball, T. Bremner, H.J. Sue, Crystallization behavior and morphological characterization of poly(ether ether ketone), Polymer 55 (2014) 5255–5265.
[7] J.N. Hay, J.I. Langford, J.R. Lloyd, Variation in unit cell parameters of aromatic polymers with crystallization temperature, Polymer 30 (1989) 489–493.
[8] X.L. Ji, X.F. Qiu, W.J. Zhang, Z.S. Mo, H.F. Zhang, Z.W. Wu, Variation in unit cell parameters with crystallization temperature in poly(ether diphenyl ether ketone), Polym. J. 30 (1998) 601–603.
[9] N.T. Wakelyn, Variation of unit cell parameters of poly(arylene ether ether ketone) film with annealing temperature, J. Polym. Sci., Part C 25 (1987) 25–28.
[10] J.N. Hay, D.J. Kemmish, J.I. Langford, A.I.M. Rae, The structure of crystalline PEEK, Polym. Commun. 25 (1984) 175–178.
[11] D.R. Rueda, F. Ania, A. Richardson, I.M. Ward, F.J. Balta Calleja, X-Ray diffraction study of die drawn poly(aryletherketone)(PEEK), Polym. Commun. 24 (1983) 258–260.
[12] J. Shimizu, T. Kikutani, Y. Ookoshi, A. Takaku, The crystal structure and the refractive index of drawn and annealed poly(ether-ether-ketone) (PEEK) fibers, Seni Gakkai Shi 41 (1985) T461–T467.
[13] A.V. Fratini, E.M. Cross, R.B. Whitaker, W.W. Adams, Refinement of the structure of PEEK fibre in an orthorhombic unit cell, Polymer 27 (1986) 861–865.
[14] W.A. Pisani, M.S. Radue, S. Chinkanjanarot, B.A. Bednarcyk, E.J. Pineda, K. Waters, R. Pandey, J.A. King, G.M. Odegard, Multiscale modeling of PEEK using reactive molecular dynamics modeling and micromechanics, Polymer 163 (2019) 96–105.
[15] C. Bas, P. Battesti, N.D. Albérola, Crystallization and melting behaviors of poly (aryletheretherketone)(PEEK) on origin of double melting peaks, J. Appl. Polym. Sci. 53 (1994) 1745–1757.
[16] D.J. Kemmish, J.N. Hay, The effect of physical ageing on the properties of amorphous PEEK, Polymer 26 (1985) 905–912.
[17] C.N. Velisaris, J.C. Seferis, Crystallization kinetics of polyetheretherketone (peek) matrices, Polym. Eng. Sci. 26 (1986) 1574–1581.
[18] Y. Wang, Y. Wang, Q. Lin, W. Cao, C. Liu, C. Shen, Crystallization behavior of partially melted poly (ether ether ketone), J. Therm. Anal. Calorim. 129 (2017) 1021–1028.
[19] P. Cebe, S.Y. Chung, S.D. Hong, Effect of thermal history on mechanical properties of polyetheretherketone below the glass transition temperature, J. Appl. Polym. Sci. 33 (1987) 487–503.
[20] A.A. Mehmet-Alkan, J.N. Hay, The crystallinity of poly(ether ether ketone), Polymer 33 (1992) 3527–3530.
[21] P. Wang, R. Ma, Y. Wang, W. Cao, C. Liu, C. Shen, Comparative study of fullerenes and graphene nanoplatelets on the mechanical and thermomechanical properties of poly(ether ether ketone), Mater. Lett. 249 (2019) 180–184.
[22] A.A. Mehmet-Alkan, J.N. Hay, The crystallinity of PEEK composites, Polymer 34 (1993) 3529–3531.
[23] G. Ellis, M. Naffakh, C. Marco, P.J. Hendra, Fourier transform Raman spectroscopy in the study of technological polymers Part 1: poly(aryl ether ketones), their composites and blends, Spectrochim. Acta A 53 (1997) 2279–2294.
[24] J.D. Louden, Crystallinity in poly(aryl ether ketone) films studied by Raman spectroscopy, Polym. Commun. 27 (1986) 82–84.
[25] J.K. Agbenyega, G. Ellis, P.J. Hendra, W.F. Maddams, C. Passingham, H.A. Willis, J. Chalmers, Applications of Fourier Transform Raman spectroscopy in the synthetic polymer field, Spectrochim. Acta A 46 (1990) 197–216.
[26] B.J. Briscoe, B.H. Stuart, P.S. Thomas, D.R. Williams, A comparison of thermal- and solvent-induced relaxation of poly(ether ether ketone) using Fourier transform Raman spectroscopy, Spectrochim. Acta A 47 (1991) 1299–1303.
[27] B.H. Stuart, B.J. Briscoe, A Fourier transform Raman spectroscopy study of poly (ether ether ketone)/polytetrafluoroethylene (PEEK/PTFE) blends, Spectrochim. Acta A 50 (1994) 2005–2009.

[28] C. Bas, Crystallization kinetics of poly(aryl ether ether ketone) Time-temperature-transformation and continuous-cooling-transformation diagrams, Eur. Polym. J. 31 (1995) 911–921.
[29] P. Cebe, S.D. Hong, Crystallization behaviour of poly(ether-ether-ketone), Polymer 27 (1986) 1183–1192.
[30] C. Fougnies, P. Damman, D. Villers, M. Dosière, M.H.J. Koch, Time-resolved SAXS, WAXS, and DSC study of the annealing of poly(aryl ether ether ketone) (PEEK) from the glassy state, Macromolecules 30 (1997) 1385–1391.
[31] C. Fougnies, P. Damman, M. Dosière, M.H.J. Koch, Time-resolved SAXS, WAXS, and DSC study of melting of poly(aryl ether ether ketone) (PEEK) annealed from the amorphous state, Macromolecules 30 (1997) 1392–1399.
[32] L. Martineau, F. Chabert, G. Bernhart, T. Djilali, Mechanical behavior of amorphous PEEK in the rubbery state, in: Proceedings of the 17th European Conference on Composite Materials ECCM17, vol. 17, Germany, Munich, 2016, p. 10.
[33] T.Y. Ko, E.M. Woo, Changes and distribution of lamellae in the spherulites of poly (ether ether ketone) upon stepwise crystallization, Polymer 37 (1996) 1167–1175.
[34] X. Tardif, B. Pignon, N. Boyard, J.W.P. Schmelzer, V. Sobotka, D. Delaunay, C. Schick, Experimental study of crystallization of PolyEtherEtherKetone (PEEK) over a large temperature range using a nano-calorimeter, Polym. Test. 36 (2014) 10–19.
[35] L. Martineau, F. Chabert, B. Boniface, G. Bernhart, Effect of interfacial crystalline growth on autohesion of PEEK, Int. J. Adhesion Adhes. 89 (2019) 82–87.
[36] D.J. Blundell, B.N. Osborn, The morphology of poly(aryl-ether-ether-ketone), Polymer 24 (1983) 953–958.
[37] N.J. Everall, J.M. Chalmers, R. Ferwerda, J.H. van der Maas, P.J. Hendra, Measurement of poly(aryl ether ether ketone) crystallinity in isotropic and uniaxial samples using Fourier transform-Raman spectrocopy: a comparison of univariate and partial least-squares calibrations, J. Raman Spectrosc. 25 (1994) 43–51.
[38] B.H. Stuart, Polymer crystallinity studied using Raman spectroscopy, Vib. Spectrosc. 10 (1996) 79–87.

Appendix (A)

To calculate the degree of crystallinity .

Appendix 1

from X-ray test The degree of crystallinity or the area of the crystal diffraction peaks is determined from the equation by using equation A-1 ,

$$\chi c = \frac{Ac}{Ac+Aa} \qquad \textbf{(A-1)}$$

χc : The degree of crystallinity .

Ac: The area of crystalline peaks of diffraction .

Aa: The area of amorphous peaks of diffraction .

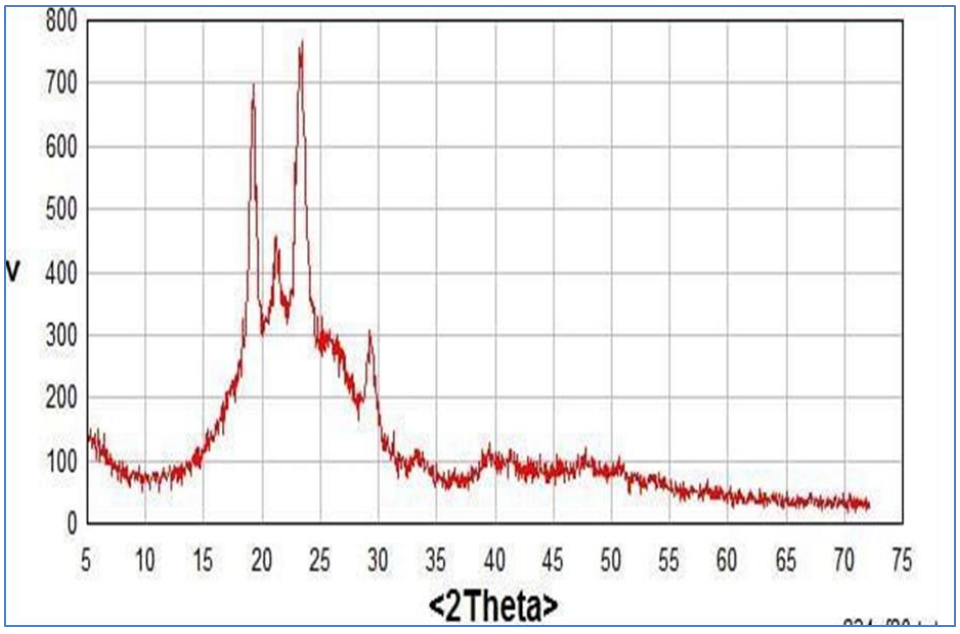

For pure PEEK

Ac=780

Aa=480

$\chi c = \frac{780}{780+480} * 100\%$

χc =61.9

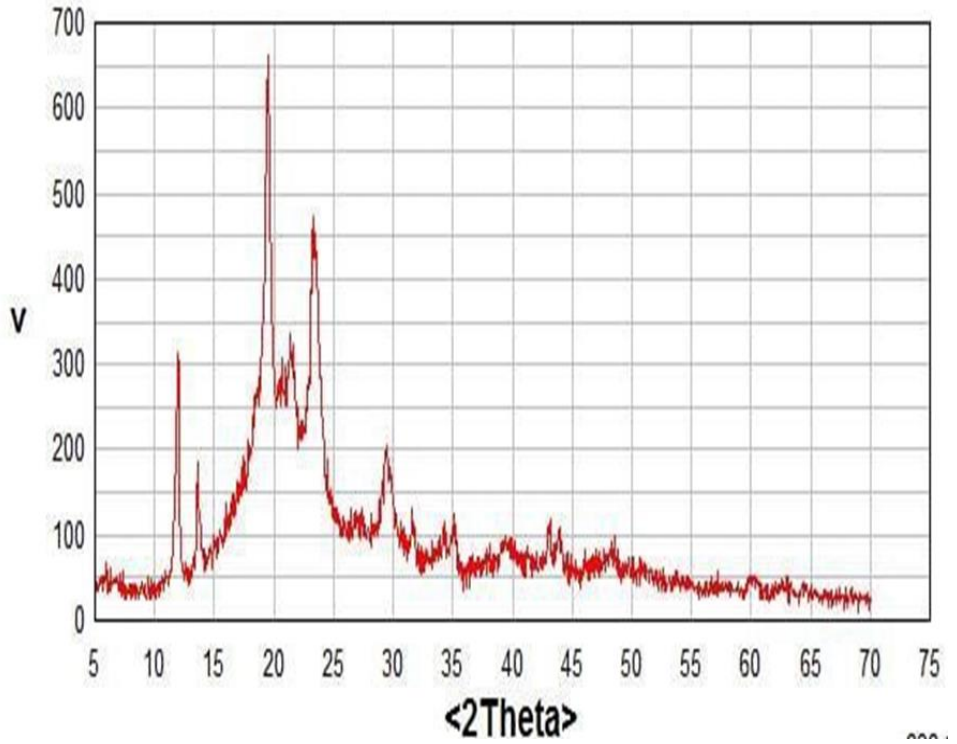

For PEEK+20%Carbon fiber.

Ac=760

Aa=230

$\chi c = \frac{760}{760+230} * 100\%$

$\chi c = 76.8\%$

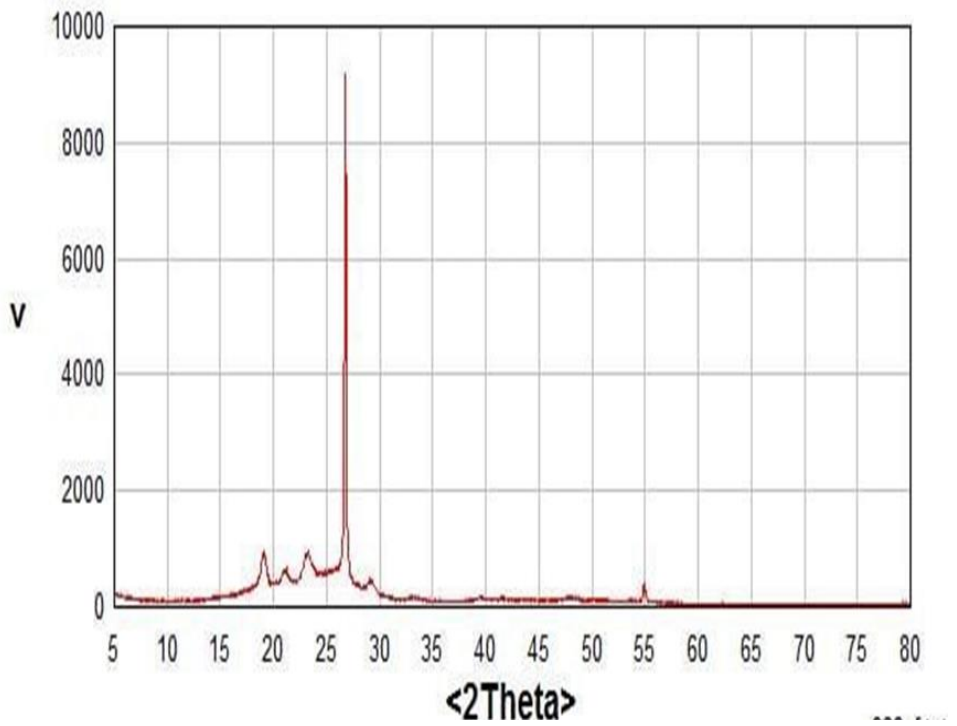

For PEEK+30% Carbon fiber.

Ac= 9000

Aa=1000

$\chi c = \frac{9000}{9000+1000} * 100\%$

$\chi c = 90\%$

Appendix 2

To calculate the Degree of crystallinity χc from density test , Knowledgeable the amorphous phase theoretical density ρa and the Crystalline phase theoretical density ρc, 1.263g $^{-3}$ and 1.400 g^{-3} respectively.

$$\chi c = \frac{\rho - \rho a}{\rho c - \rho a} * 100\% \qquad \textbf{(A-2)}$$

χc : The degreee of crystallinity.

ρ : The density of Calculated in the laboratory.

ρa : The amorphous phase density.

ρc : The Crystalline phase density.

For pure PEEK

$\chi c = \frac{1.3122-1.263}{1.400-1.263} * 100\%$, $\chi c = 35.9\ \%$

For PEEK+20% CF

$\chi c = \frac{1.3375-1.263}{1.400-1.263} * 100\%$, $\chi c = 54.4\%$

For PEEK+30% CF

$\chi c = \frac{1.3838-1.263}{1.400-1.263} * 100\%$, $\chi c = 88.2\%$

Appendix 3

To calculate the degree of crystallinity by using DSC test according to the following equation (A-3) .

$$\chi c = \Delta H_{exp} / \Delta H^{*}. W_f \qquad \textbf{(A-3)}$$

χc : The degree of crystallinity.

ΔH_{exp} : The experimental heat of fusion determined from DSC .

ΔH^{*} : The heat of fusion of fully crystalline PEEK 130J/g .

W_f : The weight fraction of PEEK in the blend.

From result of DSC Test for Pure PEEK

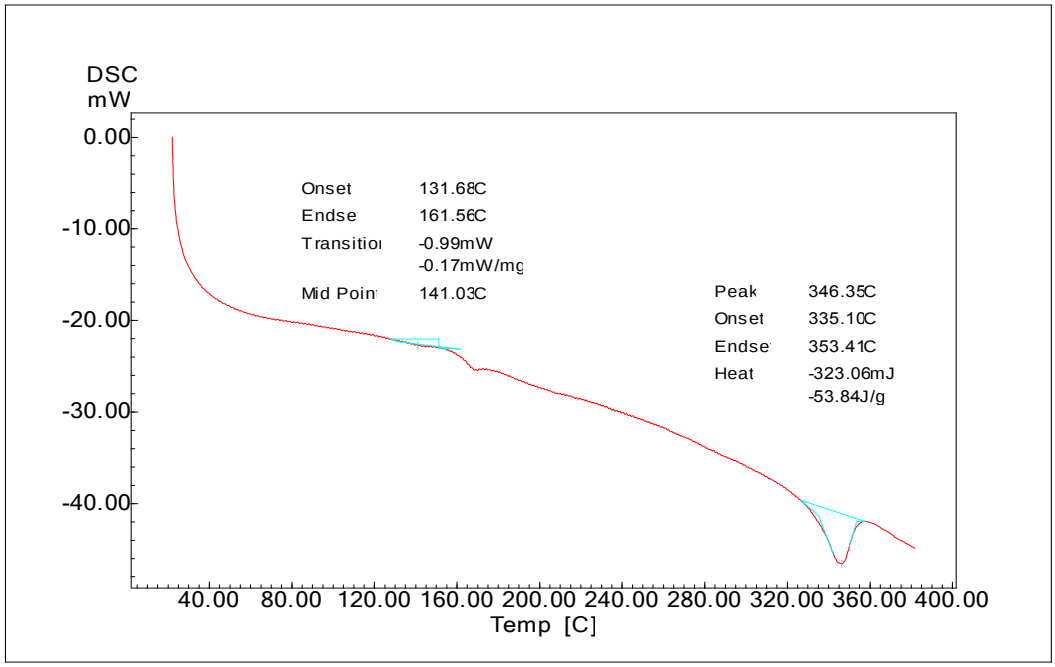

$$\chi c = \frac{53.84}{130} * 100\% \quad , \quad \chi c = 41.42\%$$

From result of DSC for PEEK+20%CF

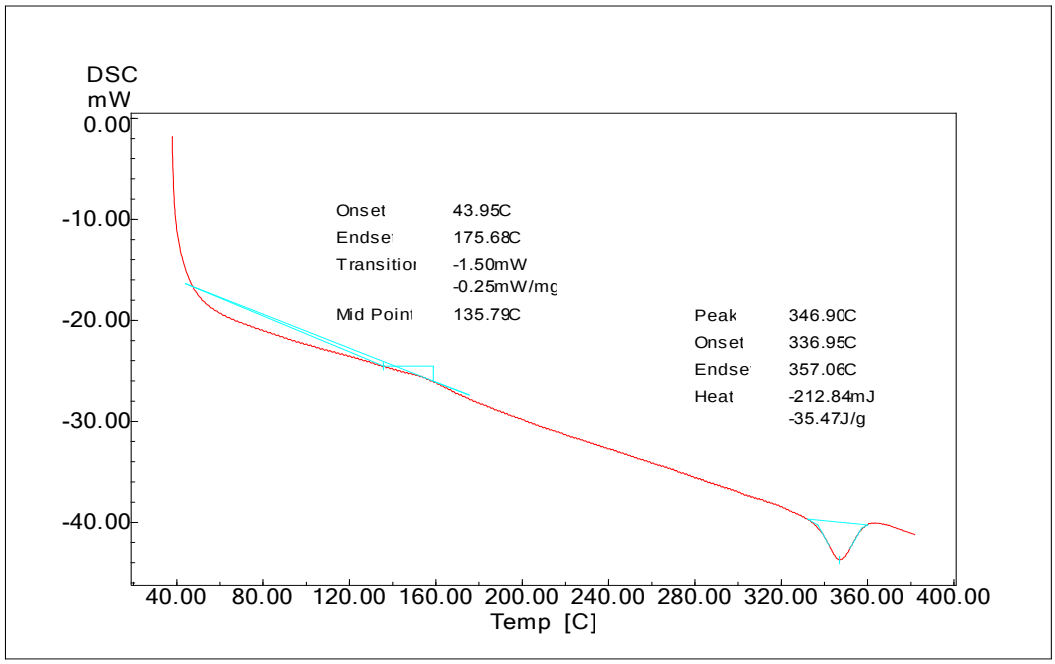

$$\chi c = \frac{35.47}{130} * 0.8 * 100\% \quad , \quad \chi c = 21.83\%$$

From result of DSC for PEEK+20%CF

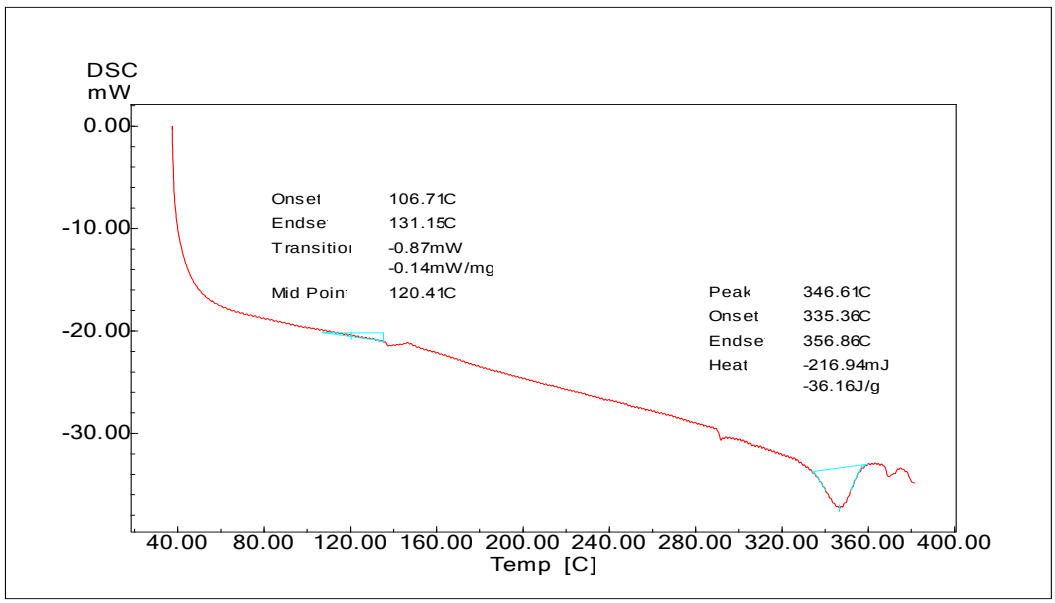

$$\chi c = \frac{36.16}{130} * 0.7 * 100\% \quad , \quad \chi c = 19.47\%$$

Appendix (B)

Appendix 1

To calculate stress and strain from load and deformation curve .

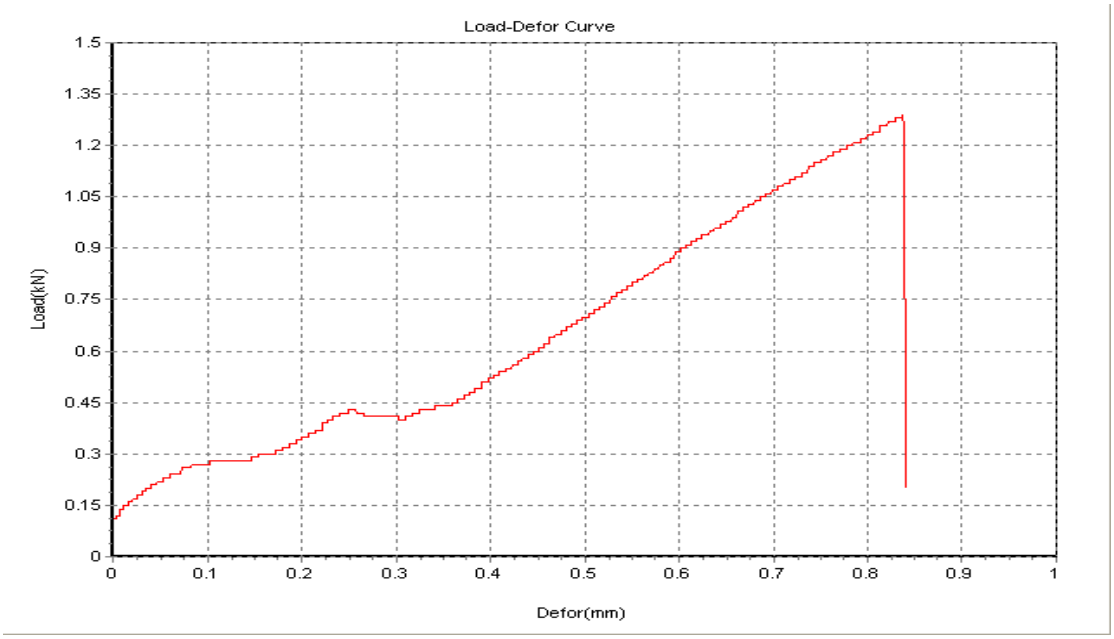

For pure PEEK

Stress = $\frac{\boldsymbol{Load}}{\boldsymbol{Cross\ section\ area}}$ **(B-1)**

A = Thickness*width = 4mm*6mm=24mm

Stress at (0.15)=$\frac{0.15*1000}{24} = 6.25\ Mpa$

Stress at (0.3) =$\frac{0.3*1000}{24} = 12.5\ Mpa$

Stress at (0.45)=$\frac{0.45*1000}{24} = 18.75\ Mpa$

Stress at (0.6)=$\frac{0.6*1000}{24} = 25\ Mpa$

Stress at (0.75)=$\frac{0.75*1000}{24} = 31.25\ Mpa$

Stress at (0.9)=$\frac{0.9*1000}{24} = 37.5\ Mpa$

Stress at (1.05)=$\frac{1.05*1000}{24} = 43.75\ Mpa$

Stress at (1.2)=$\frac{1.2*1000}{24} = 50\ Mpa$

Strain = $\Delta L/L$ **(B -2)**

Strain at (0.1)= $\frac{0.1}{40} = 0.0025$ mm^2

Strain at (0.2)= $\frac{0.2}{40} = 0.005$ mm^2

Strain at (0.3)= $\frac{0.3}{40} = 0.0075$ mm^2

Strain at (0.4)= $\frac{0.4}{40} = 0.01$ mm^2

Strain at (0.5)= $\frac{0.5}{40} = 0.0125$ mm^2

Strain at (0.6)= $\frac{0.6}{40} = 0.015$ mm^2

Strain at (0.7)= $\frac{0.7}{40} = 0.0175$ mm^2

Strain at (0.8)= $\frac{0.8}{40} = 0.02$ mm^2

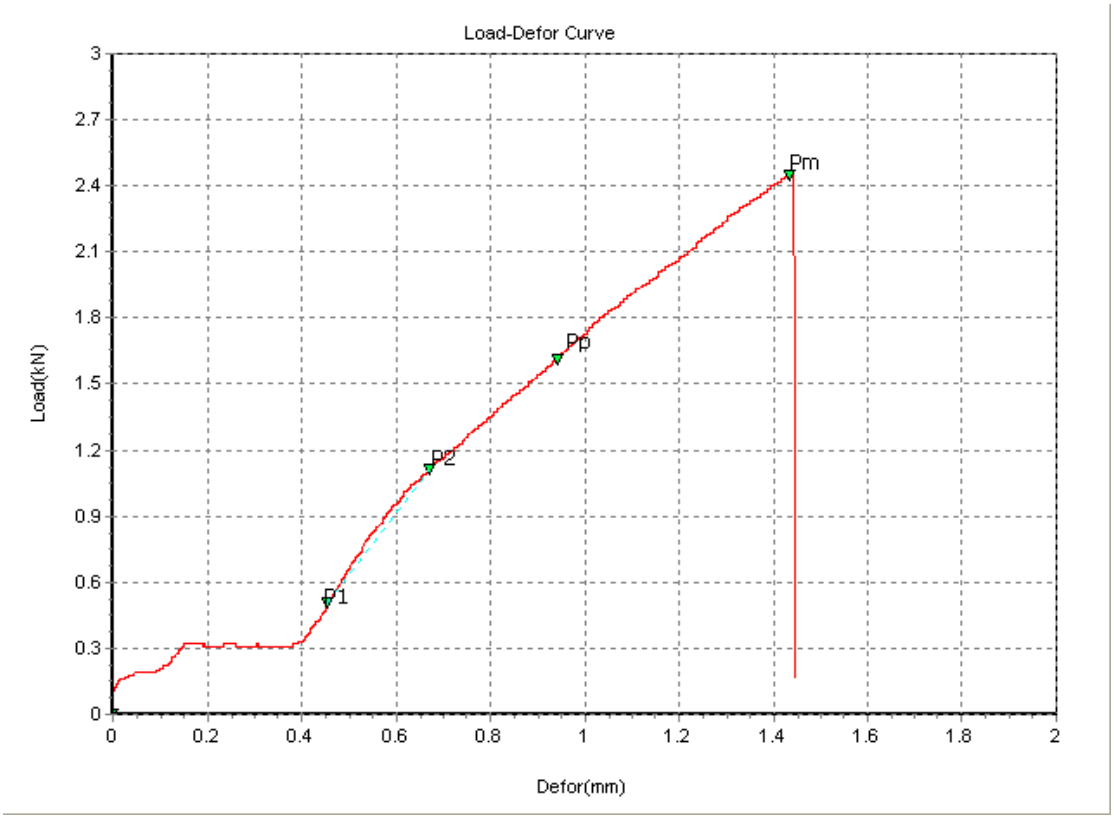

For PEEK+20%carbon fiber

Stress at (0.3)= $\frac{0.3* 1000}{24} = 12.5\ Mpa$

Stress at (0.6) $= \frac{0.6*1000}{24} = 25\ Mpa$

Stress at (0.9) $= \frac{0.9*1000}{24} = 37.5\ Mpa$

Stress at (1.2) $= \frac{1.2*1000}{24} = 50\ Mpa$

Stress at (1.5) $= \frac{1.5*1000}{24} = 62.5\ Mpa$

Stress at (1.8) $= \frac{1.8*1000}{24} = 75\ Mpa$

Stress at (2.1) $= \frac{2.1*1000}{24} = 87.5\ Mpa$

Stress at (2.4) $= \frac{2.4*1000}{24} = 100\ Mpa$

Stress at (2.5) $= \frac{2.5*1000}{24} = 104.2\ Mpa$

Strain at (0.2) $= \frac{0.2}{40} = 0.005$

Strain at (0.4) $= \frac{0.4}{40} = 0.01$

Strain at (0.6) $= \frac{0.6}{40} = 0.015$

Strain at (0.8) $= \frac{0.8}{40} = 0.02$

Strain at (1) $= \frac{1}{40} = 0.025$

Strain at (1.2) $= \frac{1.2}{40} = 0.03$

Strain at (1.4) $= \frac{1.4}{40} = 0.035$

Strain at (1.45) $= \frac{1.45}{40} = 0.0365$

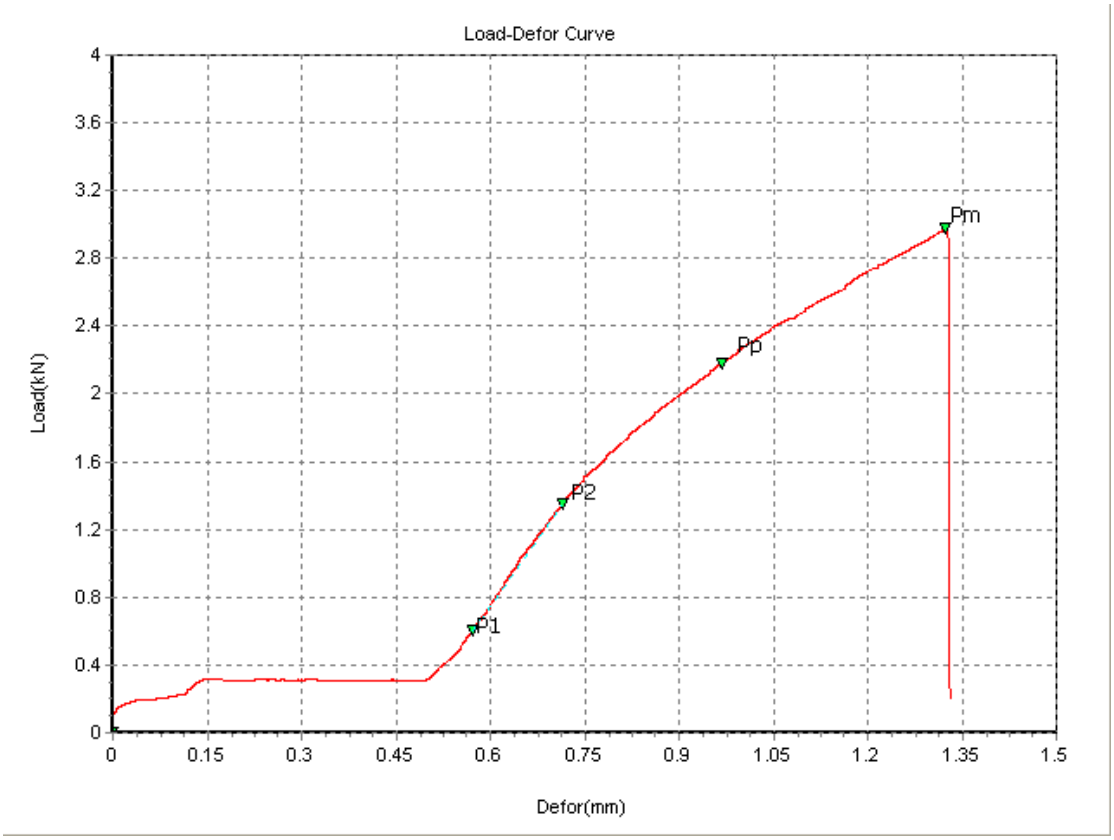

For PEEK+30%carbon fiber

Stress at (0.4)=$\frac{0.4*1000}{24} = 16.7\ Mpa$

Stress at (0.8)=$\frac{0.8*1000}{24} = 33.3\ Mpa$

Stress at (1.2)=$\frac{1.2*1000}{24} = 50\ Mpa$

Stress at (1.6)=$\frac{1.6*1000}{24} = 66.7\ Mpa$

Stress at (2)=$\frac{2*1000}{24} = 83.3\ Mpa$

Stress at (2.4)=$\frac{2.4*1000}{24} = 100\ Mpa$

Stress at (2.8)=$\frac{2.8*1000}{24} = 116.7\ Mpa$

Stress at (3)=$\frac{3*1000}{24} = 125\ Mpa$

Strain at (0.15)=$\frac{0.15}{40} = 0.0038$

Strain at (0.3)=$\frac{0.3}{40} = 0.075$

Strain at (0.45)=$\frac{0.45}{40} = 0.01125$

Strain at (0.6)=$\frac{0.6}{40} = 0.015$

Strain at (0.75)=$\frac{0.75}{40}$=0.01875

Strain at (0.9)=$\frac{0.9}{40} = 0.0225$

Strain at (1.05)=$\frac{1.05}{40} = 0.02625$

Strain at (1.2)=$\frac{1.2}{40} = 0.03$

Strain at (1.35)=$\frac{1.35}{40} = 0.034$

Appendix C

To calculate elastic modulus

E = $\frac{\boldsymbol{\sigma}}{\boldsymbol{\varepsilon}}$

For pure PEEK

E = $\frac{25-18.75}{0.01-0.0075} = 1250\ MPa = 1.25\ GPA$

For PEEK+20%CF

E =$\frac{62.5-37.5}{0.02375-0.015} = 2857\ MPa = 2.8511\ GPa$

For PEEK+30%CF

E = $\frac{66.7-50}{0.015-0.01125} = 4453.3\ MPa = 4.4533\ GPa$

Appendix D

To calculate the impact strength from fracture energy

For Pure PEEK

Thickness =3.53 mm **,**Width =10.8 mm **,** Length = 55mm

The fracture energy = 0.35 J

Impact strength = $\frac{Fracture\ energy}{cross\ section\ area} = \frac{J}{m2}$

A(cross section area)= 3.53*10.8

= 38.124/1000= 0.038124 m^2

Impact strength = $\frac{0.35}{0.038124}$ = 9.2 J/m^2

For PEEK+20%CF

Thickness =4 mm , Width = 9.7mm , Length=55mm

The fracture energy =0.65 J

A(cross section area) = 4*9.7

=38.8/1000= 0.0388 m^2

Impact strength = $\frac{0.65}{0.0388}$ =16.75 J/m^2

For PEEK+30%CF

Thickness=4mm , Width= 9.72mm, Length=55mm

The fracture energy = 0.85 J

A(cross section area) = 4*9.72

= 38.88/1000=0.03888 m^2

Impact strength = $\frac{0.85}{0.03888}$ = 21.86 J/m^2

References

References

1. Gowariker, V. R., Viswanathan, N. V. and Shreedhar, J. Polymer Science, New Age International, New Delhi, 2005.

2. Stephen Z.D. Cheng, Shi Jin, in Handbook of Thermal Analysis and Calorimetry, vol 3, pp1-828 , 2002

3. D.W. Van Krevelen, Revised by and K. Te Nijenhuis, in Properties of Polymers (Fourth Edition), 2009

4. Harold F. Giles Jr John R. Wagner, Jr., in Extrusion (Second Edition), N9781437734812, 2014.

5. Sabu Thomas, Mohammed Arif P., ... Nandakumar Kalarikkal, in Crystallization in Multiphase Polymer Systems, 2018.

6. Takashi Yamamoto, Molecular Dynamics Modeling of Crystal-Melt Interfaces and Growth of Chain folded Lamellae, Adv. Polym. Sci., 2005.

7. Professor Marianne Gilbert, in Brydson's Plastics Materials (Eighth Edition), N 978-0-323-35824-8, pp 169-204, (2017)

8. Anshuman Shrivastava , in Introduction to Plastics Engineering, N978-0-323-39500-7 , (2018)

9.G. W. Ehrenstein; Richard P. Theriault Polymeric materials: structure, properties, applications. Hanser Verlag. pp. 67–78. ISBN 978-1-56990-310-0(2001).

10. Autar K. Kaw, "Mechanics of Composite Material", Preface to theSecond Edition, International Standard Book Number-10: 0-8493-1343-0(Hardcover), Printed in the United States of America, 2006.

11. Yongming Liu, Sankaran Mahadevan , "Probabilistic Fatigue Life Prediction of Multidirectional Composite Laminates", Elsevier Ltd ,Box 1831-B, Nashville, TN 37235, Vanderbilt University, USA , 2004.

12. Prof .Dr. Najim A .Saad, and Dr. Ahmed F. Hamzah, "Study of Fatigue Behavior of Polyphenylene Sulfide (PPS) Basis Composite

Materials Reinforced with Glass Fiber and Carbon", the International Journal of Engineering and Technology, Volume 3, No.4, ISSN 2049-3444, PP 1- 15, 2013.

13. M. Gahleitner, D. Mileva, R. Androsch, D. Gloger, D. Tranchida, M. Sandholzer, P. Doshev, Crystallinity-Based Product Design: Utilizing the Polymorphism of Isotactic PP Homo- and Copolymers , Vol 31, 618, 2016.

14.Günter R., Jens-Uwe S., Polymer crystallization: observations, concepts, and interpretations, Lecture Notes in Physics, Vol. 606, Springer-Verlag Berlin Heidelberg, 7, 2003.

15. Mittal Vikas, Optimization of Polymer Nano composite Properties, Wiley, 13.1, 2010.

16. GW Becker, Ludwig Bottenbruch, Rudolf Binsack, D. Braun: Engineering Thermoplastics. Polyamides. Hanser Verlag, (in German),1998 .

17. Georg Menges, Edmund Haberstroh, Walter Michaeli, Ernst Schmachtenberg: Plastics Materials Science Hanser Verlag, , ISBN 3-446-21257-4, 2002

18. Prof. Dr. Najim A .Saad, Asist. Prof. Dr. Mohammed S. Hamzah،and Dr. Ahmed F. Hamzah, "Numerical and Experimental -Investigation for Tensile Properties of Polyphenylene Sulfide Basis Composite Material", the Iraqi Journal for Mechanical and Engineering, Special Issue for the Second International Scientific Conference, College of Engireeng Material, PP 1-22 Babylon University , Iraq, 2013.

19. John Chalmers Robert Meier Molecular characterization and analysis of polymers , Amsterdam, 24th October 2008

20. Harold F. Giles Jr, Eldridge M. Mount ,John R. Wagner Jr, The definitive processing guide and handbook , William Andrew; 1st edition (December 17, 2007)

21. L. H.(Lensil Howard) Sperling , Polymeric multicomponent materials: An introduction. New York, January , 1997

22. Joachim Ulrich and Torsten Stelzer Handbook of Industrial Crystallization , pp. 266 - 289, Cambridge University Press , 14 June 2019

23.Wilbrand Woebcken, Klaus Stöckhert, HBP Gupta: Plastics Encyclopedia. (in German) Hanser Verlag, 1998, ISBN 3-446-17969-0

24. Patil, N; Balzano, L; Portale, G; Rastogi "A Study on the Chain−Particle Interaction and Aspect Ratio of Nanoparticles on Structure Development of a Linear Polymer". 43 (16), p 6749–6759, S (July 2010).

25. Michael Thielen, Klaus Hartwig, Peter Gust: Blow molding of plastic articles Hanser Verlag, ISBN 3-446-22671-0, (2006).

26. H.J.M. Kramer, G.M. van Rosmalen, in Encyclopedia of Separation Science, 2000

27. Wang, Haopeng; Jong K. Keum; Anne Hiltner; Eric Baer; Benny Freeman; Artur Rozanski; Andrzej Galeski "Confined Crystallization of Polyethylene Oxide in Nanolayer Assemblies",Science. 323 (5915): 757–760, (6 February 2009).

28. Joachim Nentwig: Plastic films, , ISBN 3-446-40390-6 , (in German) Hanser Verlag, (2006).

29. Martin Bonnet " Plastics in engineering applications: properties, processing and practical use of polymeric materials", ISBN 3-8348-0349-9, (in German), 2008.

30. Courtney, T. H. "Mechanical Behavior of Materials", Waveland Press , 392-396, (2005).

31. Andrew J. Peacock; Allison R. Calhoun "Polymer chemistry: properties and applications" Hanser Verlag ISBN 978-1-56990-397-1 , pp. 286–287, (2006).

32. Ágnes Tímár- Balázsy; Dinah Eastop Chemical principles of textile conservation. Butterworth-Heinemann, ISBN 978-0-7506-2620-0, p 11 (1998).

33. Fazeli, Mahyar; Florez, Jennifer Paola; Simão, Renata Antoun "Improvement in adhesion of cellulose fibers to the thermoplastic starch matrix by plasma treatment modification"2018

34. Elhajjar, Rani; La Saponara, Valeria; Muliana, Anastasia, eds. (2017). Smart Composites: Mechanics and Design (Composite Materials). CRC Press. ISBN 978-1-138-07551-1.[page needed]

35. McEvoy, M. A.; Correll, N. (19 March 2015). "Materials that couple sensing, actuation, computation, and communication". Science. 347 (6228): 1261689. doi:10.1126/science.1261689. PMID 25792332.

36. Juan Alfredo Erni, "The Development Of Unidirectional And Multidirectional Composite Models Using A Modified Weibull Failure Distribution; Theory, Analysis And Applications", M.Sc. Thesis, Arizona State University, (2007).

37. Joshua Rast, "Characterizing the Fatigue Damage in Non-Traditional Laminates of Carbon Fiber Composites Using Radiography", M.Sc. Thesis, Georgia Institute of Technology, (2009).

38. David Richardson, "Composite Design Fundamentals", Faculty of

Engineering and Technology, University of the West of England, (2011).

39. Daniel B. Miracle and Steven L. Donaldson, "Introduction to Composites", , ASM Handbook Vol 21, (2001).

40. Salar Bagherpour, "Fibre Reinforced Polyester Composites", Islamic Azad University, Department of Materials Science and Engineering، Najafabad-Branch, Iran, (2012).

41. ME ChemE/MBA Jaeun Chung, "Nano scale Characterization of

Epoxy Interphase on Copper Microstructures", Berlin (2006).

42. P.K. Mallick, "Fiber Reinforced Composite", third edition Materials،Manufacturing, Department of Mechanical Engineering University of Michigan-Dearborn, copyright © by Taylor & Francis Group،LLC.(2007).

43. K.Rajasekar, “Experimental Testing of Natural Composite Material” IOSR Journal of Mechanical and Civil Engineering (IOSR-JMCE) eISSN: 2278-1684,p-ISSN: 2320-334X, Volume 11, Issue 2 Ver. III (Mar- Apr. 2014).

44. Géraldine Theiler, “PTFE- and PEEK-Matrix Composites for Tribological Applications at Cryogenic Temperatures and in Hydrogen”, Tag der wissenschaftlichen Aussprache: 6. Mai 2005.

45.Parina Patel, T. Richard Hull,“Mechanism of Thermal Decomposition of Poly (Ether Ether Ketone) (PEEK) From a Review of Decomposition Studies”, Published in Polymer Degradation andStability 95, 709-718, University Of Central Lancashire, UK, 2010.

46.Daniel Gay,Suong V. Hoa, Stephen W. Tsai, “CompositeMaterial (Design and Application)”, copyright ©by CRC Press LLC،United States of America ,2002.

47. John Walling, “Replacing Metals with PEEK (Poly ether ether ketone)”, University of Michigan, United States, 2013.

48. Steven M. Kurtz, " PEEK Biomaterials Handbook " , William Andrew is an imprint of Elsevie, Chapter 7, pp.81-91, 2012.

49. Adell, R., Lekholm, U., Rockler, B., Branemark, P.I., " A 15-year Study of Osseointegrated Implants in the Treatment of the Edentulous jaw " , Int. J. Oral Surg.,Vol. 10, , pp.387–416, 1981

50. F.C. Campbell, “Manufacturing Technology for Aerospace Structural Materials”, Copyright© Elsevier Ltd, 2006.

51. D.P. Jones, D.C. Leach, D.R. Moore, Mechanical properties of poly(ether-ether-ketone) for engineering applications, (1985).

52. Zhang, M. and J. Li, "Carbon nanotube in different shapes" Materials Today, V 12, N(6),P 12-18, 2009.

53. Kathyayini, H., et al.," Catalytic activity of Fe, Co and Fe/Co supported on Ca and Mg oxides, hydroxides and carbonates in the

synthesis of carbon nanotubes" Molecular Catalysis A: Chemical, 223(1-2): p 129-136,2004.

54. Jyh-Ming Ting[1],Wen-Chen lin," Unprecedented re-growth of carbon nanotubes on in situ reactivated catalyst " Nanotechnology, 14;20(2), 2009.

55. Bianco, A., K. Kostarelos, and M. Prato, "Applications of carbon nanotubes in drug delivery" Current Opinion in Chemical Biology, 9(6): p. 674-679, 2005.

56. Peter Morgan "CARBON FIBERS and their Composites" 1st edition,10(13), 20 May (2005).

57. D.D Edie, "The effect of processing on the structure and properties of carbon fibers" 36(4): p. 345-362 , 1998.

58. Rodríguez Guerrero Alejandro , Sánchez, Narciso, Javier, Louis, Enrique, Rodríguez Reinoso Francisco , "Pressure infiltration of Al–12 wt.% Si–X (X = Cu, Ti, Mg) alloys into graphite particle preforms"Acta Materialia, 54(7), p. 1821-1831, 2006.

59. Wang, W.G., B.L. Xiao, and Z.Y. Ma, "Evolution of interfacial nanostructures and stress states in Mg matrix composites reinforced with coated continuous carbon fibers" Composites Science and Technology, 72(2): p. 152-158. 2012.

60. Hamid Khayyam, Minoo Naebe ,Omid Zabihi, Reza R. Zamani, Stephen Atkiss, Bronwyn Fox ," Dynamic Prediction Models and Optimization of polyacrylonitrile)PAN) Stabilization Processes for Production of Carbon Fiber" IEEE Transaction on Industrial Informatics, 11(4): p. 887-896. 2015.

61. S . Chand, "Review Carbon fibers for composites" ,of Materials Science, 35:p. 1303-1313, 2000.

62. long Xia a , Binbin jia a , Jun Zeng b ,Jincheng b "Wear and mechanical properties of carbon fiber reinforced copper alloy composites" Materials Characterization, 60(5): p. 363-369. 2009.

63. Moonhee lee [a] , Yongbum choi [b*], Kenjiro sugio [b],Kazuhiro Matsugi [b] , Gen Sasaki [b]," Effect of aluminum carbide on thermal conductivity of the unidirectional CF/Al composites fabricated by low pressure infiltration process" , Composites Science and Technology 97: p. 1-5. 2014.

64. Frank, E., et al., Carbon fibers: Precursor systems, processing, structure, and properties. Angewandte Chemie - International Edition, 53(21): p. 5262-5298,2014.

65. Tony Roberts, The Carbon Fiber Industry The Carbon Fiber Industry: Global Strategic Market Evaluation 2006-2010, Vol. 10, pp. 93– 177, January 2006.

66. Tatsuo Oku , Carbon/Carbon Composites and Their properties ,2003

67. Scott Bader, "Crystic Composites Handbook", Copyright (c) December 2005.

68. Anvari A, "Fatigue life prediction of unidirectional carbon fiber/epoxy composite in Earth orbit" 10(5) (2014).

69 . Paul J. Walsh, Zoltek Corporation, "Carbon Fibers", this article is from ASM Handbook, Volume 21, Copyright© ASM International®, 2001.

70. Zhao, Z. and Gou, J. "Improved fire retardancy of thermoset composites modified with carbon nanofibers" Sci. Technol. Adv Mater(2009).

71. Ryosuke Matsuzaki 1, Masahito Ueda 2, Masaki Namiki 2, Tae-Kun Jeong 2, Hirosuke Asahara 2, Keisuke Horiguchi 1, Taishi Nakamura 1, Akira Todoroki 3, Yoshiyasu Hirano 4 " Three-dimensional printing of continuous-fiber composites by in-nozzle impregnation"6 23058(2016).

72. T. Vu-Khanh and J. Denault, " Polymer-Matrix Composites ", for 6thTech, pp, 473-482,(1991).

73. Alexander Tregub, Hannah Harel, and Gad Marom g, "The Influence of Thermal History on The Mechanical Properties of Poly(Ether Ether Ketone) Matrix Composite Materials" , Elsvier , 48(1–4), P. 185–190 The University of Trento/ Italy,1993.

74.G. Swallowe, J. Fernandez, S. Hamdan, " Crystallinity Increases in Semi Crystalline Polymers During High Rate Testing " de Physique IV Colloque, , 07 (C3), pp.C3-453-C3-458, 1997.

75. Bhanu Nandan, L. D. Kandpal, G. N. Mathur " Crystallization and melting behavior of poly(ether ether ketone)/poly(aryl ether sulfone) blends" ,90(11), P. 2906-2918, India 2003.

76. M.C. Kuo, C.M. Tsai, J.C. Huang M. Chen , " composites reinforced by nano-sized SiO2 and Al2O3 particulates", Materials Chemistry and Physics 90 , 185–195 ,Taiwan (2005)

77. Liliana. Nohara, Evandro L. Nohara, Andreza Moura, Joseane M. R. P. Gonçalves, Michelle L. Costa, Mirabel C. Rezende," Study of crystallization behavior of poly(phenylene sulfide),16(2), June 2006.

78. M. Rahail Parvaiz, Smita Mohanty, Sanjay K. Nayak and P. A. Mahanwar[2] Polyetheretherketone (PEEK) Composites Reinforced with Fly Ash and Mica 9, No.1, pp.25-41, 2010

79. T. Yu, C. M. Wu, C. Y. Chang, C. Y. Wang, S. P. Rwei, "Effects of crystalline morphologies on the mechanical properties of carbon fiber reinforcing polymerized cyclic butylene terephthalate composites", 6(4), 318–328, 2011.

80. Lanzhu Zhang, Min Li and Hui Hu, " Study on mechanical properties of PEEK composites", 476-478, pp 519-525, Trans Tech Publications, Switzerland (2012).

81. R. Hemanth, M. Sekar, B. Suresha "Effects of Fibers and Fillers on Mechanical Properties of Thermoplastic Composites " Advances in Chemical Science 2 (28-35), India 20th April (2014).

82. Iskender Ozsoy , Askin Demirkol, Abdullah Mimaroglu Huseyin Unal Zafer Demir, " The Influence of Micro- and Nano-Filler Content on the Mechanical Properties of Epoxy Composites" Mechanical Engineering 61(10),p 601-609 , 04-28(2015)

83. S. Selvam , K. Marimuthu "Development and Investigation of Mechanical Properties of PEEK Fine Particles Reinforced UHMWPE Composites" 0973-4562 Volume 11, Number 2 (2016) pp 1298-1303

84. Jianhua Li, Yatao Wang, Xiaodong Wang and Dezhen Wu,

" Development of Polyoxymethylene/PolylactideBlends for a Potentially Biodegradable Material: Crystallization Kinetics, Lifespan Prediction and Enzymatic Degradation Behavior", , 11, 1516, 2019

85. Dong Hyun Kim, Yeon Taek Hwang, Hak Sung Kim , "Investigation of Mechanical and Hygroscopic Properties for the Semi-crystalline Polypropylene Polymer Via Experiments and Molecular Dynamics" Precision Engineering and Manufacturing-Green Technology, 8(1),p 177-191 ,(2020)

86. M.Doumeng , L.Makhlouf , F.Berthet,O.Marsan K.Delbé,J.Denape, F.Chabert,"A comparative study of the crystallinity of polyetheretherketone by using density, DSC, XRD, and Raman spectroscopy techniques " 93, January 2021, 106878.

87. M. Doumeng,L.Makhlouf,FlorentinBerthet, O.Marsan,K.Delbé,Jean Denape, F.Chabert A comparativestudyof thecrystallinity of Polyetheretherketone by using density, DSC,XRD, and Raman spectroscopytechniques, 25 September 2020.

88. D.J. Blundell, B.N. Osborn, The morphology of poly(aryl-ether-ether-ketone),Polymer 24 (1983) 953–958.

89. Roger Brown, "Handbook of Polymer Testing", copyright ©Rapra Technology Limited, UK, 2002.

90. Averous L, Fringant C, Moro L, Plasticized starch-cellulose interactions in polysaccharide composites, Polymer, 42, 6565-6572, 2001

91. Kasiama, Mizolo Ginette, "Engineering Polymers Based on 1, 1-Diphenylethylenederivatives: Polymer Substrates as Precursors for Membrane Development", University Of South Africa, 2012.

92. Barbara H. Stuart, "Infrared Spectroscopy: Fundamentals and Application copy right at John Wiley & Sons, 25 June 2004.